Development of Novel CO_2-Selective Thin-film Mixed Matrix Membrane: Role of Amine Carrier and Filler Material on the Membrane Behaviour

A Thesis

Submitted in Partial

Fulfilments of the Requirements for the Degree of

DOCTOR OF PHILOSOPHY

by

Mridusmita Barooah
(136107039)

Department of Chemical Engineering

Indian Institute of Technology Guwahati

Guwahati, Assam 781039

November 2019

Dedicated

To

My Parents and My Mentor

Department of Chemical Engineering
Indian Institute of Technology Guwahati
Guwahati, Assam 781039

STATEMENT

I hereby declare that the content embodied in this thesis entitled "**Development of Novel CO_2-Selective Thin-film Mixed Matrix Membrane: Role of Amine Carrier and Filler Material on the Membrane Behaviour**" is the result of investigations carried out by me, Miss Mridusmita Barooah at the Department of Chemical Engineering, Indian Institute of Technology Guwahati, Guwahati, India, under the guidance of Prof. Bishnupada Mandal. In keeping with the general practice of reporting scientific observations, due acknowledgements have been made wherever the work described is based on the findings of other investigators.

November, 2019 Mridusmita Barooah

Department of Chemical Engineering
Indian Institute of Technology Guwahati
Guwahati, Assam 781039

CERTIFICATE

It is certified that the work described in this thesis, entitled "**Development of Novel CO_2-Selective Thin-film Mixed Matrix Membrane: Role of Amine Carrier and Filler Material on the Membrane Behaviour**", done by **Ms. Mridusmita Barooah** (Roll No. 136107039) for the award of degree of Doctor of Philosophy is an authentic record of the results obtained from the research work carried out under my supervision in the Department of Chemical Engineering, Indian Institute of Technology Guwahati, India and this work has not been submitted elsewhere for the award of any other degree or diploma.

This thesis in my opinion, has reached the standard fulfilling the requirements for the award of the degree of Doctor of Philosophy in accordance with the regulations of the institute.

November, 2019

(**Prof. Bishnupada Mandal**)
Professor
Department of Chemical Engineering
Indian Institute of Technology Guwahati
Guwahati 781039, India

ACKNOWLEDGEMENTS

The completion of this thesis would have not been possible without the support and encouragement of various people and Institution. I take this opportunity to thank all those people and Institution who have been an integral part in successful completion of this thesis.

At the onset, I express my sincere thanks to my research supervisor ***Professor Bishnupada Mandal*** *for his valuable guidance, scholarly inputs and consistent encouragement towards the completion of my research work. His continuous support towards research and freedom to think, plan and execute my ideas towards my work has provided a good basis for the present thesis. His positive attitude, encouragement, valuable guidance towards the research helped me to perform and complete the research objectives. His support in doing the experiments, analysis of the data and preparing the manuscripts are invaluable. I am fortunate enough to complete my thesis under his supervision. It has really been a notable working experience with him.*

Besides my supervisor, I am obliged to my doctoral committee chairman ***Prof. G. Pugazhenthi****, Department of Chemical Engineering for his useful suggestion during the course of my research. I would also like to thank* ***Prof. Chandan Das,*** *Department of Chemical Engineering and* ***Dr. Lal Mohan Kundu,*** *Department of Chemistry, for their valuable suggestion during my progress seminars.*

My special thanks to ***Prof. Sasidhar Gumma*** *of Chemical Engineering Department for his experience and helping nature in several ways of my Ph.D life. I am also grateful to all the* ***faculty members*** *and* ***Staffs*** *of Department of Chemical Engineering for providing me necessary facilities for analysis of data.*

I acknowledge with thanks the ***Department of Science and Technology (DST),*** *New Delhi, Government of India, INDIA (Grant No. DST/TSG/NTS/2015/73) for the financial support for my research work.*

I would also acknowledge the ***Analytical Lab Facility (Department of Chemical Engineering), Centre of Excellence for Sustainable Polymers (CoE-SusPol), Central***

***Instruments Facility**, Department of **Physics** of **IIT Guwahati,** and **CSIR-North East Institute of Science and Technology (NEIST), Jorhat** for providing me the necessary instrument facility which has been very important in this research work.*

*I would like to thank all my **seniors**, **labmates**, **juniors**, **friends** and other **well-wishers** who helped me to complete my research.*

*I also thank my **sister** for showering their love, care and also being my editor and proof-reader many times. I thank my brother, brother-in-law, sister-in-law for their support throughout my Ph.D period. Finally, I express my gratitude to the most important people in my life, **my beloved parents** for showering their love, care, sacrifices and encouragement which have made it possible for me to come so far. I owe this to you. This would not have been possible without your support.*

Midusmita Barooah

Contents

Abstract

The main objective of the present work is to study the CO_2 separation from fossil fuel combusted power plants using CO_2-selective thin-film composite dense polymeric and mixed matrix membrane containing different combinations of amine carriers and inorganic as well as hybrid fillers. The primary focus is to achieve CO_2-selective membrane by facilitated transport mechanism having impressively high CO_2 permeability along with high CO_2/N_2 selectivity at temperature and pressure values closely resembling the actual industrial flue gas conditions. Poly (vinyl alcohol) (PVA) was used as base polymeric material due to its excellent hydrophilic nature and good film-forming ability. Thermal stability of PVA has been improved by using formaldehyde (HCHO) as cross-linking agent. Poly (ethylene glycol) (PEG) was used as the polymer blend. Various combinations of amines acting as fixed and mobile carriers such as polyethyleneimine (PEI), triethylenetetramine (TETA) and piperazine glycinate (PG) were utilized to improve the CO_2 transport property. Silica prepared by Stober's process and zeolitic imidazolate framework-8 (ZIF-8) metal-organic framework (MOF) was used as filler material. The filler particles were further functionalized by amine functional groups such as 3-aminopropyltrimethoxysilane (3-APTMS) and polyethyleneimine (PEI) and utilized for gas separation studies. Different combinations of amine carriers and functionalized and unfunctionalized filler materials were introduced into the polymer hydrogel in the preparation of CO_2-selective polymer and mixed matrix membranes.

Characterization studies such as TGA, FTIR, XRD, FETEM, FESEM and XPS were done for the active layer which was found to be optically transparent to visible light and mechanically stable to be handled. The TGA curve analysed the sample weight loss in percentage (%) with temperature. The FTIR analysis confirmed the functional groups present in the sample. The X-ray diffraction pattern for all the amine doped membranes obtained by XRD analysis displayed a semi-crystalline structure with peaks at 2Θ angles of 20^o. The FETEM and FESEM analysis determined the surface morphology of the membrane surface and the XPS analysis validated the quantitative and qualitative nature of the chemical state of the membrane surface.

Gas stream containing 20 % CO_2 and 80 % N_2 by volume was utilized to study the transport properties (CO_2 and N_2 permeance and CO_2/N_2 selectivity) across the membrane. The effect of temperature (60 to 110 ºC), and sweep side water flow rate (0.0 to 0.075 ml/min) on the performance of the membranes were analysed. Several membranes have been synthesized for the gas permeation. The cross-linked PVA/PG/ZIF-8 mixed matrix membrane having a constant active layer thickness of 4 µm showed optimum performance with CO_2 permeance of 109 GPU and CO_2/N_2 selectivity of 385 at temperature of 100 °C, feed/sweep water flow rate of 0.03/0.05 ml/min and feed/sweep absolute pressure of 2.5/1.2 atm, respectively. Both polymer and mixed matrix membranes showcased promising potential for CO_2 separation from flue gas streams thus showing huge scope for large-scale CO_2 capture studies.

For the disposal possibilities of the membranes, currently landfill is one viable option available. The components present in the membrane considered in this work comprise of Poly (vinyl alcohol) (PVA), Amine carriers, and Filler materials. PVA is a biocompatible, biodegradable polymer and does not harm much. The amines generally degrade over a span of 4-5 years which is the typical life span of a membrane. The filler materials present in very less percentage in the membrane is not toxic in nature and hence can be disposed in the landfills. The other alternative options available include direct reuse. However, if the performance of the membranes is not within the range for secondary application, then it can be utilized for alternative end-of-life option and finally goes to local landfill for disposal possibilities.

List of Tables

List of Figures

CHAPTER 1

CO_2 Emission and Capture Overview, Mixed Matrix Membrane, Literature Review and Research Objectives

CHAPTER 1

CO_2 Emission and Capture Overview, Mixed Matrix Membrane, Literature Review and Research Objectives

This chapter presents an overview on the importance of CO_2 separation and its impact on environmental ecology and climate change. It also emphasizes on various CO_2 capture technologies presently available. This chapter highlights the importance of membrane technology over the conventional technologies. This section also reviews various membranes employed for CO_2 separation with special focus on mixed matrix membranes and its fabrication techniques. The different CO_2 capture methods, specifically membrane technologies for CO_2 separation using facilitated transport mechanism have been focused. Based on the gaps and challenges, the research objectives were defined.

1.1. Introduction on CO_2 emissions

With rapid industrialization, the study on control of greenhouse gas emission is of immense importance. The greenhouse gases which absorb and emit the radiant energy from the Sun throughout the atmosphere increase the global surface temperature [1, 2]. Among the various greenhouse gases (CO_2, H_2O, CH_4, N_2O, O_3, CFCs), the capture of CO_2, a primary greenhouse gas present in Earth's atmosphere is of primary concern [3]. The increase in CO_2 concentration has huge adverse environmental impact such as global warming, ocean acidification, carbon fertilization and the rise in sea level among others. As reported by the Mouna Loa Observatory in 2019, scientist recorded the first ever increase in CO_2 level to 415 parts per million (ppm), the highest ever with 800,000 years of data [4]. With such a surge, if efficient measures are not taken the CO_2 concentration is expected to rise to alarming level of 750 ppm by 2100 [5]. The primary source of CO_2 emission includes fossil fuel basically from thermal and coal-based power plants. The other sources contributing to the emission of CO_2 include deforestation, volcanic outgassing, combustion and emission from transport vehicles. Among them, fossil fuels alone contribute to emission of 24 billion tons of CO_2 per year [6, 7]. According to a study reported recently, India is the fourth largest CO_2 emitter in the world and accounts

for 7 percent of global emission. The International Energy Agency (IEA) had predicted that India would be among the top three CO_2 emitters of the world by 2030. Owing to this situation, the study of carbon capture and sequestration (CCS) is of considerable importance with capture studies from fossil fuel sources. The CCS technology is basically divided into the following three stages: (1) CO_2 capture from combustion exhaust (i.e. flue gas), (2) CO_2 transportation usually by pipelines, road tankers, ships and (3) CO_2 utilization in industrial application such as urea production and storage (i.e. underground storage) [8, 9]. The CO_2 from the combustion stack is compressed to liquid CO_2 and transported via pipelines or ships for safe storage. Injection deep into the water bodies and storage in rock formations as dry ice are some of the commonly used storage technologies. In the CCS technology, the capture study alone contributes to 70-90 % of the total operating cost of the entire technology [10]. Thus, the development of new technology for reducing CO_2 capture cost is a matter of prime concern for scientist across the globe. The primary capture technologies include post-combustion, pre-combustion and oxy-combustion for CO_2 capture. Each of these categories has been critically discussed henceforth highlighting on its benefits and usage.

Among the available capture techniques, post-combustion capture is the simplest and most effectively utilized technology since the capture step can be easily implemented after the combustion process and is readily installed into the industrial power plants [11]. Post-combustion technique comprises treatment of CO_2 from the exhaust gases on the product side. The restriction of this technique is the capture of CO_2 at low concentration of CO_2 (3-20 %) in comparison to large volume of N_2 in the gas stream, operation at low pressure (around 1 atm) and high temperature (120-180 °C) [12]. The pre-combustion technique refers to the capture of CO_2 prior to combustion process. It is applicable to integrated gasification combined cycle power plants (IGCC) consisting basically of carbon monoxide (CO) and hydrogen (H_2) in the presence of steam and oxygen under pressure and heat. The CO is converted to CO_2 and additional hydrogen is produced by water gas shift reaction from which the CO_2 is separated [13]. In oxy-combustion method, the oxygen (O_2) used for combustion is first separated from air and then the fuel is combusted in pure oxygen. Thus the flue gas contains only oxygen- rich and nitrogen-

free atmosphere producing high purity CO_2 (> 99 %) separated from water vapour by condensing the water through cooling and compression. The challenge in this technique lies in the production of pure oxygen keeping in mind the cost effectiveness of the process [14]. Table 1.1 depicts typical operating conditions of flue gas stream from various sources.

Table 1.1 Typical application condition of CO_2 separation from flue gas stream from different sources

Stream source	**CO_2 concentration**	**CO_2 partial pressure(bar)**
Gas turbine	3-4	0.03-0.04
Fired boilers of oil refinery and petrochemical	8	0.08
Natural gas fired boiler	7-10	0.07-0.10
Oil fired boilers	11-13	0.11-0.13
Coal fired boilers	12-14	0.12-0.14
IGCC after combustion	12-14	0.12-0.14
Blast furnace (after combustion)	27	0.27
Cement process	14-33	0.14-0.33

1.2. Separation technologies for CO_2 capture

The techniques used for CO_2 separation can be classified into physical and chemical process. The post-combustion CO_2 capture from flue gas can be carried out industrially by processes such as (1) amine absorption, (2) adsorption, and (3) cryogenic distillation. However, for higher efficiency hybrid systems can also be employed such as membrane system integrated with solvent absorption.

1.2.1. Amine based absorption for CO_2 capture

Amine absorption classified into physical and chemical process is a conventional technology widely developed for CO_2 capture. It removes CO_2 by exposing the flue gas stream to an aqueous amine solution [15]. The CO_2 reversibly reacts with amine forming a soluble carbonate salt and subsequently the CO_2 released by heating the salt solution in a separate stripping column [16]. Alkanolamines containing primary, secondary and tertiary amines such as monoethanolamine (MEA), diethanolamine (DEA), 2-amino-2-methyl-1-propanol (AMP) and N-methyldiethanolamine (MDEA) are commonly used absorbents for CO_2 capture. However, a minor portion of the amines are degraded or emitted to the air to degrade into some toxic undesirable substances harmful for the environment. This technology is also restricted by high energy requirement, corrosive nature and high solvent regeneration cost [17].

1.2.2. Adsorption based CO_2 capture

The separation of CO_2 from gas stream dates back to 1950's wherein molecular sieves, alumina, silica materials were used as adsorbents to remove traces of CO_2 from air. The adsorption process can be vastly divided into thermal swing adsorption (TSA) and pressure swing adsorption (PSA). For CO_2 capture, the adsorbents should have desirable characteristics of low heat capacity, accelerated kinetics, high selectivity, absorptivity, high thermal and mechanical stability. Physical adsorbents such as silica gel, molecular sieves, alumina etc. or chemical adsorbents such as hydrotalcites and limestone has been used [18, 19]. Amine based adsorbents though broadly used but low capacity and high cost add to their utility limitations.

1.2.3. Cryogenic distillation based CO_2 capture

Cryogenic distillation is widely used commercially for streams having high CO_2 concentrations (> 90 %) and separates CO_2 at extremely low temperature. The steps involved in the process comprises of compression, refrigeration and separation. These technologies directly produce liquid CO_2 which makes the CO_2 capture and transportation comparatively easier than other techniques. However, this complex process, consumes high energy and is costlier than other technologies which limit its industrial use [20, 21].

1.3. Advanced membrane technology based CO_2 capture

The conventional separation techniques have huge energy requirement with high regeneration cost and hence serves as hindrance for its large-scale operation. Hence, the research is oriented towards alternate cost-effective and energy-efficient based technology called the membrane separation. It is hugely preferred over the traditional conventional techniques due to its advantages of less energy consumption, light weight, space efficiency and compact modular design. These methods do not require any separating agent and hence no regeneration cost is taken into consideration. Although, the study of gas permeation is 150 years old, significant improvement with generation of new synthetic membrane materials with high gas separation performance has been observed in the recent decade. Morphology of the polymer plays a significant role in the case of gas transport and separation through polymer membranes. The focus of this thesis is on the development of potential membrane techniques that could serve as an efficient alternative to the age old used conventional ones for industrial CO_2 separation processes. Membranes which are semi-permeable barrier separates a particular gas component from the rest component in the mixture making the permeate rich in a particular gas. Permeation rate of a membrane depends upon sizes or diffusion coefficient of the molecules present in the membrane. The possible membrane separation mechanisms can be widely classified as solution-diffusion mechanism, Knudsen diffusion, capillary condensation, surface diffusion and molecular sieving mechanism. Based on the materials used, membranes can be broadly classified into (1) Organic membranes, (2) Inorganic membranes, and (3) Mixed matrix membranes.

Organic or polymer membranes are the most widely used commercial membranes in gas separation due to its advantages of low cost and efficient separation efficiency. The polymers used are either rubbery or glassy polymers based on their glass transition temperature [22, 23]. The principle separation mechanism of polymer membranes is the solution-diffusion mechanism. Robeson's in the early 1990s confirmed that the polymers with high selectivity exhibited low permeability and vice-versa. The constraint of this membrane came to be popularly known as Robeson's upper bound limitation [24-26]. In the Robeson's plot, the selectivity was plotted as a function of CO_2 permeability (Barrer). However, for large-scale application of gas separation membranes high CO_2

permeance along with high selectivity plays a pivotal role. Also, organic membranes are restricted by low thermal, mechanical and chemical stability. Hence, there have been innumerable studies on improving the gas separation properties of these type of membranes. Some of the common methods include polymer blending, use of amines as carrier, incorporation of both organic and inorganic fillers as well as cross-linking mechanism [27, 28].

Inorganic membrane normally exhibits high separation ability and operates at fairly high temperatures. However, the long-term application of these membranes is restricted by its high cost and brittle nature. Some common example of inorganic membranes used for gas separation application includes zeolite and silica membranes [29]. Another major class of advanced membrane material is mixed matrix membranes (MMM), developed by researchers in the mid 1980's. These membranes combine the synergistic effect of both polymeric and inorganic materials. These membranes are discussed in detail.

1.4. Mixed matrix membranes

The separation performance of polymer membranes when used alone is restricted by the trade-off limitation in permeability and selectivity. Again, pure inorganic membranes have disadvantages of high fabrication cost and handling difficulties with most being brittle. These limitations are envisioned to be overcome by advanced membrane material called mixed matrix membranes. It typically contains two phases: a continuous polymer phase and dispersed inorganic filler phase wherein the latter is distributed within the polymer matrix. The inorganic particle can be of varied types depending on their shape, structure and surface chemistry and include zeolites, activated carbon, carbon molecular sieves (CMS), silica and nano-sized particles. Robeson reviewed the upper bound with the latest available data in 2008 and reported that many MMM study approach exceeded the upper bound behaviour. However, the fabrication of defect-free mixed matrix membrane is possible only with excellent dispersion of inorganic particles which give higher performance than typical polymeric membranes [30-35]. Figure 1.1, shows the schematic representation of mixed matrix membrane with inorganic material embedded into the polymeric matrix.

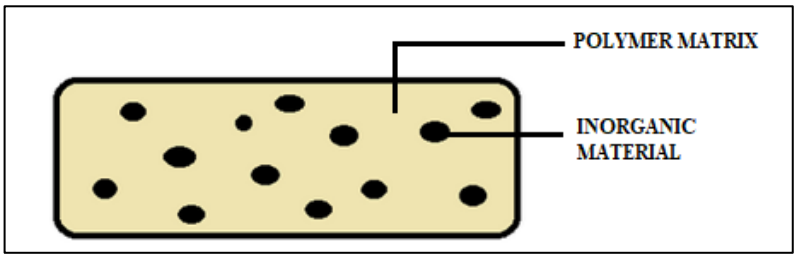

Figure 1.1 Schematic representation of mixed matrix membrane with inorganic material embedded into the polymeric matrix

1.5. Fabrication of mixed matrix membrane

The mixed matrix membrane fabrication is similar to the synthesis procedure of polymer membrane. A good polymer-particle interface is a key to preparation of defect-free mixed matrix membrane. It includes the preparation of polymer solution and pre-treatment of the inorganic filler, mixing of the polymer solution and particle, casting on to a porous polymeric support and subsequent drying and heat treatment [36]. However, poor interaction between the polymer and particle could cause deterioration in the separation performance of the membrane. The factors commonly contributing to the poor interface morphology includes low adhesion between the polymer and particle phase, partial blockage of the particle pores by polymer chain, and polymer chain rigidification. The repulsive force between polymer and filler leads to the development of interface voids. Figure 1.2 displays the different conditions of interfacial morphology in a mixed matrix membrane. Figure 1.2(a) represents the defect-free ideal morphology which occurs under perfect interfacial interaction between the polymer and the filler particle phase. The poor compatibility between the polymer and particle phase gives rise to the formation of interfacial voids as represented by Figure 1.2(b). This leads to increased gas permeability and the change in particle size leading to reduced selectivity. In the case of formation of dense polymer layer surrounding the filler particle, restriction in the mobility of polymer chain around the dense layer leads to decline in gas permeability as shown in Figure 1.2(c). Sometimes, the plugging of filler pore seals the particle size thereby exhibiting decline in gas permeability as represented in Figure 1.2(d).

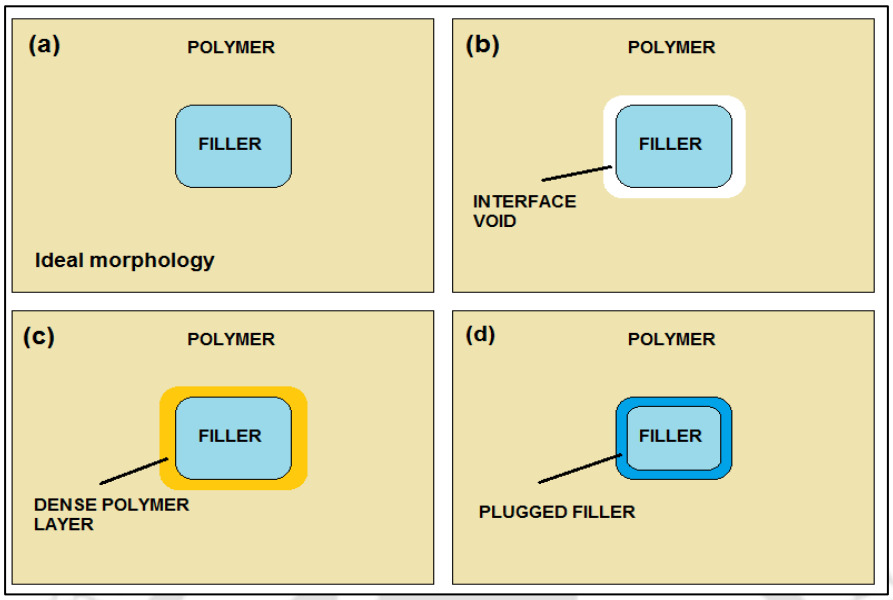

Figure 1.2 Schematic representation of various morphology in mixed matrix membrane (a) Ideal morphology, (b) Interface void surrounding the filler particle, (c) Dense polymer layer surrounding the filler particle and (d) Plugged filler formed during mixed matrix membrane formation.

Thus to obtain the desired gas separation properties, morphology, chemical and mechanical stability, mixed matrix membrane should have the following properties: (1) Homogeneous dispersion of particles in the organic matrix to avoid agglomeration which might result in the loss of selectivity, and (2) A highly defect-free polymer-particle interface guaranteeing no formation of interface voids that negatively affects the separation performance. In order to avoid any agglomeration of inorganic particles into the polymer matrix, the following three synthesis procedure can be adopted: (1) The particles and the polymer are dispersed into the solvent separately and thereafter the polymer solution is added into the particle suspension solution, (2) The particle is dispersed into the solvent followed by stirring and then added to the polymer solution to obtain homogeneous mixture of polymer and the particle, and (3) The polymer is dissolved into the solvent and thereafter the filler particles are added into the polymer solution. Out of the three synthesis procedure adopted, the first two procedures have the dilute solutions with low viscosity thus giving ample chance for agglomeration of the particles to not take place and better dispersion of the inorganic particles.

1.6. Selection of membrane material

1.6.1. Polymer materials for the bulk matrix formation

The polymers used for gas separation membrane preparation are basically divided into two types: rubbery and glassy polymer. Rubbery polymers allow chain segmental motion around the main chain bond compared to glassy polymers which possess rigid chain structure with persistent length thereby making it viable to be applied for natural gas purification involving high pressure condition. The membranes having extremely thin selective layer achieves high CO_2 permeance. Also, better separation performance in mixed matrix membranes can be observed by choosing polymers which have high selectivity compared to high permeability. The polymer selection should be such that it ensures good adhesion between the polymer and inorganic particles. The gas transport through polymer membrane basically follows solution-diffusion mechanism whereby separation is based on the solution and diffusion of the gas molecules in the membrane material. The gas molecules first dissolve in the feed side of the membrane, diffuse through the membrane by a concentration gradient and then finally desorbs on the permeate side of the membrane. Thus, the polymer material having high affinity for CO_2 molecules provides high CO_2 permselectivity. The CO_2 transport can also be accomplished by facilitated transport mechanism or reactivity selective mechanism, whereby a 'carrier' introduced into the polymer matrix reacts reversibly with CO_2 and forms CO_2–carrier reaction product at the membrane feed side, which diffuses along its concentration gradient to the permeate side of the membrane. The CO_2 is released from the CO_2–carrier reaction product at the permeate side, regenerates the carrier which react with another CO_2 molecule on the feed side. The CO_2 transport by facilitated transport mechanism results in both high CO_2 permeability and selectivity and shows improved results when compared to transport by solution-diffusion mechanism alone. The common polymers used for mixed matrix membrane include polyethersulfone (PES), polycarbonate (PC), poly(arylketones), poly(arylethers), poly(vinyl acetate) (PVA_c), poly(2,6-dimethyl-1,4- phenylene oxide) (PPO), cellulose acetate (CA), polyimide, polyetherimide, PIM-1, poly(ether-block-amide) (Pebax) and poly(vinylamine) (PVA_m).

1.6.2. Inorganic materials used as fillers

The inorganic material used in MMM can be either porous or non-porous types. Porous particles act as molecular sieving agent and separate on the basis of shape or size of the gas molecules. The inorganic particles with pore size of mesoporous range (between 2nm and 50 nm) and micro-porous range (less than 2nm) are generally used for mixed matrix membrane fabrication [37]. The selection of inorganic filler is based on various factors such as particle size, its adsorption capacity with the targeted gas molecule, surface chemistry, and functional groups.

1.6.2.1 Zeolites

Zeolites are commonly utilized as inorganic material in mixed matrix membranes [38, 39]. These are aluminosilicates with open 3D-structure having uniform cavities and channels. The proper selection of zeolite particle is essential to obtain high performance MMM. Although zeolites embedded into glassy polymers exhibit high mechanical stability compared to rubbery polymers, it leads to the formation of interfacial voids leading to decrement in selectivity with increase in permeability. However, the challenge lies in the preparation of void-free MMMs. As reported in literature, zeolite-4A with PES increased the CO_2 permeance by ~4 folds and CO_2/N_2 selectivity by ~2 folds and when blended with Matrimid improved the O_2 permeance to 0.06 GPU to 0.02 GPU while the O_2/N_2 selectivity almost remained the same [40]. To tackle the restrictions observed, modification techniques such as coating with highly permeable silicone rubber or addition of plasticizer to increase the flexibility of the polymeric matrix have been incorporated.

1.6.2.2. Carbon molecular sieves (CMS)

Carbon molecular sieves (CMS) are highly porous materials and their fine pore size distribution ensures high gas permeability as potential filler for MMM. The size of the pore opening of CMS (3-5 Å) is close to the size of gas molecules which allows precise discrimination of certain gas species. An 45 % and 20 % increase in CO_2/CH_4 and O_2/N_2 selectivity by using CMS and matrimid mixed matrix membrane has been reported [41, 42].

1.6.2.3. Activated carbon

Activated carbon is another commonly and easily available filler material in mixed matrix membrane. Incorporating activated carbon into acrylonitrile butadiene copolymer (ABS) increased the CO_2 permeability by 40-600 % and CO_2/CH_4 selectivity by 40-100 % for CO_2/CH_4 mixture. The author attributed these effects to the good adhesion properties between activated carbon and ABS and superior selectivity of ABS itself [43].

1.6.2.4. Silica

Silica nanoparticles are classified into non porous silica and ordered mesoporous silica. These are normally incorporated to the polymer matrix through sol-gel reaction leading to the development of nano-scale particles well dispersed in the polymer matrix. The increased interaction between the silanol groups present in silica and CO_2 polar gases results in improved gas solution effect thereby leading to increased gas permeability. Also, the presence of silica particles induces morphological changes at the interface resulting in increased amorphous region of the MMM and enhanced permeability and selectivity [44, 45]. Mesoporous silica such as MCM-41, MCM-48 and SBA-15 exhibit excellent mechanical and thermal stability. However, the blockage of pore needs to be restricted to achieve high separation performance.

1.6.2.5. Carbon nanotubes (CNTs)

Carbon nanotubes (CNTs) containing nano-scale diameter and large length/diameter ratio when fused in membranes provides one-dimensional nano-channels that act as alternate paths for CO_2 to transport through membranes. The dispersion and alignment of the nanotubes along with high cost are the main challenges encountered when used for mixed matrix membranes. The hydrophobic nature of the CNT hinders its good dispersion in the matrix, and hence functionalization strategies either by physical or chemical treatment is required [46-48]. Weng et al. [47] reported PBNPI/MWCNT MMM with acid-treated CNT. The acid-treatment enhanced the permeabilities and selectivities of H_2, CO_2 and CH_4 at high MWCNT loading.

1.6.2.6. Metal-organic framework (MOF)

Metal–organic frameworks (MOFs) are large emerging class of nano-porous hybrid materials with porous crystalline structures [48]. It contains a metal in the centre with various organic linkers. It possesses unique characteristic of large surface area (> 1000 m^2g^{-1}), controlled porosity, highly tailorable organic framework, regulated pore structure and tunable pore sizes thereby attracting immense attention as a potential candidate for mixed matrix membranes [49-51]. Zeolitic imidazolate frameworks (ZIFs), a subfamily of MOFs consisting of metal ions linked by imidazolate linkers integrates the desirable high surface area, pore size tunability of MOFs and the structural diversity of zeolites thereby showing great potential in gas separation studies. By varying the organic linkers of imidazolate ligands and metal ions (zinc or cobalt), various ZIF materials can be tuned according to its usability and requirement. Some of the most common MOFs used in mixed matrix membrane include copper-benzene-1, 3, 5-tricarboxylic acid (Cu-BTC) [52], metal-organic framework-5 (MOF-5) [53], zeolitic imidazolate framework-7 (ZIF-7) [54] and zeolitic imidazolate framework-8 (ZIF-8) [55]. For CO_2 separation, the aperture size of ZIF is close to the kinetic diameter of CO_2 (3.3 Å) thereby making it a highly suitable filler material in MMMs. Defect-free ZIF-7/Polyether block amide (PEBAX) MMM was fabricated and high permeability and high selectivity was achieved at high filler loading. With incorporation of ZIF-8 fillers into the soft domain of PEBAX, the CO_2 permeance enhanced by 4 folds compared to neat PEBAX membrane [56]. The fabricated ZIF-8/ polysulfone (PSf) membrane showed that the gas separation properties of permeance and selectivity increased at 8 wt % ZIF-8 loading than lean PSf membrane [57]. Surface modified ZIF-8 using 2-benziimidazole, and 2-aminobenziimidazole organic ligands with Matrimid® resulted in high CO_2 permeance and a slight decrement in CO_2/CH_4 selectivity [58]. MMMs with poly (vinyl chloride)-g-poly(oxyethylene methacrylate) (PVC-gPOEM) as organic phase and ZIF-8 as inorganic phase reported enhancement in CO_2 permeance and CO_2/N_2 selectivity than bare PVC-g-POEM which could be attributed to the better interfacial interaction of ZIF-8 and POEM phases [59]. Figure 1.3 shows the schematic diagram of transport of gases in a mixed matrix membrane comprising of polymer matrix and filler.

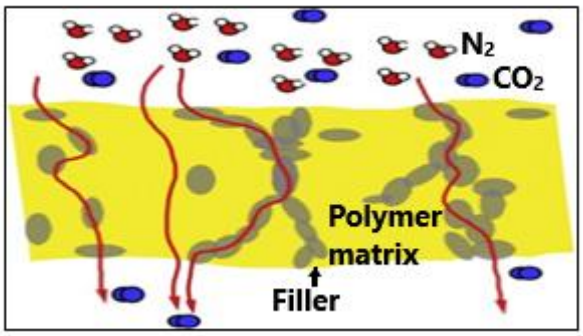

Figure 1.3 Schematic diagram of gas transport in a mixed matrix membrane comprising of a polymer matrix and filler (ideal condition)

1.7. Gas separation performances in mixed matrix membranes

To calculate the MMM gas permeance, permeation properties of continuous and dispersed phase must be taken into account. However, the models such as Maxwell model, Bruggeman model, Lewis-Nielsen model and Pal model proposed only deal with ideal morphology [60].

1.7.1. Maxwell model

The Maxwell model for predicting MMM performance was originally developed to predict the electrical conductivity in composite materials. The effective state composite permeability is given by,

$$P_{eff} = P_c \frac{nP_d + (1-n)P_c + (1-n)(P_d - P_c) + \Phi_d}{nP_d + (1-n)P_c - n(P_d - P_c)\Phi_d} \quad (1.1)$$

where, P_{eff} is the effective permeability of mixed matrix membrane, P_c is the continuous phase permeability, P_d is the dispersed phase permeability, Φ_d is the volume fraction of the dispersed phase, and n is the particle shape factor, ranging from 0 to 1.

1.7.2. Bruggeman model

This model was originally developed to predict the dielectric constant in composite materials. The equation for the permeation for random dispersion of spherical particles is given by the following equation:

$$\frac{P_{eff}}{P_c} = \frac{1}{(1-\Phi_d)} \frac{\frac{P_{eff}}{P_c} - \frac{P_d}{P_c}}{1-\frac{P_d}{P_c}} \tag{1.2}$$

However, at high particle loading this model is not applicable.

1.7.3. Lewis- Nielsen model

This model was originally developed to predict the elastic modulus of polymer composite. It was further adapted to predict the permeability in mixed matrix membranes.

$$P_{eff} = \left(\frac{1+2\Phi(\lambda_d - 1)/(\lambda_d + 2)}{1-\Psi\Phi(\lambda_d - 1)/(\lambda_d + 2)} \right) \tag{1.3}$$

$$\psi = 1 + \left[\frac{(1-\Phi_{Max})}{\Phi_{Max}^{\,2}} \right] \Phi \tag{1.4}$$

Where λ_d is the permeability ratio: $(\frac{P_d}{P_c})$, ψ is the effective volume fraction of filler, Φ is the filler fraction and Φ_{Max} is the maximum filler fraction.

1.7.4. Pal model

This model was originally introduced to determine the thermal conductivity of composite. The permeability is given by,

$$\left(1-\frac{\Phi}{\Phi_{Max}}\right)^{-\Phi_{Max}} = \left(\frac{\lambda_d - 1}{\lambda_d - P_{eff}}\right)\left(P_{eff}\right) \tag{1.5}$$

Where Φ_{Max} is the maximum filler fraction, $\boldsymbol{\lambda_d}$ is the permeability ratio and P_{eff} is the effective permeability of mixed matrix membrane.

1.8. Preparation technique of mixed matrix membranes

For the formation of defect-free polymer-inorganic nanocomposite membrane, the fabrication techniques play a major role and are of the following categories.

1.8.1. Solution blending

Solution blending is largely applied due to its easy fabrication and operation ability and its suitability for wide range of inorganic particles. In this process, the inorganic particles are added and dispersed into the polymer solution by stirring. In some cases, sonication is also applied for effective distribution of the filler particles. However, if not efficiently dispersed, particle agglomeration may occur which degrades the MMM performance. Using this technique, polysulfone (PSf)/ZrO_2 nanocomposite membranes was prepared and the membrane permeance increased as the ZrO_2 weight fraction increased [61]. Also as per literature, the fabrication of Cellulose/Al_2O_3 nanocomposite membrane was done using solution blending [62].

1.8.2. In-situ polymerization

In-situ polymerization involves the mixing of inorganic particles on organic monomer followed by polymerization. This type of preparation technique provides strong interaction between the particle and organic matrix. An example of in-situ polymerization is TiO_2 nanopowder/omethacrylic acid dispersions to produce nanocomposite membrane of poly (methacrylic acid) (PMA)/ TiO_2 [63, 64]. Another example is the preparation of PEG/silica and poly (propylene glycol) (PPG)/silica membrane by radical polymerization of 2, 2 -azobisisobutyronitrile (AIBN) [65, 66]. Fabrication of poly (ether imide) (PEI)/SiO_2 nanocomposite membrane by in-situ polymerization in another such technique [67].

1.8.3. Sol–gel

The sol–gel method is the most widely-established technique for nanocomposite membrane preparation. This method has potential advantage of moderate reaction condition and easy control over the concentration, textural and surface properties. In this method, the inorganic precursors mixed into the polymer solution further hydrolyse and condenses into well-dispersed nanoparticles in the polymer matrix. Additionally, the organic and inorganic ingredients are dispersed at the molecular or nanometer level thus leading to homogeneous membrane solution. Literature reported sol–gel method preparation of polyacrylonitrile (PAN)/tetraethoxysilane (TEOS) nanocomposite membrane showing commendable performance in O_2/N_2 separation [68]. Poly (1-

trimethylsilyl-1-propyne) (PTMSP)/silica nanocomposite membrane by polymerization of TEOS in PTMSP was also reported [69].

1.9. Literature review on mixed matrix membrane for CO_2 separation

The important literatures on CO_2 separation by various mixed matrix membrane have been discussed below:

The gas permeation and sorption properties of poly (amide-12-b-ethyleneoxide) (Pebax1074)/SAPO-34 mixed matrix membrane for CO_2/CH_4 and CO_2/N_2 separation was reported. Zeolite SAPO-34 was used to improve the $CO_2/CH_4/N_2$ gas separation performance compared to neat Pebax1074 membrane. Permeance and selectivity of the MMMs were studied at different operating conditions. The thermal, morphological and mechanical properties of MMM was analysed by differential scanning calorimetry (DSC), scanning electron microscopy (SEM) and tensile analysis. The results showed excellent improvement in CO_2/CH_4 selectivity (about 70 %) and CO_2/N_2 selectivity (about 15 %) at 20 wt % SAPO-34 loading [70]. Polyimide mixed matrix membranes for CO_2 separation was reported using carbon–silica nanocomposite (CSM) filler fabricated by solution casting method. CSMs were prepared by a hard template synthesis technique to get a tuneable porosity and surface chemistry. SEM images of the synthesized MMM confirmed good adhesion and dispersion of fillers within the polymer matrix. Significantly improved CO_2 mixed gas selectivity and permeance for CO_2/N_2 and CO_2/CH_4 gas mixture at 8.9 atm and 35 ºC were achieved with addition of the fillers. For gas mixtures with a 50:50 (CO_2: N_2) feed composition, 2-fold and 6-fold increase of the mixed gas selectivity (up to 42.5) and permeance (upto 0.39 GPU) compared to unfilled PI was achieved [71]. The effects of the acid-base catalysis conditions and silica loading weight of the PPO-silica mixed matrix membrane prepared by in-situ sol-gel method for H_2/CO_2 separation were investigated. The functional groups, crystalline structure, thermal stability and morphology of the MMMs were examined using FTIR, XRD, SEM, TEM, AFM, and TGA, respectively. The results indicate that the in-situ sol-gel method to synthesize PPO-silica MMMs is beneficial for improving the adhesion between the silica and polymer and for the silica dispersion. The additives significantly enhanced the thermal stability of the membranes. Compared to pure PPO membrane, the PPO-silica

MMMs prepared with 10 wt % acid-silica loading exhibited the best H_2/CO_2 separation properties. Enhancement in H_2 permeance and H_2/CO_2 separation ratio was observed [72]. Hybrid brominated sulfonated poly (2, 6-diphenyl-1, 4-phenylene oxide) and SiO_2 nanocomposite membranes for CO_2/N_2 separation was reported. 90 % brominated-10 % sulfonated PPO_{dp} (BSPPOdp9010) as representative material formed flexible membrane with higher CO_2 permeance of 1.16 GPU and selectivity (=36) compared to pure poly (2, 6-dimethyl-1, 4-phenylene oxide) (PPO_{dm}) membranes [73]. Facilitated transport mixed matrix membranes incorporated with amine-functionalized MCM-41 into poly (ether-block-amide) (Pebax MH 1657) were characterized by SEM, DSC, tensile test, dynamic mechanical analysis (DMA), and XRD. The results indicated that incorporation of PEI-MCM-41 generated stronger interfacial interactions and resulted in higher polymer chain rigidification at the filler–polymer interface compared to unmodified MCM-41. The as-prepared FT-MMM showed increased gas permeance and selectivity results. The highest ideal selectivities for CO_2/CH_4 and CO_2/N_2 of 41 and 102 at a CO_2 permeance of 20 GPU were reported. Compared to the membrane with pristine MCM-41, the permeance, the ideal CO_2/CH_4 selectivity and CO_2/N_2 selectivity of the PEI-MCM-41-doped membrane increased by 102.3 %, 115.8 % and 96.1 %, respectively, at 20 wt % filler loading and surpassed the 2008 Robeson upper bound line [74]. SAPO-34/polyetherimide mixed matrix membrane for CO_2/CH_4 separation was synthesized using different amounts of SAPO-34 (0 to 10 wt %) dispersed in the polymer precursor dissolved in DCE solvent. The mixed matrix membrane with 5 wt % SAPO-34 content exhibited best performance with CO_2/CH_4 ideal selectivity of 60. Based on mixed gas permeances and time-lag measurements, the separation of CO_2 and CH_4 was found to be dominated by the difference in the gas solution effect. The SAPO-34 decreased CH_4 transport by increasing its diffusion pathway. Particle agglomeration was observed at 10 wt % zeolite loading in the polymeric matrix [75]. In SPEEK/amine-functionalized TiO_2 submicrospheres mixed matrix membranes for CO_2 separation, TiO_2 submicrospheres (300 nm) were amine-functionalized through facile two-step method using dopamine (DA) and polyethyleneimine (PEI) in succession. Grafting PEI with abundant amine groups onto the titania fillers remarkably increased the content of facilitated transport sites in the membrane, leading to increment in gas permeance as well as selectivity. The highest ideal selectivity of the SPEEK/TiO_2–DA–PEI membranes for CO_2/CH_4 and

CO_2/N_2 reported were 58 and 64, respectively, with a CO_2 permeance of 32 GPU. The mechanical and thermal stabilities of the membranes showed enhancement compared to pure SPEEK membrane [76]. The effect of addition of zeolitic imidazolate framework-8 (ZIF-8) MOF filler material on the poly (vinyl alcohol) (PVA)/ piperazine glycinate (PG) solution for the MMM formation was reported. Detailed thermal, mechanical, structural and microscopic analysis revealed strong interaction and compatibility between the ZIF-8 filler and polymer matrix. The PVA/PG membrane loaded with 5 wt % ZIF-8 (PVA/PG/ZIF-8) exhibited high CO_2 permeance of 82 GPU and CO_2/N_2 selectivity of 370 which was 82.2 % and 76 % higher compared to pure PVA/PG membrane [77]. The separation of binary mixtures of CO_2/CH_4 and CO_2/N_2 on mixed matrix membrane containing Zn $(pyrz)_2(SiF_6)$ metal-organic framework synthesized by facile sono-chemical method with crosslinked polyethylene oxide polymer matrix was reported. CO_2/CH_4 and CO_2/N_2 mixture gas permeation tests revealed that separation properties of mixed matrix membrane significantly improved compared to pure polymeric membrane owing to the selective CO_2 uptake and transport in $Zn(pyrz)_2(SiF_6)$ crystal. The $Zn(pyrz)_2(SiF_6)$/XLPEO mixed-matrix membrane increased the CO_2 permeance (GPU) from 9 to 13 and CO_2/N_2 selectivity from 19 to 29 for CO_2/N_2 (20/80) binary gas mixture at 25 ^oC temperature and 1 atm upstream pressure compared to pure XLPEO [78]. Mixed matrix membranes fabricated by incorporating as-prepared metal-organic frameworks into sulfonated poly (ether ether ketone) (SPEEK) investigated the gas separation performance of MMMs in both dry and humidified state. The addition of the sulfonated metal–organic framework increased the selectivity of the membranes for CO_2/CH_4 and CO_2/N_2 systems by increasing the CO_2 solution, and the diffusion of gases through the porous metal-organic frameworks led to the simultaneous increase in CO_2 permeance. The highest ideal selectivity for CO_2/CH_4 and CO_2/N_2 observed were 50 and 53 (at a CO_2 permeance of 37 GPU in humidified state. The increased total water in MMMs led to increased CO_2 permeance and the increased bound water resulted in improved CO_2/N_2 gas selectivity [79]. Poly (vinylidene fluoride) based mixed matrix membranes comprising metal-organic frameworks such as CuBTC, CuBDC, MIL-53(Al) and NH_2-MIL-53(Al) for gas separation applications were characterized by FTIR, XRD, SEM and TGA techniques. 10 wt % loading of CuBTC in PVDF showed 43.6 and 118.7 % permeance enhancement for He and CO_2 compared to the pure membrane. Moreover, the

high selectivity enhancement of 96 % was observed for CO_2/CH_4. In regards to CuBDC, 37.5 and 117 % permeance increase for He and CO_2 was reported for 15 % loading. Furthermore, the best selectivity was related to CO_2/CH_4 in which 109.3 % increase was achieved relative to the pure membrane. The membranes containing 10 wt % of NH_2-MIL-53(Al) showed 11.25 and 22.41 % selectivity enhancement for He/CH_4 and CO_2/CH_4 [80].

Although most of the literature work was based on CO_2 separation from flue gas mixture, the operating conditions could not imitate the actual flue gas operating condition of pressure, temperature and CO_2 concentration. However, the work presented in this thesis imitated the industrial flue gas condition basically from coal based power plants. CO_2 concentration was maintained at 10-15 % and the operating temperature was maintained in the range of 90-120 °C which is in the range of industrial flue gas condition. Thus, the following thesis work has been motivated based on its following features.

1.10. Objectives of the thesis

The primary objectives of the thesis are:

1. Synthesis of CO_2-selective polymeric and mixed matrix membranes for CO_2 separation from flue gas by facilitated transport mechanism.

2. Improvement of the CO_2 facilitated transport by blending with different amine carriers and filler material combinations.

The following research works have been undertaken on the basis of objectives.

i. Synthesis of novel blends of poly (vinyl alcohol) (PVA)/poly (ethylene glycol) (PEG) and poly (vinyl alcohol) PVA/piperazine glycinate (PG) CO_2-selective membrane.
ii. Blending the membranes with different amine carriers for CO_2 separation by facilitated transport mechanism.

iii. Synthesis of mixed matrix membranes by using silica and zeolitic imidazolate framework-8 (ZIF-8) metal-organic framework (MOF) as filler material for enhanced CO_2 performance.

iv. Surface functionalization of the filler with 3-aminopropyl trimethoxysilane (3-APTMS) and polyethyleneimine (PEI) amine to further improve the gas transport performance.

v. Characterization of the nanomaterial and the synthesised membranes to examine the structural, morphological, microscopic and macroscopic behaviour.

vi. Optimization of membrane composition at various operating conditions of temperature and sweep water flow rate.

vii. Comparison of the performance studies of polymeric and mixed matrix membranes under similar operating conditions of temperature and sweep water flow rate using counter flow circular flat sheet membrane module.

1.11. Thesis outline

The following work describes the development of various combinations of PVA polymer membrane and mixed matrix membrane for CO_2 separation. In-depth study on the synthesis of filler material, various combinations of polymer and mixed matrix membrane, compatibility studies, characterization techniques and gas performance studies have been carried out.

On the basis of the above discussion, thesis work has been divided into seven chapters. A brief overview of each chapter is presented.

Chapter 1: This chapter presents an overview on the CO_2 emission from different point source and its impact on overall environmental ecology and climate change. The various conventional technologies for CO_2 separation has been discussed with special focus on advanced membrane separation technology. It gives a brief introduction on mixed matrix membrane, fabrication technique and selection of membrane material. It also focuses on the different inorganic materials used for MMM preparation. The chapter provides a detailed study on gas separation models used in mixed matrix membranes and on the different preparation techniques of mixed matrix membranes. The chapter presents

detailed literature review that includes facilitated transport of CO_2 by mixed matrix membrane.

Chapter 2: This chapter presents a detailed study on the fundamental gas transport mechanisms with special focus on the CO_2-amine reaction mechanism involving facilitated transport mechanism.

Chapter 3: This chapter provides a detailed study on the synthesis of silica nanoparticles by sol-gel process. Thereafter, synthesis, characterization and gas permeation study of PVA/PEG membrane embedded with different loading of the synthesized silica nanoparticle was conducted. The effect of different operating condition on the transport properties (CO_2 permeance and CO_2/N_2 selectivity) was investigated.

Chapter 4: This chapter provides a detailed analysis on mixed matrix membranes (MMMs) formulated by consolidating amino-functionalized silica in PVA/PEG matrix. The silica prepared by Stober's process was amino modified with 3-aminopropyltrimethoxysilane (APTMS) coupling agent to form amino-functionalized silica (APTMS-Sil). Detailed characterization studies such as TGA, FESEM, UTM, XPS and ninhydrin assay revealed the impact of amine-functionalization on the mechanical strength of the membrane. The transport properties of the binary gas mixture (CO_2/N_2) for PVA/PEG/APTMS-Sil membrane for temperature and sweep water flow rate variation were examined.

Chapter 5: This chapter reports the synthesis of zeolitic imidazolate framework-8 (ZIF-8) embedded to the poly (vinyl alcohol) (PVA)/ piperazine glycinate (PG) facilitated transport solution. High-performance mixed matrix membrane (MMM) prepared by solution coating of PVA/PG/ZIF-8 solution on to a polyethersulfone (PES) support were utilized for CO_2/N_2 separation studies. Detailed thermal, structural and microscopic analysis of the synthesized ZIF-8 particles was conducted. The characterization studiesand the performance evaluation tests were performed for the prepared membranes. The effect of different operating condition on the transport properties (CO_2 permeance and CO_2/N_2 selectivity) was investigated.

Chapter 6: This chapter studies the incorporation of surface functionalized zeolitic imidazolate framework-8 (ZIF-8) MOF with polyethyleneimine (PEI) amine-functional moieties as filler material for fabrication of robust high-performance PVA/PG/ZIF-8@PEI mixed matrix membrane (MMM). Detailed characterization such as TGA, FESEM, UTM and XPS analysis was carried out on the synthesized membrane. The effect of sweep water flow rate and temperature for the binary gas mixture (CO_2/N_2) was studied.

Chapter 7: This chapter draws appropriate conclusions based on this study. This chapter also provides some useful recommendations for future research in the relevant field.

Some of this work has been published in reputed international journals like Journal of Membrane Science (Elsevier) and Journal of Applied Polymer Science (Wiley), and some more manuscripts are either under review/communicated or will be communicated in the future course of time. The publication details of journals/ conferences are appended in the research output section in the end.

References

[1] A. Berger, "The effect of greenhouse gases on climate." proceedings of the conference on the future energy systems and technology for CO_2 Abatement, Antwerp, Belgium, November 2002: 3-10.

[2] R.K. Pachauri and A. Resisinger, Eds. Fourth assessment report on climate change; International panel on climate change: Geneva, Switzerland, 2007.

[3] T.S. Ledley, E.T. Sundquist, S.E. Schwartz, D.K. Hall, J.D. Fellows and T.L. Killeen, Climate change and greenhouse gases, Eos Trans. AGU, 80(39) (1999) 453-458.

[4] M. Van der Hoeven, CO_2 Emissions from Fuel Combustion: Highlights; Organisation for economic co-operation and development/ International Energy Agency (OECD/IEA): Paris, 2012.

[5] Earth's CO_2 Home Page, http://co2now.org/

[6] E.S. Rubin, R.N. Cooper, R.A. Frosch, T.H. Lee, G. Marland, A.H. Rosenfeld and D.D. Stine, Realistic mitigation options for global warming, Science. 257 (1992) 148-266.

[7] UNFCCC Kyoto Protocol, revised 2013. http://unfccc.int/ kyoto_protocol/items/ 2830.php (accessed on 01/05/2013).

[8] DOE, Report of the interagency task force on carbon capture and storage, The US Department of Energy and the Environmental Protection Agency, 2010.

[9] R.S. Haszeldine, Carbon capture and storage: how green can black be?, Science. 325 (2009) 1647-1652.

[10] H. Herzog and D. Golomb, Carbon capture and storage from fossil fuel, Use Encyclopedia Energy. 1 (2004) 1-11.

[11] A.A. Olajire, CO_2 capture and separation technologies for end-of-pipe applications-A review, Energy. 35 (2010) 2610-2628.

[12] S.C. Stultz and J.B. Kitto, Steam: Its generation and use, 40th ed., The Babcock and Wilcox Company, Barberton, Ohio, 1992.

[13] D. Jansen, M. Gazzani, G. Manzolini, E.V. Dijk and M. Carbo, Pre-combustion CO_2 capture, Int. J. Greenh. Gas Con. 40 (2015) 167-187.

[14] R. Stanger, T. Wall, R. Spörl, M. Paneru, S. Grathwohl, M. Weidmann, G. Scheffknecht, D. McDonald, K. Myöhänen, J. Ritvanen, S. Rahiala, T. Hyppänen, J. Mletzko, A. Kather and S. Santos, Oxyfuel combustion for CO_2 capture in power plants, Int. J. Greenh. Gas Con. 40 (2015) 55-125.

[15] B. Dutcher, M. Fan and A.G. Russel, Amine-based CO_2 capture technology development from the beginning of 2013—A Review, ACS Appl. Mater. Inter. 7(4) (2015) 2137-2148.

[16] S. Kim, H. Shi and J.Y. Lee, CO_2 absorption mechanism in amine solvents and enhancement of CO_2 capture capability in blended amine solvent, Int. J. Greenh. Gas Con. 45 (2016) 181-188.

[17] J. Kothandaraman, A. Goeppert, M. Czaun, G.A. Olah and G.K. Surya Prakash, CO_2 capture by amines in aqueous media and its subsequent conversion to formate with reusable ruthenium and iron catalysts, Green Chem. 18 (2016) 5831-5838.

[18] C.H. Yu, C.H. Huang and C.S. Tan, A review of CO_2 capture by absorption and adsorption, Aerosol Air Qual. Res. 12 (2012) 745–769.

[19] P.A. Webley, Adsorption technology for CO_2 separation and capture: a perspective, Adsorption. 20 (2014) 225-231.

[20] G. Xu, F. Liang, Y. Yang, Y. Hu, K. Zhang and W. Liu, An improved CO_2 separation and purification system based on cryogenic separation and distillation theory, Energies. 7 (2014) 3484-3502.

[21] A.M. Yousef, W.M. El-Maghlany, Y.A. Eldrainy and A. Attia, New approach for biogas purification using cryogenic separation and distillation process for CO_2 capture, Energy. 156 (2018) 328-351.

[22] V. Abetz, T. Brinkmann, M. Dijkstra, K. Ebert, D. Fritsch and K. Ohlrogge, D. Paul, K.V. Peinemann, S. Pereira Nunes, N. Scharnagl and M. Schossig, Developments in membrane research: from material via process design to industrial application, Adv. Eng. Mater. 8 (2006) 328-358.

[23] http://synderfiltration.com/learning-center/articles/introduction-to membranes/membrane-materials-organic-inorganic/

[24] S. Kenarsari, D. Yang, G. Jiang, S. Zhang, J. Wang, A. Russell, Q. Wei and M. Fan, Review of recent advances in carbon dioxide separation and capture, RSC Adv. 3 (2013) 22739-22773.

[25] Y. Cai, Z. Wang, C. Yi, Y. Bai, J. Wang and S. Wang, Gas transport property of polyallylamine–poly (vinyl alcohol)/polysulfone composite membranes, J. Membr. Sci. 310 (2008) 184.

[26] J. Campbell, G. Szekely, R.P. Davies, D. Braddock and A.G. Livingston, Fabrication of hybrid polymer/metal organic framework membranes: mixed matrix membranes versus in situ growth, J. Mater. Chem. A. 2 (2014) 9260-9271.

[27] Y. Zhang, J. Sunarso, S. Liu and R. Wang, Current status and development of membranes for CO_2/CH_4 separation: A review, Int. J. Greenh. Gas Con. 12(2013) 84–107.

[28] Y. Zhao and W.S.W. Ho, Steric hindrance effect on amine demonstrated in solid polymer membranes for CO_2 transport, J. Membr. Sci. 415–416 (2012) 132–138.

[29] T.S. Chung, L.Y. Jiang, Y. Li and S. Kulprathipanja, Mixed matrix membranes (MMMs) comprising organic polymers with dispersed inorganic fillers for gas separation, Prog. Polym. Sci. 32 (2007) 483–507.

[30] N. Widjojo, Y. Li, L. Jiang and T.S. Chung, Recent progress and challenges on mixed matrix membranes in both material and configuration aspects for gas separation, In book: Advanced Materials for Membrane Preparation. 19 (2012) 64-82.

[31] N. Bryan, E. Lasseuguette, M.V. Dalen, N. Permogorov, A. Amieiro, S. Brandani and M.C. Ferrari, Development of mixed matrix membranes containing zeolites for post-combustion carbon capture, Energy Procedia. 63 (2014) 160-166.

[32] X. Wu, Z. Tian, S. Wang, D. Peng, L. Yang, Y. Wu, Q. Xin, H. Wu and Z. Jiang, Mixed matrix membranes comprising polymers of intrinsic microporosity and covalent organic framework for gas separation, J. Membr. Sci. 528 (2017) 273-283.

[33] J.K. Adewole, A.L. Ahmad, S. Ismail and C.P. Leo, Current challenges in membrane separation of CO_2 from natural gas: A review, Int. J. Greenh. Gas. Con. 17 (2013) 46−65.

[34] M. Barooah and B. Mandal, Enhanced CO_2 separation performance by PVA/PEG/silica mixed matrix membrane, J. Appl. Polym. Sci. 46481 (2018) 1-12.

[35] M. Wang, Z. Wang, S. Zhao, J. Wang and S. Wang, Recent advances on mixed matrix membranes for CO_2 separation, Chin. J. Chem. Eng. 25(11) (2017) 1581-1597.

[36] M.M. Khan, V. Filiz, G. Bengtson, S. Shishatskiy, M. Rahman and V. Abetz, Functionalized carbon nanotubes mixed matrix membranes of polymers of intrinsic microporosity for gas separation, Nanoscale Res. Lett. 7 (2012) 504.

[37] G. Dong, H. Li and V. Chen, Challenges and opportunities for mixed-matrix membranes for gas separation, J. Mater. Chem. A. 1 (2013) 4610–4630.

[38] C.I. Chaidou, G. Pantoleontos, D.E. Koutsonikolas, S.P. Kaldis and G.P. Sakellaropoulos, Gas separation properties of polyimide-zeolite mixed matrix membranes, Sep. Sci. Technol. 47 (2012) 950–962.

[39] M. Hussain and A. Konig, Mixed matrix membrane for gas separation: polydimethylsiloxane filled with zeolite, Chem. Eng. Technol. 35 (2012) 561–569.

[40] M.G. Süer, N. Baç and L. Yilmaz, Gas permeation characteristics of polymer-zeolite mixed matrix membranes, J. Membr. Sci. 91 (1994) 77–86.

[41] D.Q. Vu, W.J. Koros and S.J. Miller, Mixed matrix membranes using carbon molecular sieves: I. Preparation and experimental results, J. Membr. Sci. 211 (2003) 311–334.

[42] D. Qadir, H. Mukhtar and L.K. Keong, Synthesis and characterization of polyethersulfone/carbon molecular sieve based mixed matrix membranes for water treatment application, Procedia Engg. 148 (2016) 588 – 593.

[43] M. Anson, J. Marchese, E. Garis, N. Ochoa and C. Pagliero, ABS copolymer-activated carbon mixed matrix membranes for CO_2/CH_4 separation, J. Memb. Sci. 243 (2004) 19–28.

[44] N.H. Khdary and M.E. Abdelsalam, Polymer-silica nanocomposite membranes for CO_2 capturing, Arabian. J. Chem. (2017).

[45] S. Kim, E. Marand, J. Ida and V.V. Guliants, Polysulfone and mesoporous molecular sieve MCM-48 mixed matrix membranes for gas separation, Chem. Mater. 18(5) (2006) 1149–1155.

[46] S.M. Sanip, A.F. Ismail, P.S. Goh, M.N.A. Norrdin, T. Soga, M. Tanemura and H. Yasuhiko, Carbon nanotubes based mixed matrix membrane for gas separation, Adv. Mater. Res. 364 (2012) 272-277.

[47] T.H. Weng, H.H. Tseng and M.Y. Wey, Preparation and characterization of multi-walled carbon nanotube/PBNPI nanocomposite membrane for H_2/CH_4 separation, Int. J. Hydr. Energy. 34 (2009) 8707-8715.

[48] H. Furukawa, N. Ko, Y.B. Go, N. Aratani, S.B. Choi, E. Choi, A.O. Yazaydin, R. Q. Snurr, M. O'Keeffe, J. Kim and O. M. Yaghi, Ultrahigh porosity in metal-organic frameworks, Science. 329 (2010) 424-428.

[49] H. Furukawa, K.E. Cordova, M. O'Keeffe and O.M. Yaghi, The chemistry and applications of metal-organic frameworks, Science. 341 (2013).

[50] S. Kitagawa, R. Kitaura and S.I. Noro, Functional porous coordination polymers, Angew. Chem. 43 (2004) 2334-2375.

[51] K.S. Park, Z. Ni, A.P. Cote, J.Y. Choi, R. Huang, F.J. Uribe-Romo, H.K. Chae, M. O'Keeffe and O.M. Yaghi, Exceptional chemical and thermal stability of zeolitic imidazolate frameworks, Proc. Natl. Acad. Sci. U. S. A. 103 (2006) 10186-10191.

[52] S. Basu, A. Cano-Odena and I.F.J. Vankelecom, Asymmetric matrimid®/$[Cu_3(BTC)_2]$ mixed-matrix membranes for gas separations, J. Membr. Sci. 362 (2010) 478–487.

[53] E.V. Perez, K.J. Balkus Jr, J.P. Ferraris and I.H. Musselman, Mixed-matrix membranes containing MOF-5 for gas separations, J. Membr. Sci. 328 (2009) 165–173.

[54] T. Yang, Y. Xiao and T.S. Chung, Poly-/metal-benzimidazole nano-composite membranes for hydrogen purification, Energy Environ. Sci. 4 (2011) 4171–4180.

[55] M.J.C. Ordonez, K.J. Balkus Jr, J.P. Ferraris and I.H. Musselman, Molecular sieving realized with ZIF-8/Matrimid® mixed-matrix membranes, J. Membr. Sci. 361 (2010) 28–37.

[56] T. Li, Y. Pan, K.-V. Peinemann and Z. Lai, Carbon dioxide selective mixed matrix composite membrane containing ZIF-7 nano-fillers, J. Membr. Sci. 425-426 (2013) 235-242.

[57] H.B. Tanh Jeazet, S. Sorribas, J.M. Roman-Marín, B. Zornoza,´ C. Tellez, J. Coronas and C. Janiak, Increased selectivity in CO_2/CH_4 separation with mixed-matrix membranes of polysulfone and mixed MOFs MIL-101 (Cr) and ZIF-8, Eur. J. Inorg. Chem. (2016) 4363−4367.

[58] J.A. Thompson, K.W. Chapman, W.J. Koros, C.W. Jones and S. Nair, Sonication-induced ostwald ripening of ZIF-8 nanoparticles and formation of ZIF-8/polymer composite membranes, Micropor. Mesopor. Mater. 158 (2012) 292-299.

[59] H. Shin, W.S. Chi, S. Bae, J.H. Kim and J. Kim, High-performance thin PVC-POEM/ZIF-8 mixed matrix membranes on alumina supports for CO_2/CH_4 separation, J. Ind. Eng. Chem. 53 (2017) 127-133

[60] H. Cong, M. Radosz, B. Towler and Y. Shen, Polymer–inorganic nanocomposite membranes for gas separation, Sep. Purif. Technol. 55 (2007) 281-291.

[61] I. Genné, S. Kuypers and R. Leysen, Effect of the addition of ZrO_2 to polysulfone based UF membranes, J. Membr. Sci. 113 (1996) 343–350.

[62] N.M. Wara, L.F. Francis and B.V. Velamakanni, Addition of alumina to cellulose acetate membranes, J. Membr. Sci. 104 (1995) 43–49.

[63] H. Liu, Synthesis of TiO_2 nanopowder enwrapped by organic membrane with microwave induced plasma method, Huaxue Tongbao. 10 (1997) 44-46.

[64] A. Doucouré, C. Guizard, J. Durand, R. Berjoan and L. Cot, Plasma polymerization of fluorinated monomers on mesoporous silica membranes and application to gas permeation, J. Membr. Sci. 117 (1996) 143–150.

[65] N.P. Patel, A.C. Miller and R.J. Spontak, Highly CO_2-permeable and selective polymer nanocomposite membranes, Adv. Mater. 15 (2003) 729–733.

[66] N.P. Patel, C.M. Aberg, A.M. Sanchez, M.D. Capracotta, J.D. Martin and R.J. Spontak, Morphological, mechanical and gas-transport characteristics of

crosslinked poly (propylene glycol): Homopolymers, nanocomposites and blends, Polymer. 45 (2004) 5941-5950.

[67] S.P. Nunes, K.V. Peinemann, K. Ohlrogge and A. Alpers, Membranes of poly (ether imide) and nanodispersed silica, J. Membr. Sci. 157 (1999) 219–226.

[68] M. Iwata, T. Adachi, M. Tomidokoro, M. Ohta and T. Kobayashi, Hybrid sol-gel membranes of polyacrylonitrile-tetraethoxysilane composites for gas permselectivity, J. Appl. Polym. Sci. 88 (2003) 1752–1759.

[69] D. Gomes, S.P. Nunes and K.V. Peinemann, Membranes for gas separation based on poly (1-trimethylsilyl-1-propyne)-silica nanocomposites, J. Membr. Sci. 246 (2005) 13-25.

[70] H. Rabiee, S. Meshkat Alsadat, M. Soltanieh, S.A. Mousavi and A. Ghadimi, Gas permeation and sorption properties of poly(amide-12-b-ethyleneoxide) (Pebax1074)/SAPO-34 mixed matrix membrane for CO_2/CH_4 and CO_2/N_2 separation, J. Ind. Eng. Chem. 27 (2015) 223–239.

[71] M.W. Anjum, F. de Clippel, J. Didden, A.L. Khan, S. Couck, G.V. Baron, J.F.M. Denayer, B.F. Sels, and I.F.J. Vankelecom, Polyimide mixed matrix membranes for CO_2 separations using carbon-silica nanocomposite fillers, J. Membr. Sci. 495 (2015) 121–129.

[72] G.L. Zhuang, H.H. Tseng and M.Y. Wey, Preparation of PPO-silica mixed matrix membranes by in-situ sol-gel method for H_2/CO_2 separation, Int. J. Hydr. Energy. 39 (2014) 17178–17190.

[73] B. Yu, H. Cong and X. Zhao, Hybrid brominated sulfonated poly (2, 6-diphenyl-1,4-phenylene oxide) and SiO_2 nanocomposite membranes for CO_2/N_2 separation, Pro. Nat. Sci-Mater. 22(6) (2012) 661-667.

[74] H. Wu, X. Li, Y. Li, S. Wang, R. Guo, Z. Jiang, C. Wu, Q. Xin and X. Lu, Facilitated transport mixed matrix membranes incorporated with amine functionalized MCM-41 for enhanced gas separation properties, J. Membr. Sci. 465 (2014) 78–90.

[75] S. Belhaj Messaoud, A. Takagaki, T. Sugawara, R. Kikuchi and S.T. Oyama, Mixed matrix membranes using SAPO-34/polyetherimide for carbon dioxide/methane separation, Sep. Purif. Technol. 148 (2015) 38–48.

[76] Q. Xin, H. Wu, Z. Jiang, Y. Li, S. Wang, Q. Li, X. Li, X. Lu, X. Cao and J. Yang, SPEEK/amine-functionalized TiO_2 submicrospheres mixed matrix membranes for CO_2 separation, J. Membr. Sci. 467 (2014) 23–35.

[77] M. Barooah and B. Mandal, Synthesis, characterization and CO_2 separation performance of novel PVA/PG/ZIF-8 mixed matrix membrane, J. Membr. Sci. 572 (2019) 198-209.

[78] H. Gong, T.H. Nguyen, R. Wang and T.H. Bae, Separations of binary mixtures of CO_2/CH_4 and CO_2/N_2 with mixed-matrix membranes containing $Zn(pyrz)_2/(SiF_6)$ metal-organic framework, J. Membr. Sci. 495 (2015) 169–175.

[79] Q. Xin, T. Liu, Z. Li, S. Wang, Y. Li, Z. Li, J. Ouyang, Z. Jiang and H. Wu, Mixed matrix membranes composed of sulfonated poly (ether ether ketone) and a sulfonated metal-organic framework for gas separation, J. Membr. Sci. 488 (2015) 67–78.

[80] E.A. Feijani, H. Mahdavi and A. Tavasoli, Poly (vinylidene fluoride) based mixed matrix membranes comprising metal organic frameworks for gas separation applications, Chem. Eng. Res. Des. 96(2015) 87-102.

CHAPTER 2

CO_2 Separation by Reactive Polymer Membrane: CO_2-Amine Reaction by Zwitterionic Mechanism

CHAPTER 2

CO_2 Separation by Reactive Polymer Membrane: CO_2-Amine Reaction by Zwitterionic Mechanism

This chapter presents detailed study on the fundamental gas transport mechanisms and the formation of CO_2-amine complex and zwitterionic mechanism. Special focus has been given on the CO_2-amine reaction mechanism involving facilitated transport of CO_2 through the thin-film dense polymer membrane.

2.1. Fundamental gas transport mechanism in membrane

The various gas transport mechanisms for porous and non-porous membrane material can be classified into Knudsen diffusion, surface diffusion, capillary condensation, molecular sieving diffusion, and solution-diffusion mechanism [1, 2].

2.1.1. Gas transport mechanism in porous membrane

The gas transport mechanism in porous membrane occurs by Knudsen diffusion, surface diffusion, capillary condensation and molecular sieving mechanism.

2.1.1.1. Knudsen diffusion

In Knudsen diffusion, the diffusing molecules is more likely to collide with the pore wall than with other penetrant species and is best suited for pore sizes < 50 nm. The pore diameter of the gas molecule is smaller than the mean free path of the diffusing gas molecules. In the time interval between intermolecular collisions many molecule-wall collision occur and the molecules are in thermal equilibrium with the wall.

2.1.1.2. Surface diffusion

In surface diffusion mechanism, at sufficient low temperature and/or high pressure, the molecules adsorb on the surface of the pores and subsequently hop from one site to adjacent empty site by overcoming the energy barrier. The extent of surface diffusion is

determined by the mobility of the molecules and its adsorption capacity.

2.1.1.3. Capillary condensation

Capillary condensation occurs when the condensed liquid from the vapour fills on the pore spaces of the porous medium thus influencing the diffusion rate across the membrane [3]. When the pore size is small enough, the penetrants wet the pore surface sufficiently thereby creating multiple molecular layers of the adsorbed penetrant.

2.1.1.4. Molecular sieving mechanism

In molecular sieving mechanism, the gas molecules are separated based on the size exclusivity. The pore diameters of the sieves should be in the range of the gas molecules to be separated to work as molecular sieve membranes. If the membrane has pore size wherein it allows the smaller gas molecules to pass through and blocking the larger gas molecules from penetrating, a high gas separation would be achieved.

2.1.2. Gas transport in non-porous membrane

The gas transport in non-porous dense membrane occurs by either solution-diffusion or facilitated transport mechanism.

2.1.2.1. Solution-diffusion mechanism

The gas transport by "solution-diffusion mechanism" was first proposed by Thomas Graham in 1866, wherein the permeation process involved the dissolution of penetrant followed by transmission of the dissolved species through the membrane [4]. However, Fick [5] proposed the law of mass diffusion by drawing analogy from the Fourier's law of heat conduction. As per Fick, the solution-diffusion mechanism basically follows three steps: (1) adsorption of the permeate at upstream membrane side, (2) diffusion

through membrane under concentration gradient, and (3) desorption at the downstream membrane side. The slowest molecular diffusion is considered to be the rate-determining step in permeation. The penetrant flux (J) can be represented as:

$$J = -D\frac{dC}{dx} \tag{2.1}$$

where, D is the diffusion coefficient, dC/dx is the concentration gradient across the membrane. Under steady-state conditions, this equation can be represented by:

$$J_i = D_i\frac{(C_f - C_p)}{L} \tag{2.2}$$

Where, C_f and C_p are the concentration in the feed side and permeate side of the membrane and L is the membrane thickness.

Stefan and Exner [6] in the late 1870's concluded that gas permeation through soap membrane was proportional to the product of solubility coefficient (S) and diffusion coefficient (D). Later, Wroblewski [7] showed that under steady-state conditions, the diffusion and solubility coefficients are independent of concentration. The permeability coefficient *(P)* which determines the permeation capability of the membrane is defined as the product of solubility coefficient and diffusion coefficient:

$$P=D.S \tag{2.3}$$

The gas transport by polymeric material and its ability to separate a mixture is determined by its selectivity. In a binary mixture, the selectivity also termed as separation factor is determined as the ratio of their permeability coefficient [8, 9].

$$\alpha_{i/j} = \frac{P_i}{P_j} = \left(\frac{D_i}{D_j}\right) \times \left(\frac{S_i}{S_j}\right) \tag{2.4}$$

where $\alpha_{i/j}$ is the ideal selectivity.

2.1.2.2. Facilitated transport mechanism

To utilize the membrane technology as alternative to conventional technologies, membranes should have high selectivities along with high permeability. To serve this purpose, transport mechanism by reversible complexation reaction commonly termed as facilitated transport mechanism is included along with the solubility and diffusivity mechanism. The carrier molecule which is either fixed or mobile reacts with CO_2 molecule through a selective reversible chemical reaction.

2.2. Reactive polymer membrane

Reactive polymer membrane for CO_2 separation involves use of amines as carrier that reacts rapidly, selectively and reversibly with CO_2. The amines can be classified as primary, secondary and tertiary amines based on the number of carbon containing groups attached to the nitrogen atom. Based on the structure, amines can be further classified as sterically hindered and sterically unhindered amine. A sterically hindered amine is a primary amine in which the amino-group is fixed to tertiary carbon atom or a secondary amine in which the amino-group is fixed to at least one secondary or tertiary carbon atom [10, 11]. Some of the amines which have been industrially utilized include monoethanolamine (MEA), diethanolamine (DEA), triethylenetetramine (TETA), tetraethylenepentamine (TEPA), pentaethylenehexamine (PEHA). Figure 2.1 shows the schematic representation of gas transport by reactive polymer membranes. The principle reaction mechanism when amine solutions are used to absorb the CO_2 may be represented by the zwitterionic mechanism as explained.

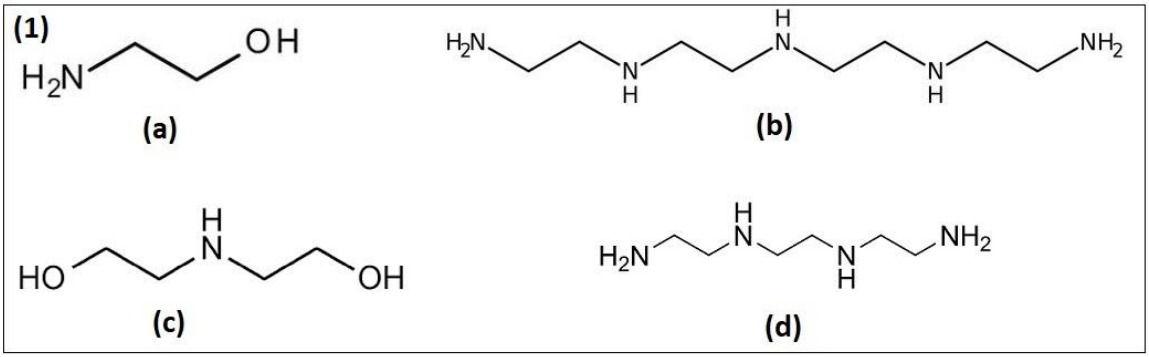

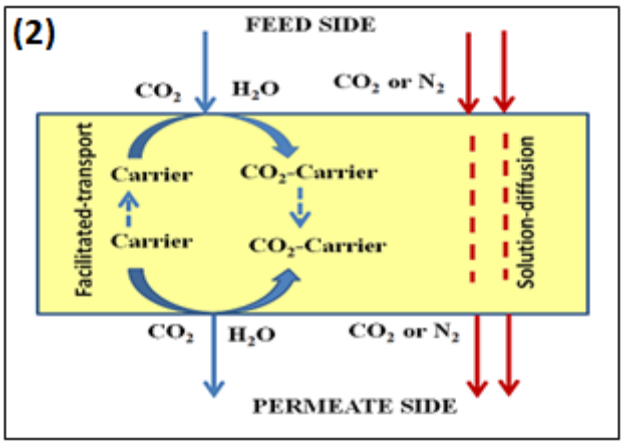

Figure 2.1 (1) Chemical structure of (a) MEA, (b) TEPA, (c) DEA and (d) TETA amine, (2) Schematic representation of gas transport by reactive polymer membrane.

2.2.1. Zwitterionic mechanism

As proposed by Caplow [12] and Danckwerts [13], zwitterionic mechanism is one of the popular two-step mechanism for CO_2-amine reaction in which the zwitterion is formed as an intermediate. The CO_2-amine reaction can be classified as a two-step reaction: CO_2 first reacts with alkanolamine to form zwitterion which is then transferred to the second molecule. The second molecule which is a base can be amine, (OH^-) ion or H_2O. However, Versteeg and van Swaaij [14] established that the deprotonation reaction with (OH^-) ion as base is insignificant as compared to amine and water molecules. This base then deprotonates the zwitterion by base catalyzed to form carbamate ion. The CO_2 reacts in aqueous amine solution to form either bicarbonate or carbamates. The amine carrier reversibly and rapidly reacts with CO_2 molecules thereby promoting facilitated

transport mechanism. According to this mechanism, reaction between CO_2 and the amine leads to the formation of a zwitterion as shown by Equation (R2.1):

$$CO_2 + RR'NH \rightleftharpoons RR'NH^+COO^- \quad \text{(R2.1)}$$

Where, RR'NH represents a primary or secondary amine and $RR'NH^+COO^-$ represents the zwitterion. This zwitterion is further deprotonated by base, b, in the next step to form carbamate ion as follows:

$$RR'NH^+COO^- + b \rightleftharpoons RR'NCOO^- + bH^+ \quad \text{(R2.2)}$$

Where, $RR'NCOO^-$ is the carbamate ion. If the base, b, in the reaction described by Equation (R2.2) is the amine itself, the carbamate formation can be represented as:

$$RR'NH^+COO^- + RR'NH \rightleftharpoons RR'NCOO^- + RR'NH_2^+ \quad \text{(R2.3)}$$

By considering Equation (R2.1) and (R2.3), the overall reaction can be represented as:

$$CO_2 + 2RR'NH \rightleftharpoons RR'NCOO^- + RR'NH_2^+ \quad \text{(R2.4)}$$

Where $RR'NH_2^+$ is the protonated amine. If the amine is sterically hindered, the zwitterion reacts with water and amine more readily to form bicarbonate ion:

$$RR'NH^+COO^- + H_2O \rightleftharpoons HCO_3^- + RR'NH_2^+ \quad \text{(R2.5)}$$

In this case, the overall reaction can be represented by considering Equation (R2.1) and (R2.5) as:

$$CO_2 + RR'NH + H_2O \rightleftharpoons HCO^-_3 + RR'NH^+_2 \quad \text{(R2.6)}$$

The carbamate ion of the sterically hindered amine is unstable and readily undergoes hydrolysis to form bicarbonates and release free amine molecules:

$$RR'NCOO^- + H_2O \rightleftharpoons HCO_3^- + RR'NH \quad \text{(R2.7)}$$

These free amine molecules can again react with CO_2. From the above equation it can be inferred that in case of sterically hindered amines, large amount of bicarbonate ion is formed compared to carbamate ions.

2.2.2. Base catalysis mechanism

As explained by Donaldson and Nguyen [15], tertiary amines (RR'R"N) do not react directly with CO_2 and usually accelerate the hydration reaction of CO_2. The kinetics does not vary too much and is considered to be a first-order reaction with respect to amine concentration. The equation can be represented as:

$$CO_2 + RR'R''N + H_2O \rightleftharpoons RR'R''NH^+ + HCO_3^- \quad \text{(R2.8)}$$

2.2.3. Termolecular mechanism

The termolecular mechanism was proposed by Crooks and Donnellan [16] whereby one molecule of amine react simultaneously with one molecule of CO_2 and one molecule of base (b). The reaction takes place in a single step whereby an amine is bonding with CO_2 and simultaneously proton transfer takes place via loosely-bound encounter complex as the intermediate:

$$CO_2 + RR' \cdots b \rightleftharpoons RR'NCOO^- \cdots bH^+ \quad \text{(R2.9)}$$

This complex further dissociates to form reactant molecules (CO_2 and amine).

2.2.4. Aqueous solution chemistry

The water effect on the CO_2-amine reaction plays a great importance. The water dissociation reaction can be represented by:

$$H_2O \rightleftharpoons H^+ + OH^- \quad \text{(R2.10)}$$

In aqueous solution, CO_2 reacts with water or its dissociated product like H^+ ion or OH^- ion as follows:

$$CO_2 + H_2O \rightleftharpoons H_2CO_3 \quad \text{(R2.11)}$$

$$CO_2 + OH^- \rightleftharpoons HCO_3^- \quad \text{(R2.12)}$$

$$HCO_3^- + OH^- \rightleftharpoons CO_3^{2-} + H_2O \quad \text{(R2.13)}$$

$$HCO_3^- + H_3O^+ \rightleftharpoons H_2CO_3 + H_2O \quad \text{(R2.14)}$$

References

[1] R. Datta, S. Dechapanichkul, J.S. Kim, L.Y. Fang and H. Uehara, A generalized model for the transport of gases in porous, non-porous, and leaky membranes. I. Application to single gases, J. Membr. Sci. 75(3) (1992) 245-263.

[2] M. Wang, J. Zhao, X. Wang, A. Liu and K.K. Gleason, Recent progress on submicron gas-selective polymeric membranes, J. Mater. Chem. A. 5 (2017) 8860-8886.

[3] U. Eickmann and U. Werner, Porous membranes in gas separation technology, Membranes and Membrane Processes. (1986) 327-334.

[4] G.S. Park, Transport principles—solution, diffusion and permeation in polymer membranes, Synthetic membranes: Science, Engineering and Applications. 181 (1986) 57-107.

[5] A. Paul, T. Laurila, V. Vuorinen and S.V. Divinski, Chapter from book thermodynamics, diffusion and the kirkendall effect in solids, 115-139.

[6] M. Askari, M.L. Chua and T.S. Chung, Permeability, solubility, diffusivity, and PALS data of cross-linkable 6FDA-based copolyimides, Ind. Eng. Chem. Res. 53(6) (2014) 2449-2460.

[7] L.M. Robeson, Z.P. Smith, B.D. Freeman and D.R. Paul, Contributions of diffusion and solubility selectivity to the upper bound analysis for glassy gas separation membranes, J. Membr. Sci. 453 (2014) 71-83.

[8] M.M. Khan, V. Filiz, G. Bengtson, S. Shishatskiy, M. Rahman and V. Abetz, Functionalized carbon nanotubes mixed matrix membranes of polymers of intrinsic microporosity for gas separation, Nanoscale Res. Lett. 7 (2012) 504.

[9] G. Dong, H. Li and V. Chen, Challenges and opportunities for mixed-matrix membranes for gas separation, J. Mater. Chem. A. 1 (2013) 4610–4630.

[10] C.I. Chaidou, G. Pantoleontos, D.E. Koutsonikolas, S.P. Kaldis and G.P. Sakellaropoulos, Gas separation properties of polyimide-zeolite mixed matrix membranes, Sep. Sci. Technol. 47 (2012) 950–962.

[11] M. Hussain and A. Konig, Mixed matrix membrane for gas separation: polydimethylsiloxane filled with zeolite, Chem. Eng. Technol. 35 (2012) 561–569.

[12] M. Caplow, Kinetics of carbamate formation and breakdown, J. Am. Chem. Soc. 90 (1968) 6795-6803.

[13] P.V. Danckwerts, The reaction of CO_2 with ethanolamines, Chem. Eng. Sci. 34 (1979) 443-446.

[14] G.F. Versteeg and W.P.M. Van Swaaij, On the kinetics between CO_2 and alkanolamines both in aqueous and non-aqueous solution-II. tertiary amines, Chem. Eng. Sci. 43 (1988) 587-591.

[15] T.L. Donaldson and Y.N. Nguyen, Carbon dioxide reaction kinetics and transport in aqueous amine membranes, Ind. Eng. Chem. Fundam. 19 (1980) 260-266.

[16] J.E. Crooks and J.P. Donnellan, Kinetics and mechanism of the reaction between carbon dioxide and amines in aqueous solution, J. Chem. Soc. Perkin Trans. 2: Phy. Org. Chem. 4 (1989) 331-333.

CHAPTER 3

Synthesis and Characterization of Novel PVA/PEG and PVA/PEG/Silica Membrane for CO_2/N_2 Separation

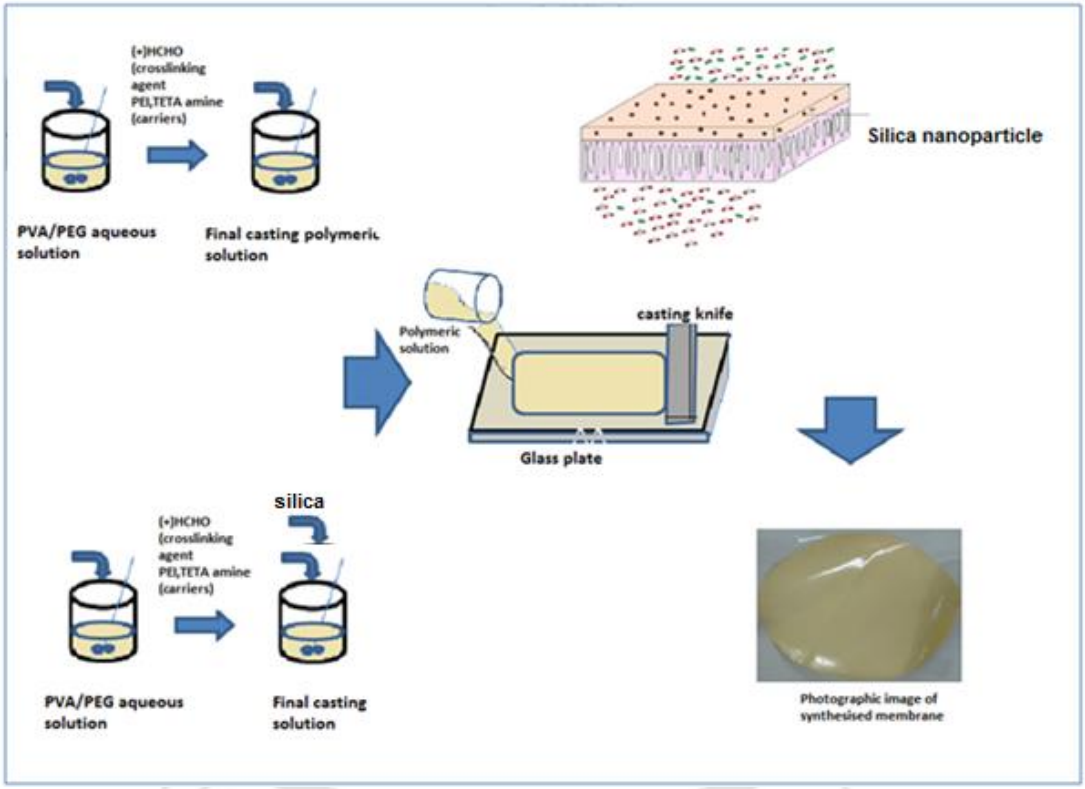

Graphical Abstract of PVA/PEG and PVA/PEG/Silica mixed matrix membrane formation

CHAPTER 3

Synthesis and Characterization of Novel PVA/PEG and PVA/PEG/Silica Membrane for CO_2/N_2 Separation

This chapter focuses on development of novel CO_2-selective membrane by embedding silica nanoparticle as filler material into the poly (vinyl alcohol) (PVA)/polyethylene glycol (PEG) matrix using solution casting methodology. In situ sol-gel technique was applied for the synthesis of hydrophilic SiO_2 nanoparticles. The close interaction between the silanol groups in the surface of SiO_2 and the polymer matrix is envisioned to increase the compatibility between the polymer-particle phase. This in turn augments the mechanical strength and separation performance of the membrane. Detailed characterization studies of the synthesised membrane were conducted. The comparative performance study of the facilitated transport polymeric membrane (PVA/PEG) and facilitated transport mixed matrix membrane (PVA/PEG/Silica) for similar temperature and sweep water flow rate variation were analysed. This work is scientifically acknowledged in the journal, ***"Journal of Applied Polymer Science".***

3.1. Introduction

The performance of polymer membrane at high temperature can be improved by polymer blending, use of cross-linking agent and mixed matrix membrane formation [1]. Mixed matrix membrane (MMM) combining the advantages of both polymeric and inorganic membranes is a highly desirable strategy to achieve high CO_2 performance [2, 3]. The common fillers used in MMM involve zeolites, activated carbon, carbon molecular sieves (CMS) and nano-sized particles. Among them, silica is considered as an attractive inorganic filler involving easy fabrication techniques, low synthesis cost and high resistance to swelling making it highly desirable for MMM application for gas separation [4-10]. The silica nanoparticles have varied industrial application such as improvement of the properties in cementitious materials [11], field of catalysis [12], drug delivery [13], chemical sensors [14], chromatography [15, 16] and liquid/gas separation applications [17, 18]. The various methods for preparation of silica nanoparticles consist of plasma synthesis [19, 20], chemical vapour deposition [21], micro emulsion

processing [22], combustion- synthesis [23], sol-gel processing [24, 25], hydrothermal techniques [26], etc. The sol-gel technique for silica preparation have been considered in this study due to its advantages of low processing condition (temperature and pressure) and dispersion of the silica nanoparticles at molecular level into the polymer matrix [27]. Poly (vinyl alcohol) (PVA), a biodegradable and water soluble polymer is environmental friendly and has excellent properties of high film forming ability, strong compatibility with amines, high thermal and chemical stability [28]. It is used as base polymer for the preparation of gas separation membrane. Formaldehyde (HCHO) is utilized as the cross-linking agent. Polyethylene glycol (PEG) is used as the polymer blend owing to the presence of polar ether groups in its chain. The polar ether (PEO) segment in PEG co-ordinates efficiently with the polar CO_2 molecule thereby increasing the membrane stability and CO_2 separation performance (CO_2 permeance and CO_2/N_2 selectivity). However, PEG when used alone results in very high crystallinity leading to reduction in the gas permeability and hence not preferred [29].

The silica/PVA hybrid material synthesized through sol-gel process depicted enhancement in the structural, thermal mechanical characteristics than pure PVA [30-32]. The silica nanoparticles incorporated into PVA/PEG matrix is envisioned to enhance the interaction between the hydroxyl group of PVA matrix and silanol groups present in the surface of SiO_2 nanomaterial. This might lead to increased compatibility between the two phases thus improving the overall mechanical strength and CO_2 transport performance [33]. Taking the above factors into consideration, the amalgamation of the film forming ability of PVA/PEG blend along with PEI and TETA as amine carrier and silica as filler material combined into a simple process could thus pave the way for efficient CO_2 separation. This work thus involves the detailed comparative CO_2 separation performance study of facilitated transport polymeric membrane (PVA/PEG) and facilitated transport mixed matrix membrane (PVA/PEG/Silica) at similar operating conditions. We envision that the addition of silica nanoparticle will improve the membrane properties significantly along with the CO_2 separation performance thereby providing a novel route of membrane preparation for large-scale carbon capture studies.

3.2. Materials

Poly (vinyl alcohol) (M_w = 130,000), polyethylene glycol (M_n = 6000), polyethyleneimine (PEI) (M_w = 25,000), and triethylenetetramine (TETA) (M_w = 146.08) were obtained from Sigma-Aldrich, USA. Pure ethanol (99 % purity), formaldehyde solution, potassium hydroxide (KOH), hydrochloric acid (HCl), tetraethylorthosilicate (TEOS) were acquired from Merck, India. Microporous polytetrafluoroethylene substrate with thickness ~150 μm (pore size ~ 0.03 μm) was purchased from Sterlitech USA. The gas cylinders: binary mixed gas (20 % CO_2 and 80 % N_2), Argon (Ar) and Helium (He) used for GC analysis was obtained from Vadilal Pvt. Ltd., India. The molecular structure of the materials used has been depicted in Figure 3.1.

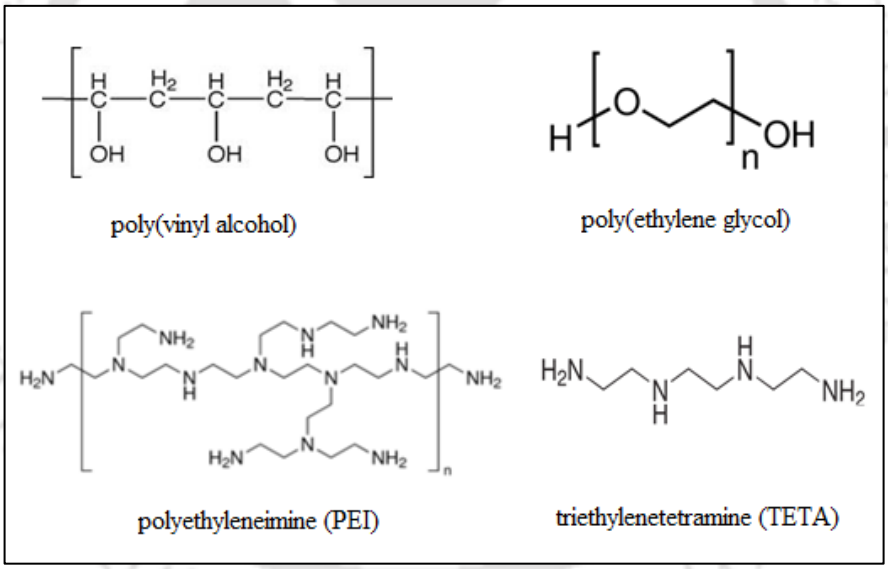

Figure 3.1 Molecular structure of materials used

3.3. Experimental

3.3.1. Synthesis of crosslinked PVA-PEG membrane

Active layer of thin-film-composite membrane was cast on the porous polytetrafluoroethylene support by solution casting methodology. Firstly, PVA polymer hydrogel was synthesized by using formaldehyde as crosslinking agent. The degree of cross-linking was fixed at 60 mol % as already optimized [34]. Secondly, crosslinked-PVA polymer hydrogel was blended with polyethylene glycol (PEG) at different PVA/PEG ratio keeping the concentration of KOH constant (10 wt %). The calculation of the amount considered is shown in Appendix 2. The dry compositions of the membrane considered were 72 wt % PVA + 18 wt % PEG, 60 wt % PVA + 30 wt % PEG, 45 wt % PVA + 45 wt % PEG and 30 wt % PVA + 60 wt % PEG.

PVA aqueous solution was prepared in a round bottom flask attached to reflux condenser and temperature was maintained in oil bath (continuous stirring; temperature ~90 °C). 60 mol % degree of cross-linking with formaldehyde (HCHO) and 10 wt % of potassium hydroxide (KOH) was added into the PVA aqueous solution to form PVA/HCHO/KOH solution. Calculated amount of polyethylene glycol (PEG) was added and stirred continuously until the formation of homogeneous casting solution by varying the PVA/PEG ratio. The solution was then centrifuged at 10,000 rpm for 30 mins to remove unwanted particle and air bubbles and finally cast on porous PTFE substrate fixed to a glass plate using casting knife. The membrane was then dried overnight in a laminar flow chamber (LabTech) under ambient condition followed by heating in an oven (Thermo Scientific Heratherm) at 120 °C for 10 h and finally used for characterization.

3.3.2. Synthesis of crosslinked PVA/PEG facilitated transport membrane

The PVA/PEG blend was chosen in the ratio of 1:0.25 (as discussed in section 3.5.1.1). 60 mol % degree of crosslinking with formaldehyde (HCHO) and 10 wt % of KOH was added into the PVA/PEG aqueous solution. Three different combination of polyethyleneimine (PEI) and triethylenetetramine (TETA) blend

was synthesized. 25 wt % PEI and 15 wt % TETA amine blend was considered. The final crosslinked PVA/PEG polymer membrane was prepared in a procedure already explained in section 3.3.1. The dense selective layer thickness of the final dried composite membrane was calculated to be ca. 27 µm as confirmed by FESEM analysis. The detailed calculation is shown in Appendix A2.1.

3.3.3. Synthesis of silica sol by in situ sol-gel process

Silica sol was synthesized by a method reported by Stober [43]. In brief, TEOS (precursor) and absolute ethanol (solvent) was added under ambient condition with continuous stirring. Thereafter, distilled water and 1N HCl (catalyst) was included to the solution. The pH of the solution was maintained at constant value (pH~2). The solution was stirred for ~3 h at 60 °C. Clear silica sol was obtained.

3.3.3.1. Reaction mechanism

The network formation of silica by sol-gel process is based on hydrolysis and condensation reaction as described by Equation (R3.1-R3.3). Schematic representation of hydrolysis and condensation (alcohol and water) reaction of TEOS and its subsequent possible PVA/silanol network structure formation is presented in Figure 3.2.

$$Si(OC_2H_5)_4 + xH_2O \rightarrow Si(OC_2H_5)_{4-x}(OH)_x + xC_2H_5OH \quad \text{(R3.1)}$$

$$\equiv Si\text{-}OC_2H_5 + \equiv Si\text{-}OH \xrightarrow{\text{Alcohol condensation}} \equiv Si\text{-}O\text{-}Si \equiv + C_2H_5OH \quad \text{(R3.2)}$$

$$\equiv Si\text{-}OH + \equiv Si\text{-}OH \xrightarrow{\text{Water condensation}} \equiv Si\text{-}O\text{-}Si \equiv + H_2O \quad \text{(R3.3)}$$

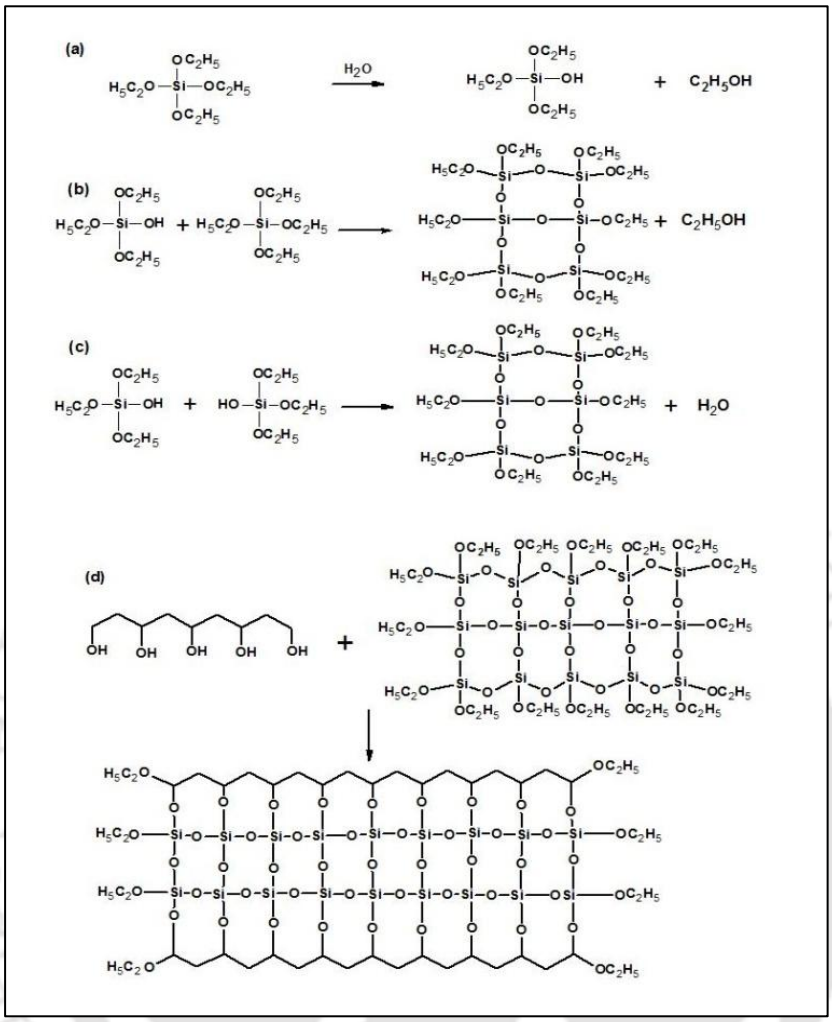

Figure 3.2 Schematic representation of hydrolysis and condensation (alcohol and water) reaction of TEOS (a,b), and PVA/silanol network structure formation (c)

3.3.4. Synthesis of crosslinked PVA/PEG/Silica mixed matrix membrane

Stoichiometric amount of HCHO, KOH, PEI and TETA was considered (as discussed in Sections 3.3.1 and 3.3.2). Thereafter, silica content with loading of 3 wt % and 6 wt % was added to form the PVA/PEG/Silica MMM. The MMM sample with silica loading of 3 wt % and 6 wt % were denoted by PVA/PEG/Sil(3) and PVA/PEG/Sil(6) respectively.

3.4. Membrane characterization

Thermogravimetric analysis (TGA) (TGA4000, Perkin-Elmer, USA) was carried out under nitrogen atmosphere, heating rate ~10 °C/min. The attenuated total reflection-fourier transform infrared spectroscopy (ATR-FTIR) (SHIMADZU, IRAffinity 1, Japan) wavenumber range (4000 to 400 cm^{-1}), 40 scans per sample and 4 cm^{-1} resolution confirmed the functional groups present in the membrane. X-ray diffraction measurement **(**Bruke D8); 2θ angles (10^{o}-60^{o}), Cu Kα radiation of wavelength λ = 1.54056 Å examined the crystallinity of the materials. The morphology and distribution of the silica nanoparticles in the synthesized membrane were investigated by FETEM and FESEM imaging. The samples were first fractured in liquid nitrogen, fixed on a stub by a carbon tape and gold coated before top surface and cross-sectional surface analysis is carried out. The surface chemical state analysis was examined by XPS spectrometer (Thermo Scientific Escalab Xi^{+}). Mono-chromated Al Kα radiation was used as the X-ray source and the results was documented by software named Avantage v5.984.

3.4.1. Gas permeation study

The mixed gas permeation experimental set-up schematic is shown in Figure 3.3. The detailed experimental protocol followed for gas permeation measurement is explained in Appendix 1. A counter-current membrane module made of stainless steel with membrane area of 51.5 cm^2 was considered. The entire module was stationed inside a thermostatic cabinet for temperature control. The CO_2/N_2 binary feed gas (20 vol % CO_2) and sweep gas (pure Argon) was fed in counter current direction in the module. The gas flow rate was controlled by mass flowmeters (Aalborg, USA). The gases were humidified by HPLC pumps (Shimadzu, Japan). The humidified gases were saturated with water vapour with a saturator installed inside the system oven. The pressure of the entire system was maintained by back pressure regulators (Swagelok, USA). The permeate and retentate gas coming out of the oven were dehumidified and the composition of the gases analysed by gas chromatograph (Varian 450 GC) having thermal conductive detector (TCD). Each condition was fixed for ~10 h until steady-state and consecutively three readings were recorded at a constant condition. The average of the readings with standard deviation represented the gas permeation data. The details

calculation procedures of CO_2 and N_2 flux, permeability and permeance along with CO_2/N_2 selectivity were discussed in appendix section (Appendix 3).

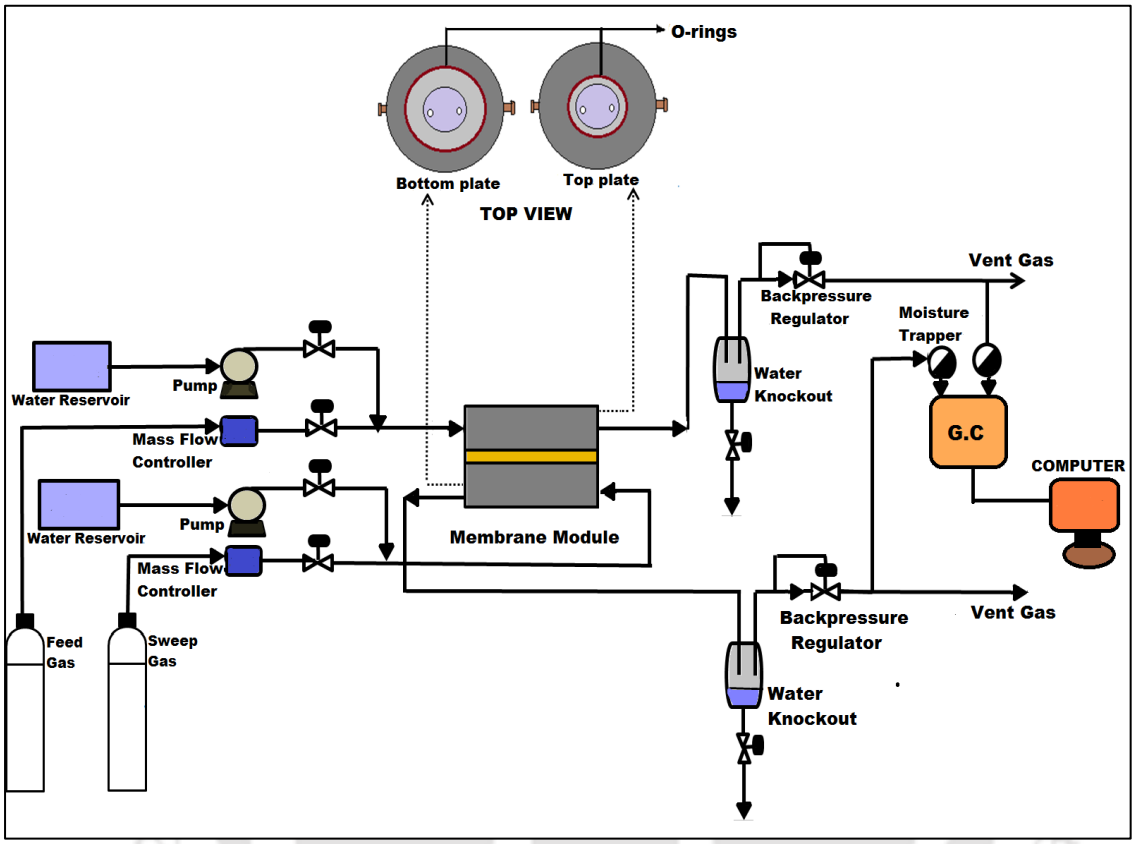

Figure 3.3 Schematic representation of gas permeation apparatus

3.5. Results and discussion

3.5.1. Thermogravimetric analysis (TGA)

3.5.1.1. TGA analysis of crosslinked PVA/PEG membrane

The thermal stabilities and weight loss regime of crosslinked-PVA-PEG blend polymers were determined by TGA curves (Figure 3.4(a)). Each TGA curve showed three weight loss regimes. The first weight loss between (30-130 ºC) is attributed to the moisture loss captured during sample preparation. The second weight loss (200-265 ºC) is associated with loss of hydroxyl groups from the polymer chain. The final weight loss between (395-510 ºC) is attributed to the polymer backbone decomposition. It was observed that PVA/PEG in the ratio 1/0.25 showed the best thermal stability.

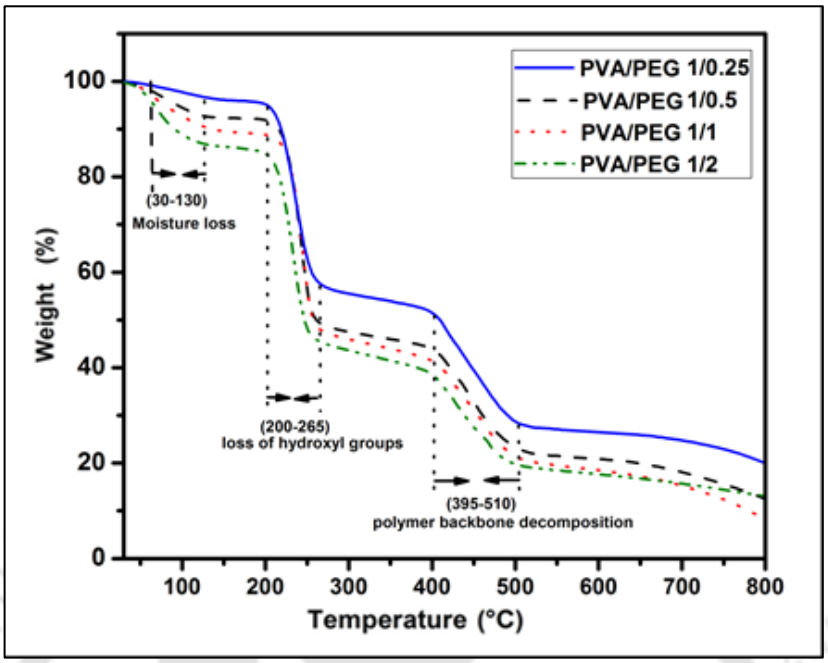

Figure 3.4 (a) TGA curve of crosslinked PVA/PEG membrane

3.5.1.2. TGA analysis of crosslinked PVA/PEG and PVA/PEG/Sil(3) membrane

The thermal stabilities and weight loss regime of crosslinked-PVA-PEG and PVA/PEG/Sil(3) membrane was determined by TGA curves (Figure 3.4(b)). Each TGA curve showed three weight loss regimes. The first weight loss between (35-150 ºC) is attributed to the moisture loss captured during sample preparation. The second weight loss (210-350 ºC) is associated with loss of hydroxyl groups from the polymer chain. The final weight loss between (450-630 ºC) is attributed to the polymer backbone decomposition. It was observed that PVA/PEG/Sil(3) membrane showed higher stability than PVA/PEG membrane.

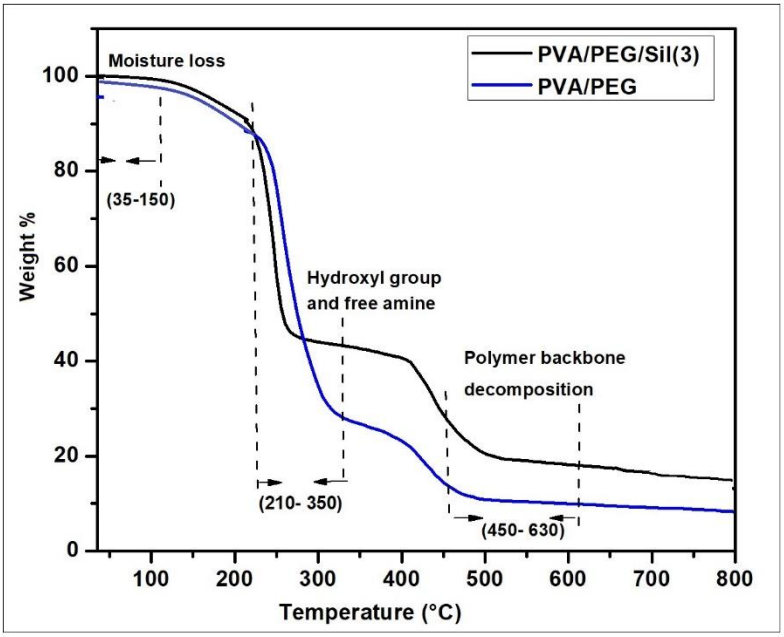

Figure 3.4 (b) TGA curve of crosslinked facilitated transport PVA/PEG and PVA/PEG/Sil(3) membrane

3.5.2. Fourier transform infrared spectroscopy analysis (FTIR)

The FTIR spectroscopy of the PVA/PEG, PVA/PEG/Sil(3), and PVA/PEG/Sil(6) membrane is shown in Figure 3.5. The broad peak ~3200 to 3400 cm^{-1} indicated the presence of hydrogen-bonded hydroxyl groups (O-H) and (N-H) groups from the amines introduced in the membrane. The sharp frequency at 2875 cm^{-1}, 1670 cm^{-1} and 1550 cm^{-1} refers to (C-H) symmetric stretching of the alkyl band, (C=C) stretching and the combination of (O-H) and (C-H) bending, respectively. The vibrational bands observed at 1450 cm^{-1} and 1320 cm^{-1} attribute to CH_2 in-plane bending and CH_2 out of plane bending [35, 36]. The peak at 1000-1110 cm^{-1} is assigned to C-O stretching vibration for PVA/PEG membrane. However, for PVA/PEG/Sil(3) and PVA/PEG/Sil(6) membrane, an increase in peak intensity at this range ascribed to the overlapping of (Si-O-C) and (Si-OH) bond affirming the presence of silica in the membrane. The peak at ~850 cm^{-1} confirmed the silanol group from silica doped membrane.

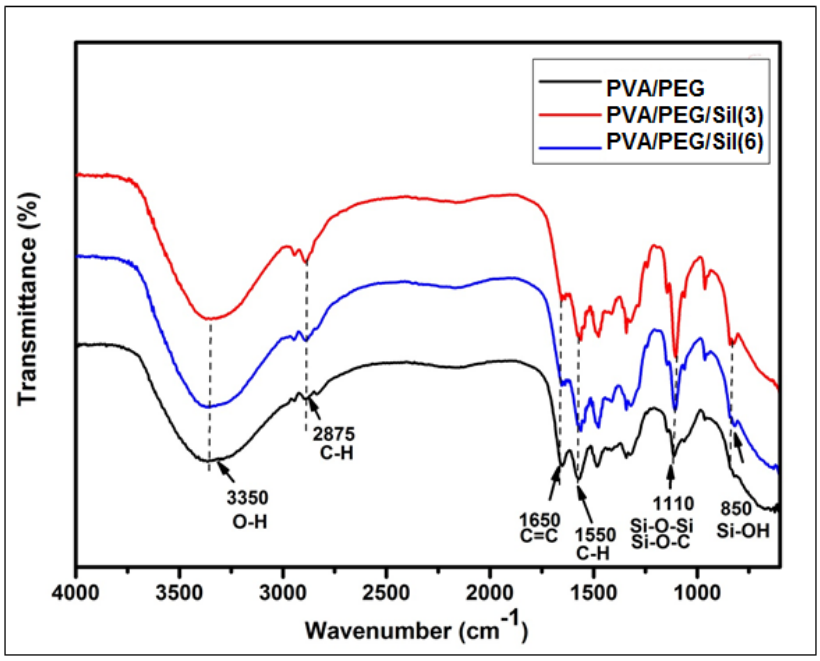

Figure 3.5 FTIR curve of crosslinked PVA/PEG, PVA/PEG/Sil(3) and PVA/PEG/Sil(6) membrane

3.5.3. X-ray diffraction analysis (XRD)

The diffraction pattern from XRD analysis confirmed (Figure 3.6) the semi-crystalline structure of PVA/PEG membrane with large peak at 2θ angle of 20º attributed to the hydroxyl group presence in its side chain [37, 38]. However, the strong interaction between the silica and PVA results in decline of crystal growth in PVA by the silica network. The incorporation of silica loading (PVA/PEG/Sil(3)) thus increased the amorphous region in the polymer chain.

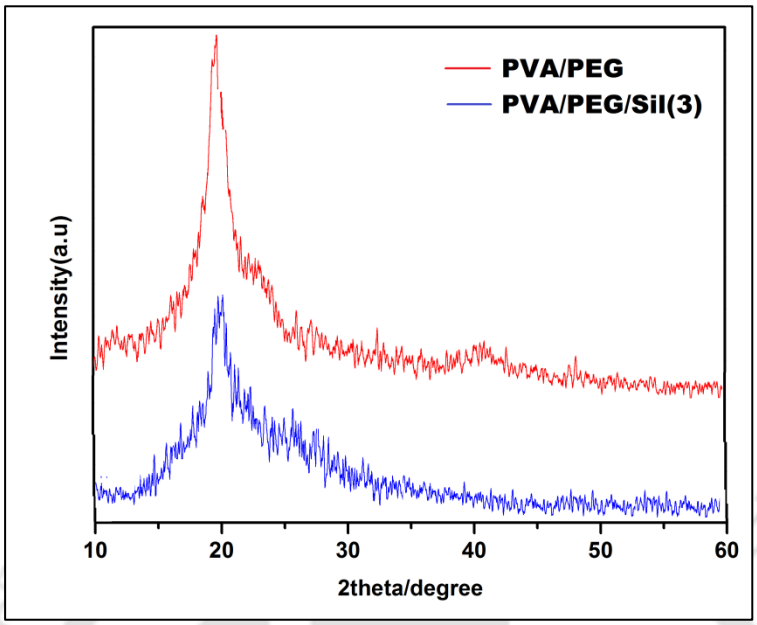

Figure 3.6 XRD curve of PVA/PEG and PVA/PEG/Sil(3) membrane

3.5.4. Field emission transmission electron microscopy analysis (FETEM)

The particle morphology of as-synthesized silica was probed by FETEM analysis as shown in Figure 3.7. The unfunctionalized silica particles confirmed uniform spherical structure with narrow particle size range of 100-150 nm confirming the formation of silica by Stober's process and the distribution of silica at loading of 3 wt %.

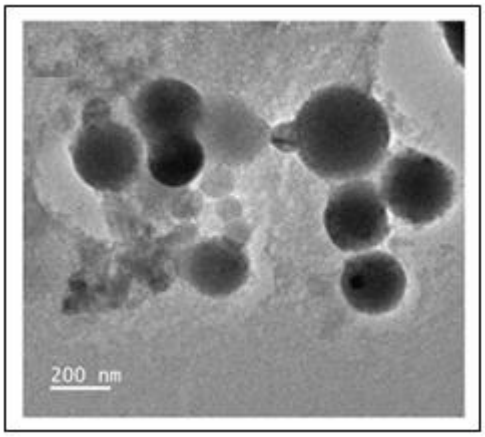

Figure 3.7 FETEM analysis of Sil loading of 3 wt %

3.5.5. Field emission scanning electron microscopy analysis (FESEM)

Field emission scanning electron microscope (FESEM) image of top surface and cross-section of membranes are shown in Figure 3.8(a-d). The cross-sectional view confirmed the presence of two distinctive layers with almost no penetration of the polymer solution into the porous substrate. Also, good dispersion of the nanoparticles is confirmed through the FESEM studies. This allows the membrane to perform at negligible mass transfer resistance of the substrate.

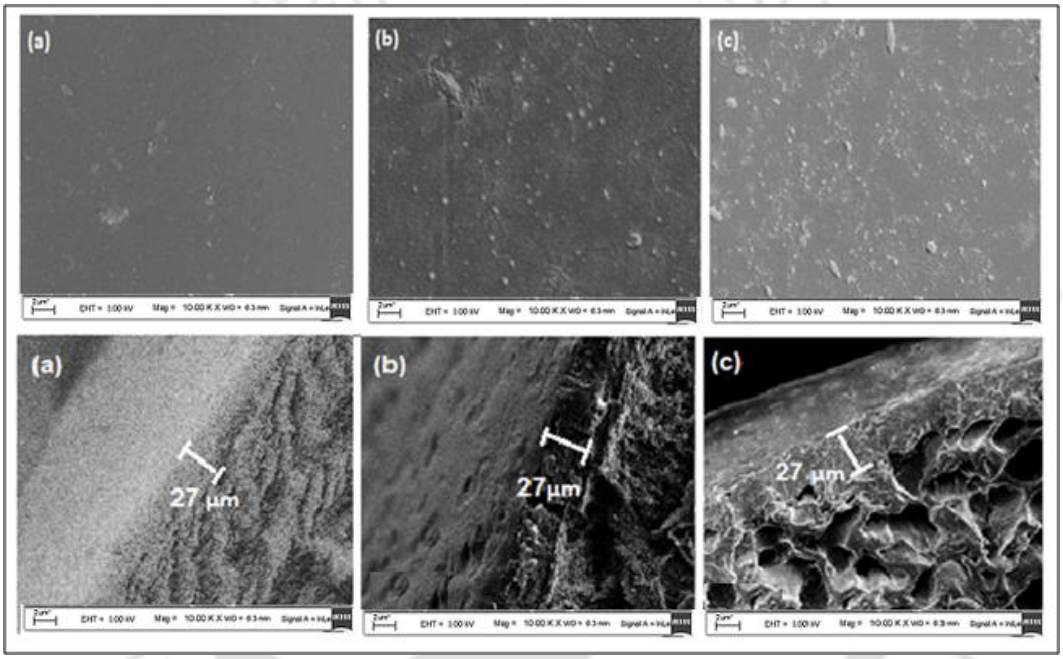

Figure 3.8 FESEM image of top surface of (a) PVA/PEG, (b) PVA/PEG/Sil(3) and (c) PVA/PEG/Sil(6) membrane and cross-sectional surface of (a) PVA/PEG, (b) PVA/PEG/Sil(3) and (c) PVA/PEG/Sil(6) membrane

3.5.6. X-ray photoelectron spectroscopy analysis (XPS)

The XPS analysis of PVA/PEG/Sil film was performed at a temperature of 24^{o}C. The survey scan (Figure 3.9) of XPS spectrum of the PVA/PEG/Sil(3) film sample showed the existence of C 1s, N 1s, O 1s and Si 2s and Si 2p peak.

3.6. CO_2 separation performance study of the membranes

The binary gas mixture has been analysed for variation in temperature (60-110 ºC) and sweep side water flow rate (0.01-0.075 ml/min). The feed gas (20 % CO_2 and balance N_2) and sweep gas (Ar) flow rates were constant at 30 and 40 ml/min, respectively.

3.6.1. Effect of temperature on CO_2 performance

The performance of PVA/PEG and PVA/PEG/Sil(3) membrane with temperature variation (range: 60 to 110 °C) was investigated (Figure 3.10 (a, b)). The feed/sweep side pressure was maintained at 2.5 atm and 1.2 atm, respectively. The effect of temperature on CO_2 and N_2 permeance and CO_2/N_2 selectivity for the membrane was analysed. The CO_2 permeance and CO_2/N_2 selectivity initially increased up to certain temperature (~100 °C) and then declined linearly with further increase in temperature. The increase in temperature increased the rate of reaction between CO_2 and carrier in presence of water. With increasing temperature, water content in the membrane lowers thus lowering the CO_2 solubility in the membrane. Also, the membrane flexibility is reduced with rise in temperature. However, the N_2 transport which solely follows solution diffusion mechanism is not affected by this phenomenon and thereby showed very slow, negligible change in N_2 permeance with temperature. This result thus suggests that water along with temperature plays a significant role for CO_2 facilitated transport. The CO_2 permeance and CO_2/N_2 selectivity increased by 75 % and 36 % for PVA/PEG/Sil(3) membrane compared to PVA/PEG membrane. These results could be attributed to the good interaction of the polymer-filler leading to substantial improvement in the CO_2 separation performance.

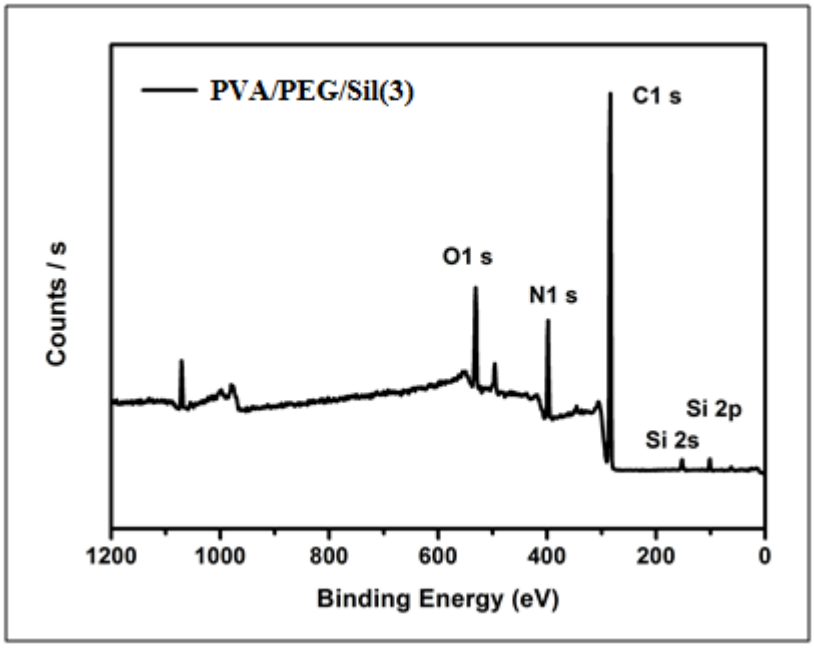

Figure 3.9 XPS survey scan of PVA/PEG/Sil(3) membrane

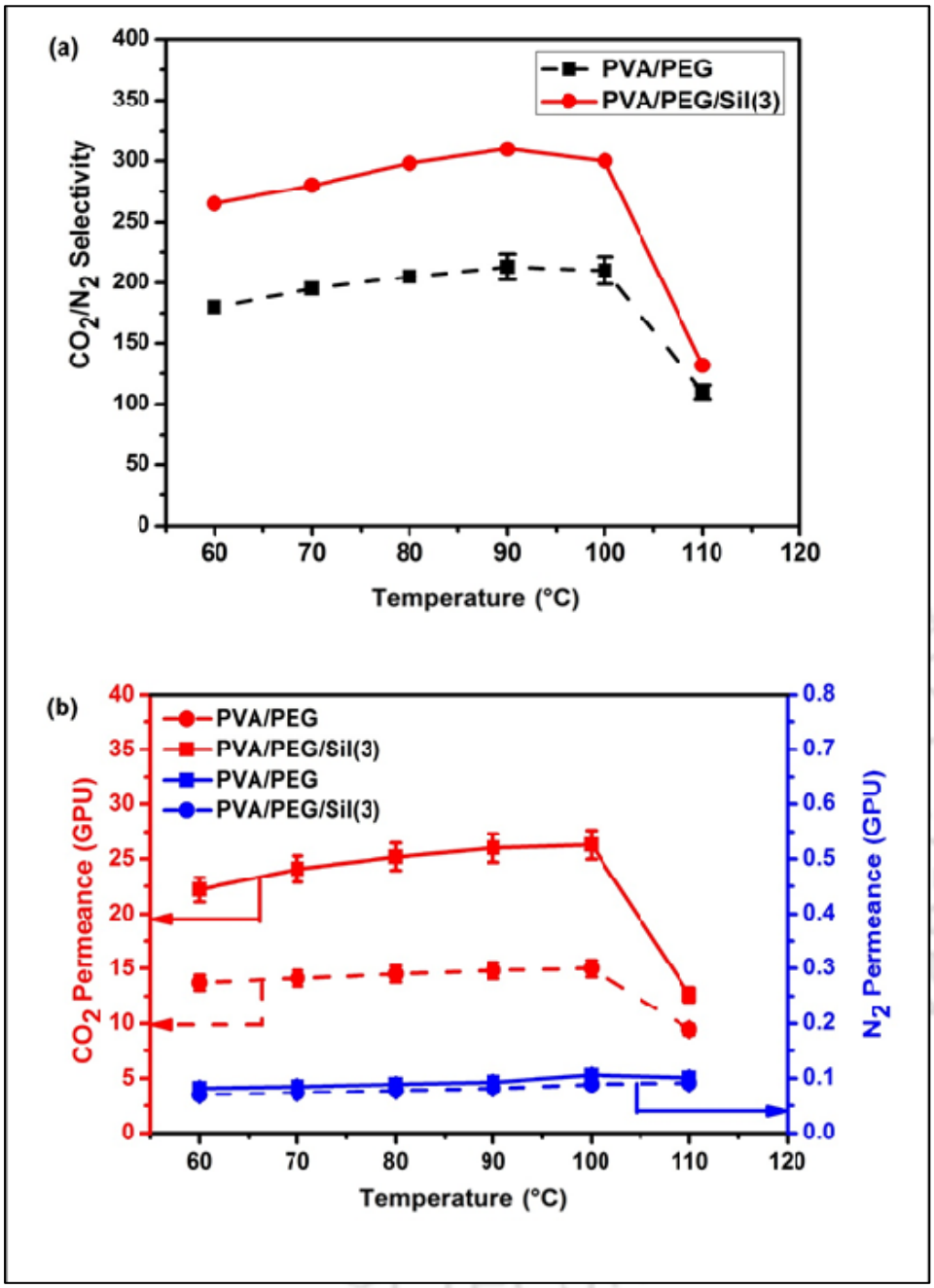

Figure 3.10 Effect of temperature on (a) CO_2/N_2 selectivity and (b) CO_2 and N_2 permeance (GPU) for PVA/PEG and PVA/PEG/Sil(3) membrane at feed absolute pressure = 2.5 atm, sweep absolute pressure = 1.2 atm, and water flow rates = 0.03/0.04 ml/min (feed/sweep)

3.6.2. Effect of sweep water flow rate on CO_2 performance

The effect of water flow rate (ml/min) in the sweep side on membrane performance was analysed with sweep side water flow rate variation from 0.01 to 0.075 ml/min. The feed side water flow rate was maintained constant at 0.03 ml/min. The pressure at the feed and sweep side was kept constant at 2.5 atm and 1.2 atm, respectively. The temperature of the system was kept constant at 100 °C. Feed gas (20 % CO_2 and balance N_2) and carrier gas (Ar) flow rates were kept constant at 30 and 40 ml/min, respectively. (Figure 3.11(a, b)) represents the sweep side water effect on CO_2/N_2 selectivity and CO_2 and N_2 permeance for PVA/PEG and PVA/PEG/Sil(3) membrane. It was observed that the CO_2/N_2 selectivity and CO_2 permeance initially increased considerably with increase in sweep water content and then became constant after a certain value. This is attributed to the increase in the mobility of CO_2-carrier complex occurring through the CO_2-carrier reactions due to the increased water retention by the membranes with higher sweep flow rate [39, 40]. However, the N_2 transport is governed solely by solution diffusion mechanism, thereby showing insignificant increase in the N_2 permeance with increase in water flow rate. Thus, it could be established that the addition of silica fillers into the polymer matrix improved the separation properties of the membrane.

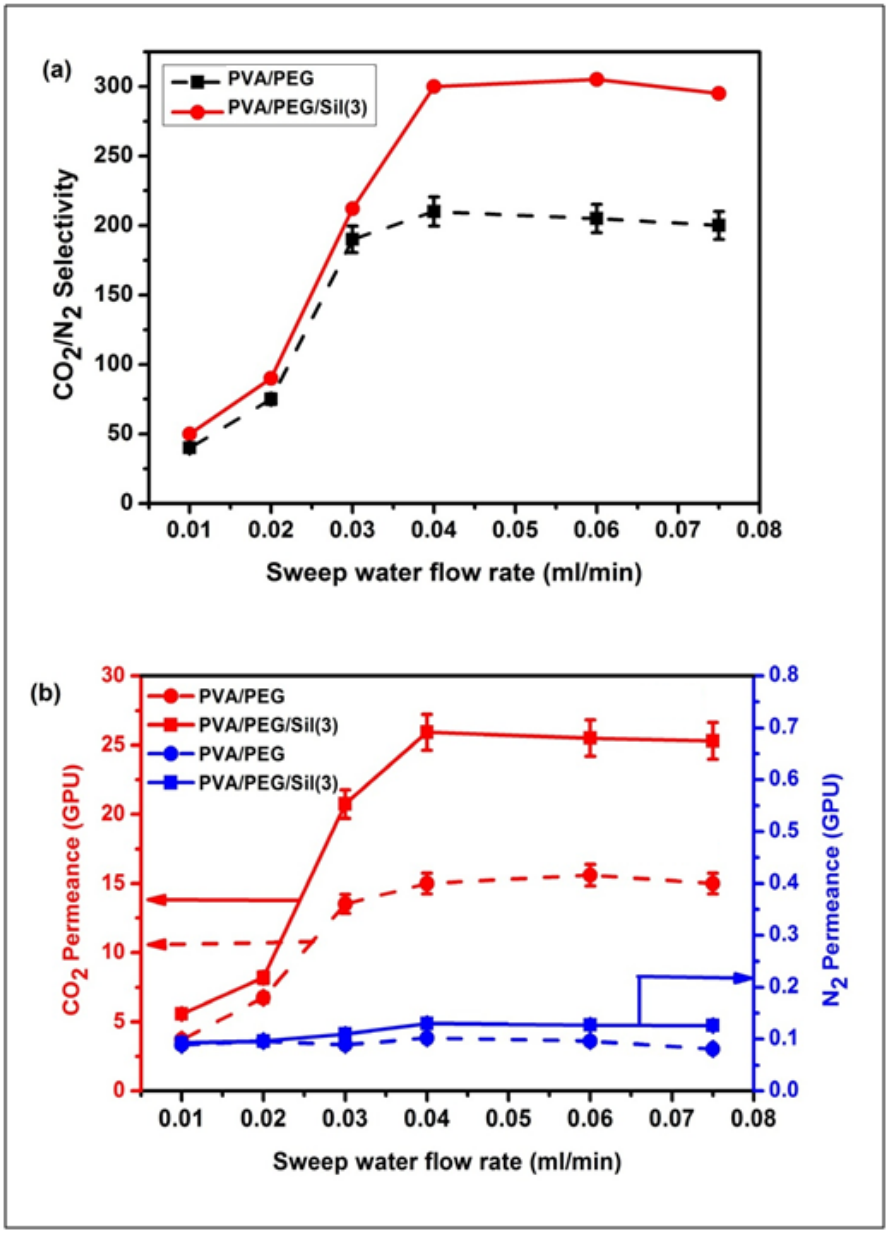

Figure 3.11 Effect of sweep side water flow rate on (a) CO_2/N_2 selectivity and (b) CO_2 and N_2 permeance (GPU) for PVA/PEG and PVA/PEG/Sil(3) membrane at 100 °C temperature with feed absolute pressure of 2.5atm, feed water flow rate of 0.03 ml/min

The bar diagram (Figure 3.12) showed 78 % increment in CO_2 permeance (GPU) for PVA/PEG/Sil(3) membrane compared to pure PVA/PEG membrane with

enhancement in CO_2/N_2 selectivity by 36 %. Thus it can be concluded that addition of silica filler into the polymeric matrix gives a substantial improvement in terms of both CO_2 permeance and CO_2/N_2 selectivity. The CO_2 permeability (Barrer) and CO_2/N_2 selectivity results for different membrane have been compared in Table 3.2.

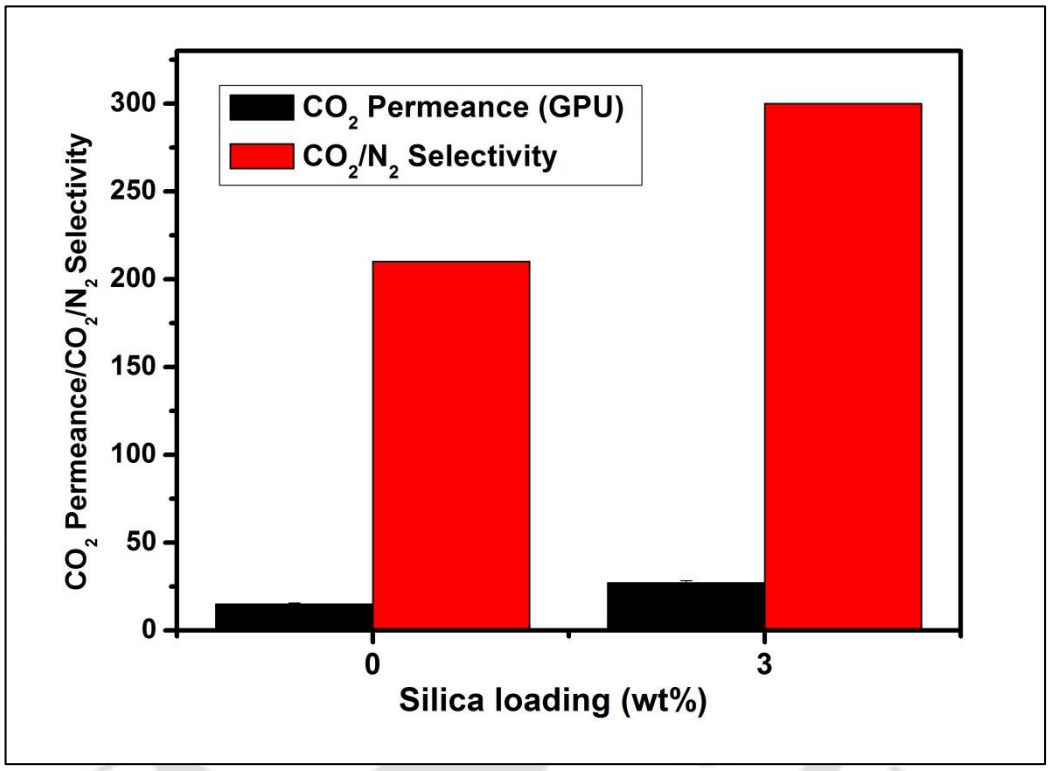

Figure 3.12 Bar diagram for CO_2 permeance (GPU) and CO_2/N_2 selectivity for PVA/PEG and PVA/PEG/Sil(3) membrane

Table 3.2 CO_2 permeability (Barrer) and CO_2/N_2 selectivity results for different membrane material

Polymer	CO_2 permeability (Barrer)	CO_2/N_2 selectivity	Thickness (µm)	Reference
2,2'-Bis(3,4-dicarboxyphenyl) hexafluoropropane dianydride(6FDA) (25 wt % silica nanoparticles)	1920	23	30-50	[16]
Polyimide (carbon-silica nanocomposite filler)	27	42.5	70-100	[36]
Polyvinylchloride(PVC) 30 wt % silica	0.1908	27.3	35	[37]
Crosslinked PVA/PEG membrane	400	210	27	This work
Crosslinked PVA/PEG/Sil(3) membrane	710	300	27	This work

3.7. Robeson's curve

The experimental results in this work when compared with polymer/silica combination reported in literature exceeded the Robeson's upper bound barrier with exceptional CO_2 separation (Figure 3.13). Thus the PVA/PEG membrane and PVA/PEG/Sil(3) membrane

exhibited higher values of CO_2 permeability (Barrer) and CO_2/N_2 selectivity as confirmed by Robeson's upper bound limit.

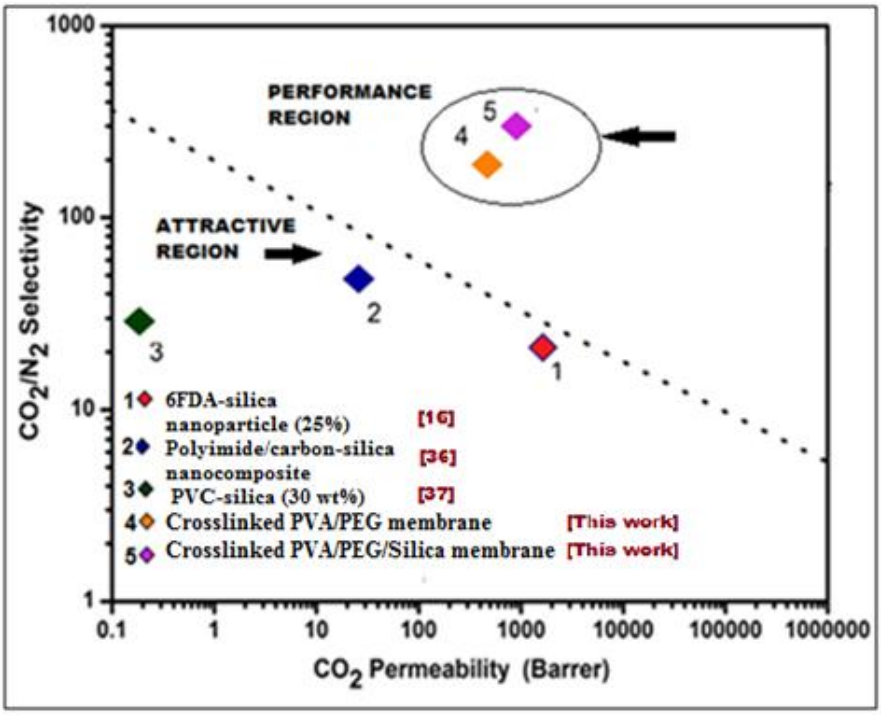

Figure 3.13 Robeson's upper bound curve of PVA/PEG and PVA/PEG/Sil(3) membrane

3.8. Conclusions

It is widely believed that the structure and separation performance of mixed matrix membrane depends on polymer-filler interaction. The synthesis of defect-free MMM is an important concern and of paramount importance. In this work, PVA and PEG polymer along with silica nanoparticle at different loading weight have been successfully synthesized. The thermal stability and crystallinity property of defect-free, homogenously dispersed PVA/PEG/Silica MMM have been analysed. FESEM study showed homogenous dispersion of the fillers in the polymer matrix. FTIR and XRD study showed the successful addition of the filler materials. Gas permeation study revealed that the temperature and sweep side water flow rate have a remarkable impact

on the CO_2 permeance, and CO_2/N_2 selectivity. The addition of 3 wt % silica content resulted in the enhancement of CO_2 permeance by 78 % and CO_2/N_2 selectivity by 36 % as compared to pristine PVA/PEG facilitated transport polymeric membrane. The synthesized crosslinked PVA/PEG and PVA/PEG/silica membrane showed impressive gas separation properties (CO_2 permeance and CO_2/N_2 selectivity) very well surpassing 2008 Robeson upper bound limitation. Because of the strong interaction between the polymer matrix and silica filler, the synthesized MMMs exhibited excellent thermal and transport properties for gas separation. With addition of small amount of silica content into the polymer matrix, it was found that the CO_2 separation properties could be enhanced many fold. Thus, we believe these results demonstrate a novel and unique membrane material that could be exploited for industrial CO_2/N_2 separation.

References

[1] J. Liao, Z. Wang, C. Gao, M. Wang, K. Yan, X. Xie, S. Zhao, J. Wang and S. Wang, A high performance PVA_m–HT membrane containing high-speed facilitated transport channels for CO_2 separation, J. Mater. Chem. A. 3 (2015) 16746-16761.

[2] S. Wang, X. Li, H. Wu, Z. Tian, Q. Xin, G. He, D. Peng, S. Chen, Y. Yin and Z. Jiang, Advances in high permeability polymer-based membrane materials for CO_2 separations, Energy Environ. Sci. 9 (2016) 1863-1890.

[3] C.I. Chaidou, G. Pantoleontos, D.E. Koutsonikolas, S.P. Kaldis and G.P. Sakellaropoulos, Gas separation properties of polyimide-zeolite mixed matrix membranes, Sep. Sci. Technol. 47 (2012) 950–962.

[4] M. Barooah and B. Mandal, Enhanced CO_2 separation performance by PVA/PEG/silica mixed matrix membrane, J. Appl. Polym. Sci. 46481 (2018) 1-12.

[5] S. Kim, E. Marand, J. Ida and V.V. Guliants, Polysulfone and mesoporous molecular sieve MCM-48 mixed matrix membranes for gas separation, Chem. Mater. 18(5) (2006) 1149–1155.

[6] S.M. Sanip, A.F. Ismail, P.S. Goh, M.N.A. Norrdin, T. Soga, M. Tanemura and H. Yasuhiko, Carbon nanotubes based mixed matrix membrane for gas separation, Adv. Mater. Res. 364 (2012) 272-277.

[7] D.Q. Vu, W.J. Koros and S.J. Miller, Mixed matrix membranes using carbon molecular sieves: I. Preparation and experimental results, J. Membr. Sci. 211 (2003) 311–334.

[8] J. Zou and W.S.W. Ho, CO_2-selective polymeric membranes containing amines in crosslinked poly (vinyl alcohol), J. Membr. Sci. 286 (2006) 310.

[9] A.F. Barquin, C.C. Coterillo and A. Irabien, Separation of CO_2-N_2 gas mixtures: membrane combination and temperature influence, Sep. Purif. Technol. 188 (2017) 197 – 205.

[10] L.P. Singh, S.K. Agarwal, S.K. Bhattacharyya, U. Sharma and S. Ahalawat, Preparation of silica nanoparticles and its beneficial role in cementitious materials, Nanomater. nanotechnol. 1(1) (2011) 44-51.

[11] J.L. Zou and X.L. Chen, Using silica nanoparticles as a catalyst carrier to the highly sensitive determination of thiamine, Microchemical J. 86(1) (2007) 42-47.

[12] W.H. De Jong and P.JA. Borm, Drug delivery and nanoparticles: applications and hazards, Int. J. Nanomedicine. 3(2) (2008) 133–149.

[13] J. Peng, J. Li, W. Xu, L. Wang, D. Su, C.L. Teoh, and Y.T. Chang, Silica nanoparticle-enhanced fluorescent sensor array for heavy metal ions detection in colloid solution, Anal. Chem. 90(3) (2018) 1628–1634.

[14] N. Na, X. Cui, T. De Beer, T. Liu, T. Tang, M. Sajid and J. Ouyang, The use of silica nanoparticles for gas chromatographic separation, J. Chromatogr. A. 1218(28) (2011) 4552-4558.

[15] C. Aydogan and Z. El Rassi, Monolithic stationary phases with incorporated fumed silica nanoparticles. Part II. Polymethacrylate-based monolithic column with "covalently" incorporated modified octadecyl fumed silica nanoparticles for reversed-phase chromatography, J. Chromatogr. A. 1445 (2016) 62-7.

[16] E. Ameri, M. Sadeghi and N. Zareia, A. Pournaghshband, Enhancement of the gas separation properties of polyurethane membranes by alumina nanoparticles, J. Membr. Sci. 479 (2015).

[17] K.S. Jang, H.J. Kim, J.R. Johnson, W.G. Kim, W.J. Koros, C.W. Jones and S. Nair, Modified mesoporous silica gas separation membranes on polymeric hollow fibers, Chem. Mater. 23 (2011) 3025-3028

[18] A. Bapat, C. Anderson, C.R. Perrey, C.B. Carter, S.A. Campbell and U. Kortshagen, Plasma synthesis of single-crystal silicon nanoparticles for novel electronic device applications, Plasma Phys. Controlled Fusion. 46 (2004).

[19] R.P. Chaukulkar, K. de Peuter, P. Stradins, S. Pylypenko, J.P. Bell, Y. Yang and S. Agarwal, Single-Step Plasma Synthesis of Carbon-Coated Silicon Nanoparticles, ACS Appl. Mater. Interfaces. 6 (2014) 19026-19034.

[20] A. Kumar, P.B. Agarwal, S. Kumar, B.C. Joshi and H. Chander, Low-pressure chemical vapour deposition of silicon nanoparticles: synthesis and characterisation, Defence Sci. J. 58(4) (2008) 550-558.

[21] T. Aubert, F. Grasset, S. Mornet, E. Duguet, O. Cador, S. Cordier, Y. Molard, V. Demange, M. Mortier and H. Haneda, Functional silica nanoparticles synthesized by water-in-oil microemulsion processes, J. Colloid Interface Sci. 341(2) (2010) 201-208.

[22] S.T. Aruna and A.S. Mukasyan, Combustion synthesis and nanomaterials, Curr. Opin. Solid State Mater. Sci. 12 (2008) 44–50

[23] L.P. Singh, S.K. Bhattacharyya, R. Kumar, G. Mishra, U. Sharma, G. Singh and S. Ahalawat, Sol-gel processing of silica nanoparticles and their applications, Adv. Colloid Interface Sci. 214 (2014) 17-37.

[24] H.N. Azlinaa, J.N. Hasnidawania, H. Noritaa and S.N. Surip, Synthesis of SiO_2 nanostructures using sol-gel method, Acta Phys. Pol. A. 129(4) (2016)

[25] I.Ab Rahman and V. Padavettan, Synthesis of silica nanoparticles by sol-gel: size-dependent properties, surface modification, and application in silica-polymer nanocomposites- a review, J. Nanomaterials. 8(2012)

[26] L. Gu, A. Zheng, K. Hou and C. Dai, One-pot hydrothermal synthesis of mesoporous silica nanoparticles using formaldehyde as growth suppressant, Micropor. Mesopor. Mater. 152 (2015) 9-15.

[27] M. Salimi, V. Pirouzfar and E. Kianfar, Enhanced gas transport properties in silica nanoparticle filler-polystyrene nanocomposite membranes, Colloid Polym. Sci. 295(1) (2016) 1-12.

[28] A. Mondal, M. Barooah and B. Mandal, Effect of single and blended amine carriers on CO_2 separation from CO_2/N_2 mixtures using crosslinked thin-film poly(vinyl alcohol) composite membrane, Int. J. Greenh. Gas Con. 39 (2015) 27-38.

[29] S. Ben Hamouda and S. Roudesli, Transport properties of PVA/PEI/PEG composite membranes: Sorption and permeation characterizations, Cent. Eur. J. Chem. 6 (2008) 634–640.

[30] H. Pingan, J. Mengjun, Z. Yanyan and H. Ling, A silica/PVA adhesive hybrid material with high transparency, thermostability and mechanical strength, RSC Adv. 7 (2017) 2450–2459.

[31] J. Li, J, Suo and R. Deng, Structure, mechanical, and swelling behaviours of poly(vinyl alcohol)/SiO_2 hybrid membranes, J. Reinf. Plast. Compos. 29 (2010) 618–629.

[32] J.H. Kim and Y.M. Lee, Gas permeation properties of poly (amide-6-b-ethylene oxide)-silica hybrid membranes, J. Membr. Sci. 193 (2001) 209–225.

[33] M. Barooah and B. Mandal, Enhanced CO_2 separation performance by PVA/PEG/silica mixed matrix membrane, J. Appl. Polym. Sci. 46481 (2018) 1-12.

[34] A. Mondal, CO_2-Selective thin-film polymer composite membranes: Improvement of thermal stability and role of amine carriers, PhD Thesis Dissertion (2014).

[35] S.G. Chaudri, B.H. Rajai and P.S. Singh, Nanoscale homogeneity of silica–poly (vinyl alcohol) membranes by controlled cross-linking via sol–gel reaction in acidified and hydrated ethanol, RSC Adv. 5 (81) (2015) 65862-65869.

[36] M.W. Anjum, F. de Clippel, J. Didden, A.L. Khan, S. Couck, G.V. Baron, J.F.M. Denayer, B.F. Sels and I.F.J. Vankelecom, Polyimide mixed matrix membranes for CO_2 separations using carbon-silica nanocomposite fillers, J. Membr. Sci. 495 (2015) 121–129.

[37] M. Mohagheghian, M. Sadeghi, M.P. Chenar and M. Naghsh, Gas separation properties of polyvinylchloride (PVC)-silica nanocomposite membrane, K. J. Chem. Eng. 31(11) (2014) 2041-2050.

[38] H. Ma, T. Shi and Q. Song, Synthesis and characterization of novel PVA/SiO_2-TiO_2 hybrid fibers, Fibers. 2 (2014) 275–284.

[39] A. Mondal and B. Mandal, CO_2 separation using thermally stable crosslinked poly (vinyl alcohol) membrane blended with polyvinylpyrrolidone/ polyethyleneimine/ tetraethylenepentamine, J. Membr. Sci. 460 (2014) 126-138.

[40] A. Mondal and B. Mandal, Synthesis and characterization of crosslinked poly (vinyl alcohol)/poly (allylamine)/2-amino-2-hydroxymethyl-1,3-propanediol/polysulfone composite membrane for CO_2/N_2 separation, J. Membr. Sci. 446 (2013) 383–394.

CHAPTER 4

Tailoring the Properties of Silica by Amino- Functionalization as Filler in Mixed Matrix Membranes for Enhanced CO_2 Separation

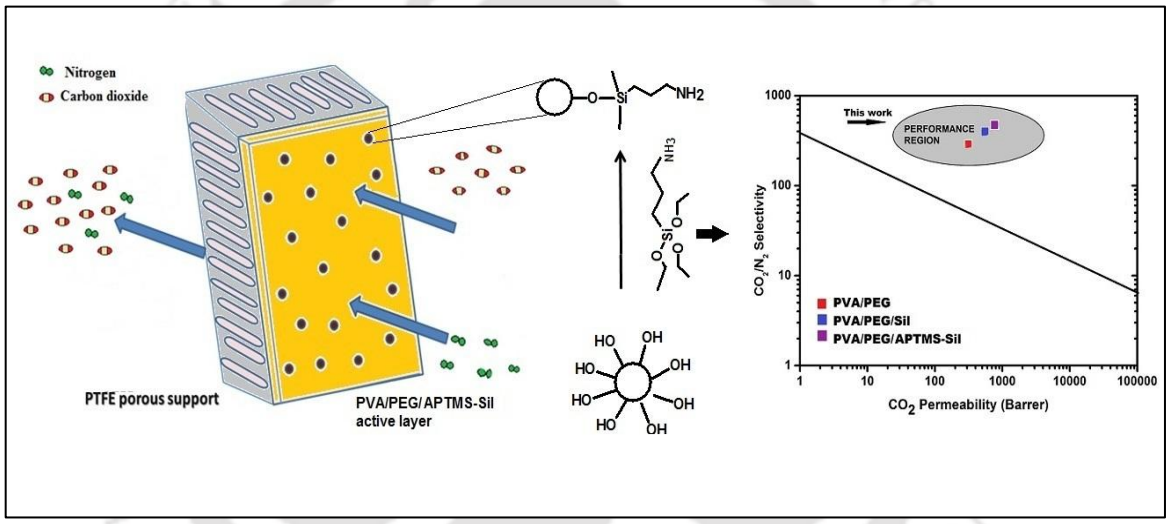

Graphical abstract of PVA/PEG/APTMS-Sil membrane and Robeson's curve

CHAPTER 4

Tailoring the Properties of Silica by Amino- Functionalization as Filler in Mixed Matrix Membranes for Enhanced CO_2 Separation

This chapter involves the preparation of mixed matrix membrane (MMM) by consolidating amino-functionalized silica in the poly (vinyl alcohol) (PVA)/polyethylene glycol (PEG) matrix. The silica prepared by Stober's process is used as filler for CO_2 separation in Chapter 3. To further improve the compatibility between the polymer and inorganic phase and enhance CO_2 transport performance, the silica nanoparticles are surface modified with 3-aminopropyltrimethoxysilane (APTMS) amino functional groups. Detailed material characterization is performed by XPS and ninhydrin assay to confirm the successful grafting of the amino group on the silica surface. We envision that this work will invigorate a cost effective route for industrial flue gas separation studies.

4.1. Introduction

Mixed matrix membranes (MMMs) integrating the synergistic effect of filler and polymer material provides a simpler approach in the synthesis of high-performance speciality membrane material. The inorganic filler such as silica, metal-organic frameworks (MOFs), carbon nanotubes, zeolites, etc. dispersed in the polymer matrix combines the attractive property of polymer easy processability along with high performance ability of fillers [1-3]. However, its large-scale application for gas separation is hugely dependent on the formation of defect-free high-performance MMM. Suitable polymer-inorganic particle combination and polymer-particle interface morphologies are the pre-requisites for the formation of void-free MMMs [4, 5].

Good compatibility of polymer matrix with selected filler is also an essential factor to ensure high selectivity and avoid undesirable characteristics of particle agglomeration, non-selective void formation and polymer rigidification which degrades the overall membrane performance. Various techniques such as surface and chemical modification, use of additives and filler combinations have been utilized to improve the interaction

with CO_2 molecules to enhance the gas transport performance. The silica particles have been functionalized with various functional groups such as amines, -NH_2, hydroxo, -OH, nitro, -NO_2, sulfonic acid, -SO_3H, etc. The bonding between the polymer backbone and the functional groups of the filler materials improves the interaction with the CO_2 molecules thereby leading to increased compatibility between the two phases. Among them, surface functionalization by amino groups provides appealing CO_2 separation performance by promoting enhanced reversible reaction/interaction between the CO_2 and amino groups [6]. The N_2 gas does not form complexes with amine groups thereby leading to enhanced CO_2/N_2 selectivity along with its permeability.

PVA/PEG polymer blend has been chosen due to its positive effect on gas separation performance. The incorporation of silica particles in the PVA/PEG matrix improved the gas permselectivity along with the structural, mechanical and thermal behaviour of the membrane as discussed in Chapter 3. Addition of silica as filler improved superior thermal behaviour, chemical stability, low cost and high specific surface area on the membrane. The enhancement in the gas separation performance with addition of silica on PVA/PEG facilitated transport membrane has been discussed in detail in Chapter 3 [16]. The PVA/PEG/Sil membrane with 3 wt % silica exhibited an impressive 78 % and 36 % increment in CO_2 permeance and CO_2/N_2 selectivity compared to PVA/PEG membrane. Taking these enhanced results as a prerogative, the silica filler has been further surface functionalized with amino functional moieties for effective CO_2 separation. Various techniques for incorporation of organosilane groups into silica surface include physical and chemical impregnation, post-synthesis grafting and co-condensation [17-22]. The surface functionalization with organosilane compound involves activating and tailoring the surface properties of silica nanoparticle with desired amino functional agents such as polyethyleneimine (PEI) [23], 3-aminopropyltrimethoxysilane (APTMS) [24], 3-aminopropyltriethoxysilane (APTS) [25]. The amino groups attached to the silica surface in the membranes thereafter forms carbamate ions that reacts reversibly and escalates the overall facilitated transport mechanism in the membrane showing significant increase of CO_2 permeance and CO_2/N_2 permselectivity [26]. The N_2 molecule in the CO_2/N_2 gas mixture does not take part in the facilitated transport mechanism and hence shows no effect on the N_2 permeance. In this chapter, improvement in the CO_2 separation property by combining the 3-aminopropyltrimethoxysilane (APTMS) functionalized silica

(APTMS-Sil) into the PVA/PEG blend matrix facilitated by polyethyleneimine (PEI) and triethylenetetramine amine carriers is envisioned to provide a novel and cost effective route for efficient CO_2 separation studies.

4.2. Materials

Poly (vinyl alcohol) (98-99 mol % hydrolyzed powder, M_w= 130,000), polyethylene glycol (average M_n=6000), 3-aminopropyltrimethoxysilane (APTMS), polyethyleneimine (M_w = 25,000), and triethylenetetramine (M_w=146.08) were supplied by Sigma-Aldrich, USA. Hydrochloric acid (HCl, 37 % purity), tetraethylorthosilicate (TEOS > 98 %), formaldehyde (37 wt % aqueous solution), ultra-pure ethanol (99 %), were provided by Merck, India. Polytetrafluoroethylene support (thickness: ~150 μm, pore size: ~0.03 μm) were obtained from Sterlitech USA. The binary feed gas (CO_2/N_2) (20/80 vol %) mixture, Argon (ultrapure) and Helium (99.999 % pure) used for the gas permeation analysis was collected from Vadilal Pvt. Ltd., India.

4.3. Experimental

4.3.1. Synthesis of amino-functionalized silica (APTMS-Sil)

The silica sol was synthesized by Stober's process [17]. Before the functionalization step, the silica nanoparticle was sonicated to remove aggregates and increase the surface available for functionalization. The APTMS functionalized silica was prepared by adding ~50 ml anhydrous toluene to the sonicated silica suspension until complete dispersion. Thereafter, calculated amount of APTMS was added and stirred at 70-80 ºC for 24 h for enhanced covalent bond between the hydroxyl groups at silica surface with the APTMS amino groups. The obtained amino-functionalized silica sample was coded as APTMS-Sil. The structural formula of PVA, APTMS and schematic representation of synthesis of APTMS functionalized silica nanoparticle are shown in Figure 4.1.

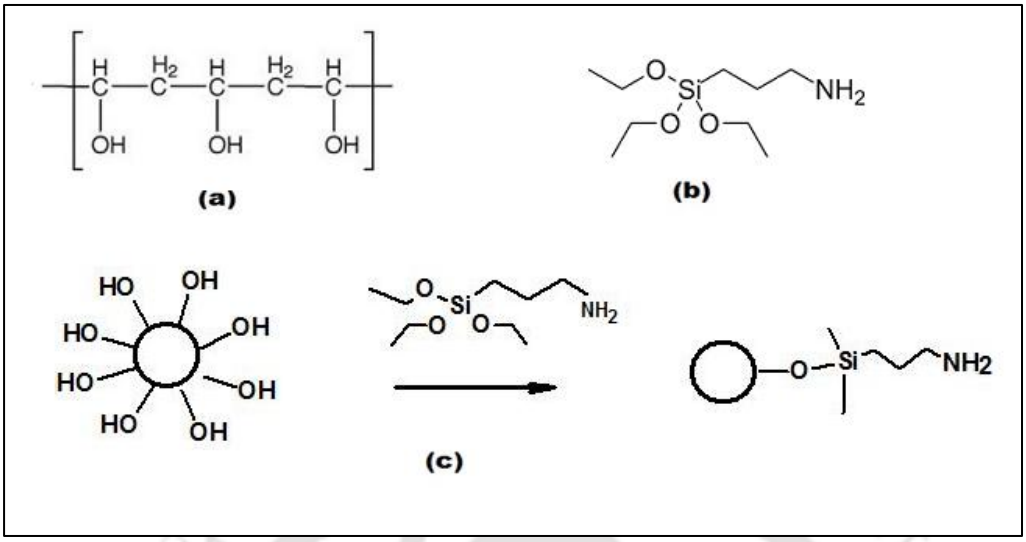

Figure 4.1 Structural formula of (a) polyvinyl alcohol (PVA), (b) 3-aminopropyltrimethoxysilane (APTMS) and (c) schematic representation of the synthesis of APTMS functionalized silica nanoparticle

4.3.2. Synthesis of crosslinked PVA/PEG/APTMS-Sil mixed matrix membrane

The crosslinked PVA/PEG polymer solution (10 wt % solid weight) was prepared [9]. Fixed amount of APTMS functionalized silica (APTMS-Sil) was appended into the homogeneous polymer solution and stirred continuously until the formation of APTMS amino-functionalized silica mixed matrix membrane (PVA/PEG/APTMS-Sil) casting solution. The solution was further sonicated for ~20 mins for homogenous dissipation of the silica nanoparticle into the matrix before finally casting on the porous PTFE support with uniform pore size of ~30 nm. The viscosity was maintained > 1200 cp to ensure no solution penetration on the porous substrate.

4.4. Membrane characterization

The ATR-FTIR (SHIMADZU, IRAffinity 1, Japan) wavenumber range (4000 to 400 cm^{-1}), 40 scans per sample and 4 cm^{-1} resolution confirmed the functional groups present in the membrane. The surface morphology and topography was analysed by FETEM and FESEM, ZEISS, USA. For FESEM analysis, the samples were fixed with a carbon tape on a stub and gold sputter coated prior to imaging. The samples for BET analysis were degassed prior to the calculation of the surface area by Bruner-Emmett-Teller method. The mechanical property of PVA/PEG and PVA/PEG/Sil film was measured using computerized universal tensile testing machine (UTM) (Model No: AEC 1112-5 KN ACD). The membrane samples were cut into rectangular shape of (3× 7cm) and tested at a room temperature of ~25 ºC. Each membrane sample was tested for at least three times and the average with least deviation was considered. The surface chemical state analysis was examined by XPS spectrometer (Thermo Scientific Escalab Xi^{+}). Mono-chromated Al Kα radiation was used as the X-ray source and the results was documented by software named Avantage v5.984.

4.5. Results and discussion

4.5.1. Fourier transform infrared spectroscopy (FTIR)

Figure 4.2 shows the FTIR spectra for pure silica and APTMS amine functionalized silica particle. The absorption peak at 3648 cm^{-1} corresponds to OH stretching of free silanol groups. The band around 1590 cm^{-1} is attributed to the NH_2 scissoring vibration. This band indicates that the silica nanoparticles were successfully functionalized by the amine groups. The bands at 2971 cm^{-1} is due to CH stretching in propyl groups.

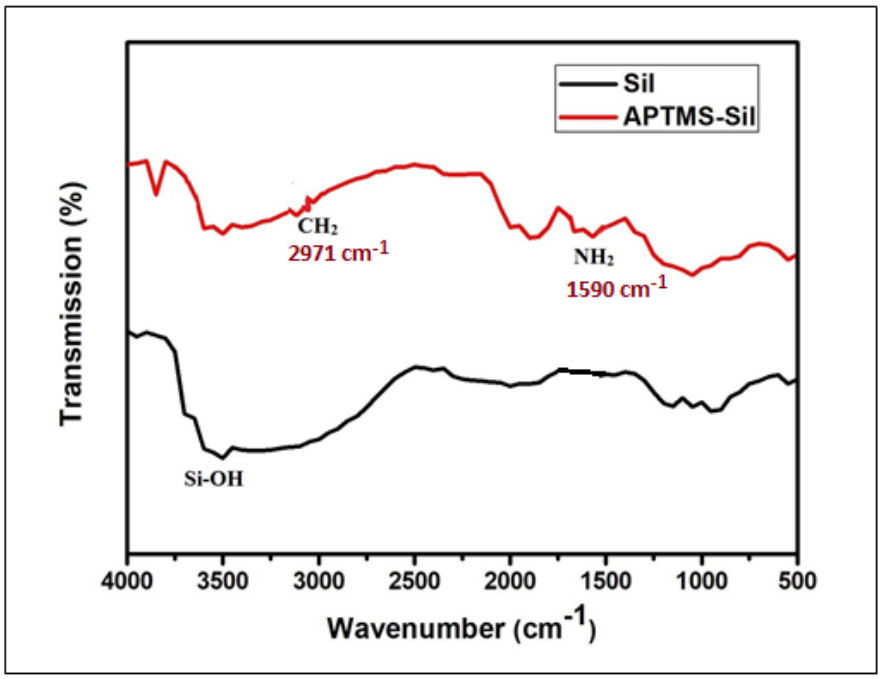

Figure 4.2 FTIR curve of Sil and APTMS-Sil

4.5.2. Field emission transmission electron microscopy analysis (FETEM)

The particle morphology of as-synthesized silica and amino-functionalized silica (APTMS-Sil) was probed by FETEM analysis as shown in Figure 4.3 (a, b). The unfunctionalized silica particles confirmed uniform spherical structure with a narrow particle size range of 100-150 nm. The APTMS-Sil exhibited identical spherical structure with slightly rougher edges attributed to the polymerization of the organic layer on the particle surface. Thus, it could be established that the amine functionalization of silica brought no significant change in the particle morphology.

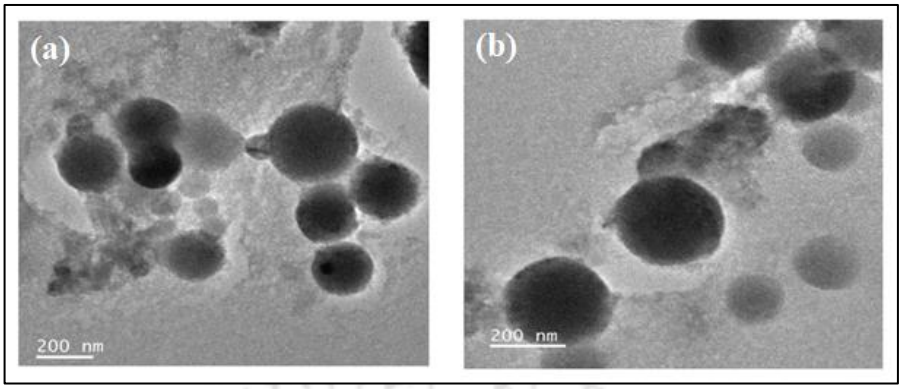

Figure 4.3 FETEM analysis of (a) Sil and (b) APTMS-Sil

4.5.3. Field emission scanning electron miscroscopy analysis (FESEM)

FESEM analysis of PVA/PEG/Sil and PVA/PEG/APTMS-Sil membranes was performed as shown in Figure 4.4 (a, b). No significant changes in the surface morphology were observed as has already been confirmed by FETEM analysis. The presence of dark spots in the PVA/PEG/APTMS-Sil membrane could be attributed to the presence of amine groups. The surface modification increased the interaction between the polymer chain and the functionalized groups. This leads to the agglomerate-free, homogeneously dispersed filler particle into the polymer matrix. These results were in synchrony with those reported in literature [43, 45].

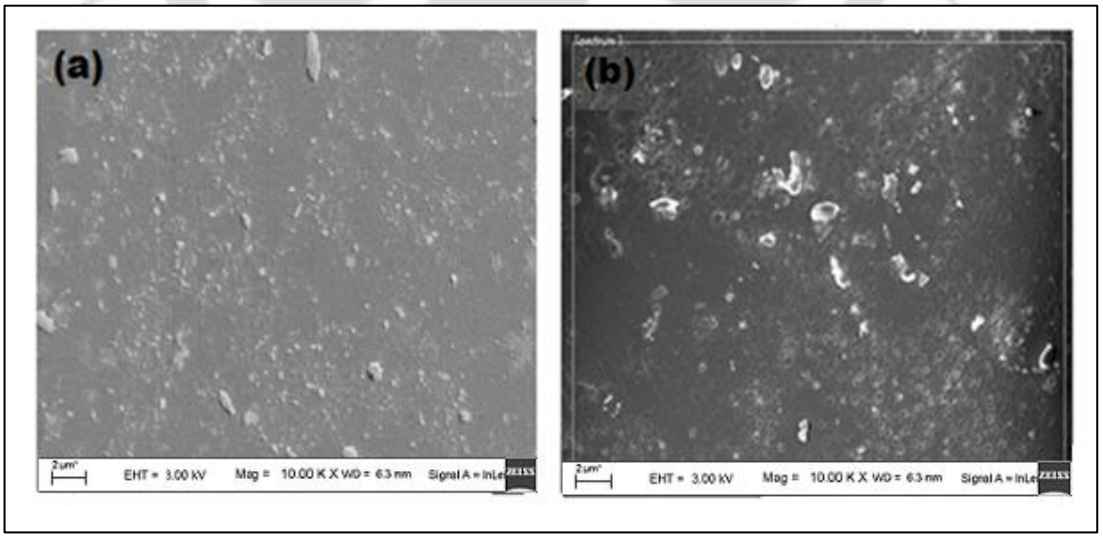

Figure 4.4 FESEM top surface analysis of (a) PVA/PEG/Sil and (b) PVA/PEG/APTMS-Sil membrane

4.5.4. Surface area analysis

The N_2 adsorption-desorption isotherm of the raw silica (Sil) and the APTMS-silica (APTMS-Sil) exhibited typical type I characteristic as indicated by Figure 4.5. It was observed that the sample retained the same isotherm thereby suggesting no change in pore shape after amine modification as already confirmed by FETEM analysis. The BET surface area and pore volume of the synthesized silica nanoparticle was reported in Table 4.1. The reduction in the surface area with amine functionalization established the surface filling by the amine moieties. The decrease in pore volume confirmed the pore being partially occupied by the amino groups thereafter confirming the successful surface functionalization of the nanofillers with APTMS [29].

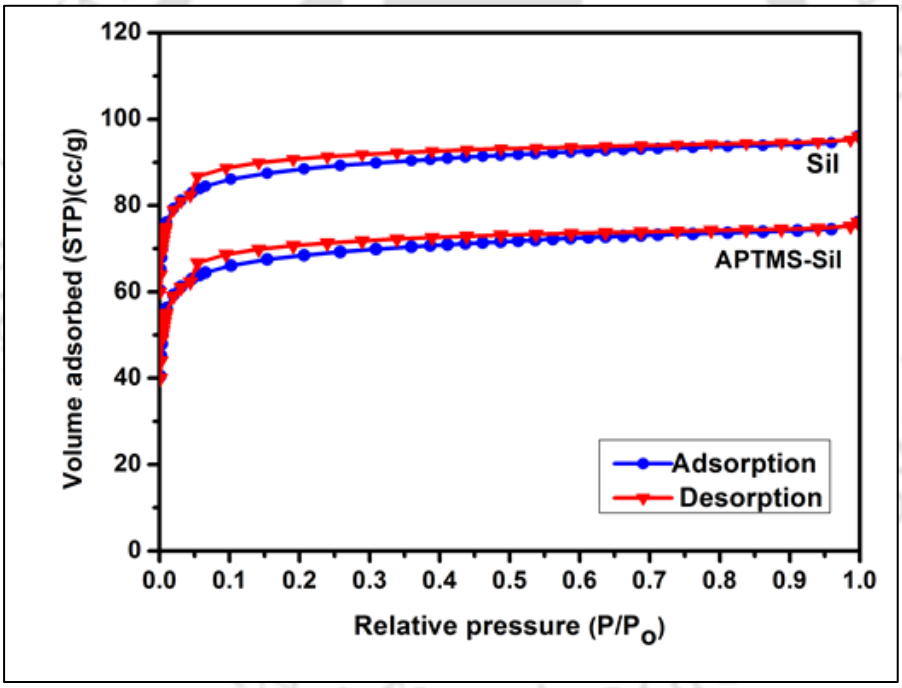

Figure 4.5 N_2 adsorption-desorption isotherm of Sil and APTMS-Sil

Table 4.1 BET surface area and total pore volume of the silica and amine-functionalized silica sample

Sample	BET surface area (m^2/gm)	Total pore volume (cm^3/gm)
Sil	**267.7**	**0.149**
APTMS-Sil	**152.3**	**0.125**

4.5.5. Mechanical strength analysis

The mechanical stability of the membranes plays a pivotal role for long-term, large-scale CO_2 separation application. The mechanical strength of PVA/PEG, PVA/PEG/Sil and PVA/PEG/APTMS-Sil membrane was analysed by a universal testing machine (UTM) kept at room temperature. The stress-strain curve (Figure 4.6) showed the positive effect of silica loading on the mechanical properties of the membranes. The crosslinked PVA/PEG film showed increment in stress with strain. It was observed that significant improvement in tensile strength was achieved with the addition of silica which further increased for amino modified silica. The tensile strength of PVA/PEG was 40.2 MPa which increased to 57.4 MPa and 86.5 MPa for PVA/PEG/Sil and PVA/PEG/APTMS-Sil membrane, respectively. The tensile strength for PVA/PEG/Sil and PVA/PEG/APTMS-Sil film showed an increment of 43 % and 115 % as compared to PVA/PEG film. This could be attributed to the enhancement in the cross-linking density and formation of dense structure with incorporation of silica. Also, the strong interaction of the inorganic particle with the polymer matrix and its uniform distribution on the organic matrix with amino-functionalization of silica leads to superior load transfer [30]. Thus, the use of coupling agent is envisaged to promote better interfacial bond between the silica filler and the PVA matrix thereby leading to higher tensile strength [14].

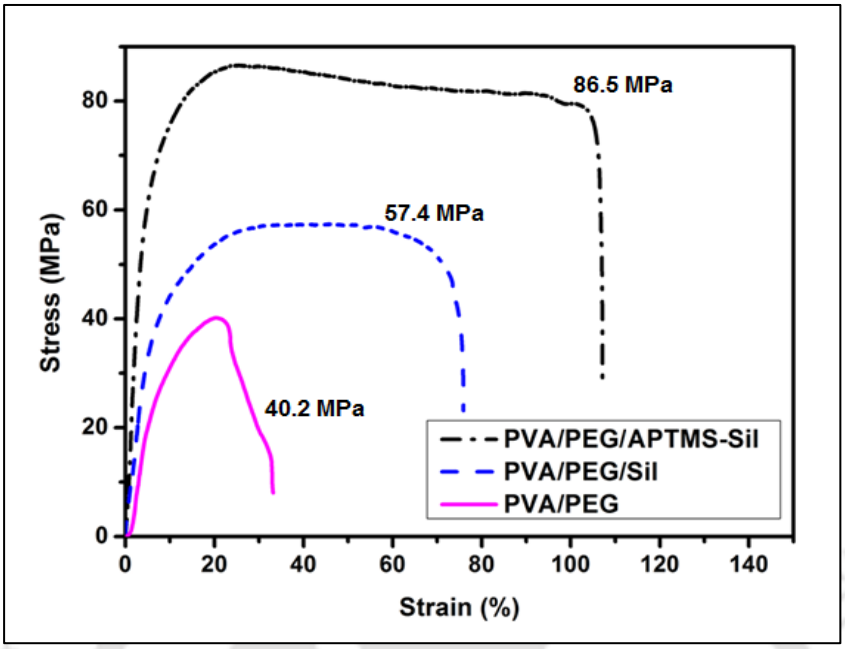

Figure 4.6 Typical stress-strain curve of PVA/PEG, PVA/PEG/Sil and PVA/PEG/APTMS-Sil membrane

4.5.6. Ninhydrin assay

The Kaiser test with ninhydrin assay confirmed the presence of APTMS on the surface modified silica (APTMS-Sil). The reaction between ninhydrin solution and amino groups leads to the formation of purple-blue complex (Ruhemann's purple) which is characteristics of ninhydrin-amino complex [31-34]. Before analysis, the unreacted APTMS was washed from the surface with ethanol. A fixed amount of amino functionalized silica sample was dispersed in 1 mL of ninhydrin solution, sonicated for 40 min and thereafter heated at 80 ºC for 20 min. A purple-blue Ruhemann's complex was formed due to the association of the ninhydrin solution with amino groups of ZIF-8. Thus the test established the successful attachment of PEI amine to the surface of the ZIF-8 filler.

4.5.7. X-ray photoelectron spectroscopy analysis (XPS)

The survey scan of XPS spectrum (Figure 4.7 a) of PVA/PEG/Sil and PVA/PEG/APTMS-Sil film (temperature ~ 24 ºC) established the presence of C, N, O, Si peaks. It also confirmed the surface composition of the silica filler with functionalization effect. The C 1s, O 1s and Si atoms contain peaks with binding energies of 285 eV, 532

eV, 152 eV (Si 2s) and 103 eV (Si 2p), respectively. The increase in the characteristic peak signal of N 1s and S 1s for PVA/PEG/APTMS-Sil film compared to PVA/PEG membrane confirmed the successful APTMS amine modification on the ZIF-8 nanocrystal surface. The high resolution spectra of C 1s and N 1s region showed strong core level transition for the element. The peak at 285.2 and 284.9 eV corresponds to the presence of (C-C) and (C-N) bonds (Figure 4.6 b). The peaks with binding energies at 285.8 and 287.5 eV corresponds to the (C-O) and (C=O) bond, respectively. The narrow scan range of N 1s peak (Figure 4.6 c) confirmed the successful addition of amino groups to the silica surface. The amino groups could be broadly classified into three different binding energies. The amines in free state, amines bonded with the O-H groups present at the surface of the particles and protonated amines were represented by binding energies of 398.2 eV, 399.6 eV and 401.8 eV, respectively [35, 36]. The presence of protonated amines indicated that carbamates are formed which explained the interaction of CO_2 molecules with the amine groups. Thus, the interaction of the silica nanoparticle with the APTMS amine moieties could be further verified by XPS analysis.

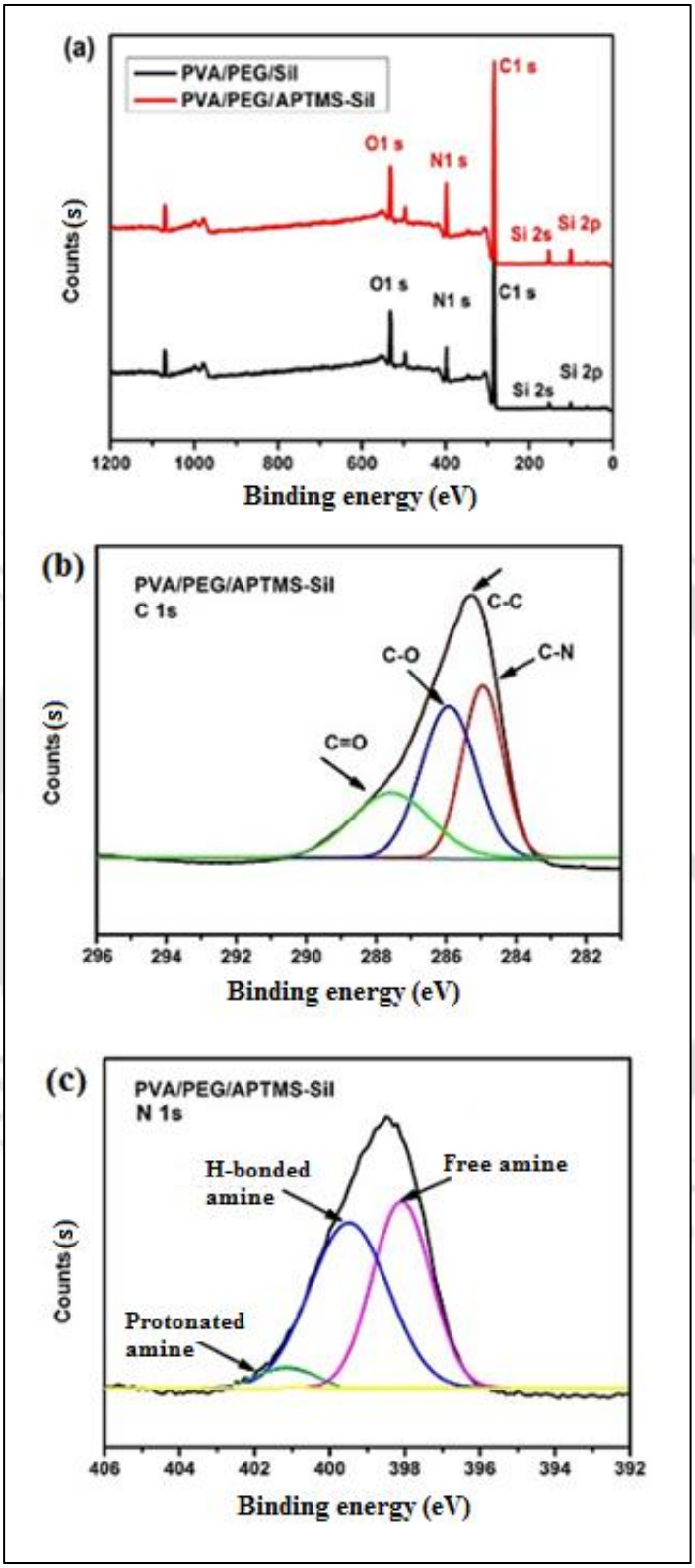

Figure 4.7 XPS analysis showing (a) survey scan of PVA/PEG/Sil and PVA/PEG/APTMS-Sil membrane, (b) C 1s peak and, (c) N 1s peak of PVA/PEG/APTMS-Sil membrane

4.6. CO_2 separation performance study of the membrane

The CO_2 separation performance of the synthesized membranes were analysed for variation of temperature (60-110 °C) and sweep water flow rate (0.01-0.075 ml/min). Binary gas (20 % CO_2 and 80 % N_2) and Argon (Ar) was used as feed and carrier gas, respectively. The effect of PVA/PEG/APTMS-Sil mixed matrix membrane on the CO_2 performance was studied. Binary feed gas mixture and sweep gas (Argon (Ar)) was considered for mixed gas permeation study.

4.6.1. Effect of temperature on CO_2 performance

The effect of temperature on the CO_2 permeance and CO_2/N_2 selectivity for the PVA/PEG/APTMS-Sil membrane was analysed. As seen in Figure 4.8(a), it was observed that with the increase in temperature up to 100 °C, the CO_2/N_2 selectivity and CO_2 permeance showed an inclination. This could be attributed by the contributed effect of the increased CO_2 solubility and diffusivity, and enhanced CO_2-amine reaction rate contributed by the carrier along with the additional amines attached to silica nanoparticle surface. The enhancement in the facilitated transport by the additional amino groups attached to the surface of the silica nanoparticle along with the PEI amines which acts as fixed carrier augments the CO_2-amine reversible reaction mechanism. This can be attributed to the increased CO_2-amine reversible rate of reaction governed by the facilitated transport mechanism in the presence of temperature and moisture content. However, at higher temperature (>100 ºC), the restriction in water content lowered the facilitated transport properties [37-39].

The PVA/PEG/APTMS-Sil membrane showed optimum CO_2 permeance and CO_2/N_2 selectivity of 36 GPU and 325 at a temperature of 100 ºC, feed and sweep side absolute pressure of 2.5 atm and 1.2 atm and feed and sweep side water flow rates of 0.03 ml/min and 0.04 ml/min, respectively.

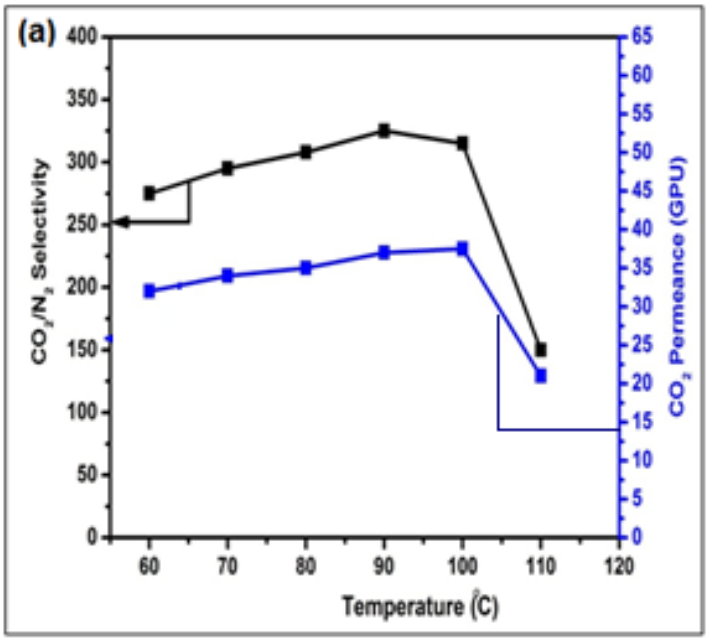

Figure 4.8(a) Effect of temperature on CO_2 permeance (GPU) and CO_2/N_2 selectivity at feed absolute pressure = 2.5 atm, sweep absolute pressure = 1.2 atm, sweep/feed water flow ratio = 1.67

4.6.2. Effect of sweep water flow rate on CO_2 performance

The change in CO_2 permeance and CO_2/N_2 selectivity with variation in sweep water flow rate from (0.01-0.075 ml/min) was analysed as shown in Figure 4.8(b). With increased sweep water content (up to 0.04 ml/min), the CO_2 permeance and CO_2/N_2 selectivity showed an uptrend. This could be attributed to the increased mobility of CO_2-carrier complex occurring through the CO_2-carrier reactions with increasing water content. At sweep water flow rate > 0.04 ml/min, both CO_2 permeance and CO_2/N_2 selectivity showed a constant value attributed to the carrier saturation inside the membrane material. Also, it is envisaged that the presence of amino modified silica nanoparticle caused disruption of the polymer chain packing thereby increasing the presence of overall fractional free volume and improving in the penetrant gas interaction. Further, the smaller molecular size and condensability of CO_2 gas molecule as compared to N_2 molecules is expected to accelerate its transport across the membrane [40, 41].

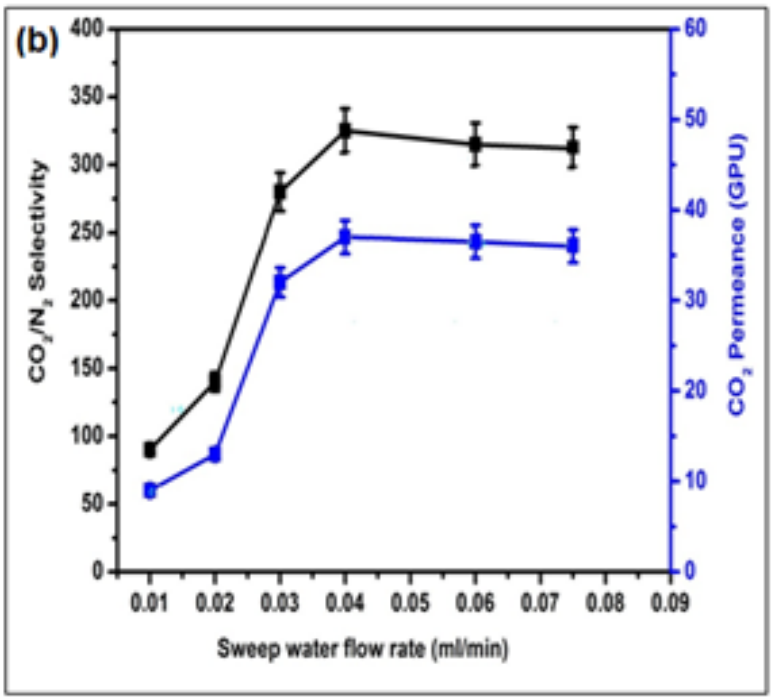

Figure 4.8(b) Effect of sweep water flow rate (ml/min) on CO_2 permeance (GPU) and CO_2/N_2 selectivity at temperature of 100 ºC, feed and sweep absolute pressure of 2.5 and 1.2 atm

The PVA/PEG/APTMS-Sil membrane showed CO_2 permeance of 36 GPU and CO_2/N_2 selectivity of 325 at fixed conditions of 100 ºC temperature, 0.03/0.04 ml/min feed /sweep water flow rate and 2.5/1.2 atm feed/sweep side pressure. These results showed significant augmentation in the CO_2 permeance (GPU) and CO_2/N_2 selectivity by 141 % and 55 % and by ~33 % and 8 % in comparison to PVA/PEG and PVA/PEG/Sil membrane, respectively. The effect of CO_2 permeance (GPU) and CO_2/N_2 selectivity on PVA/PEG, PVA/PEG/Sil and PVA/PEG/APTMS-Sil at temperature = 100 ºC, feed/ sweep water flow rate= 0.03/0.04 ml/min, and feed/sweep side pressure= 2.5/1.2 atm was represented in Figure 4.9.

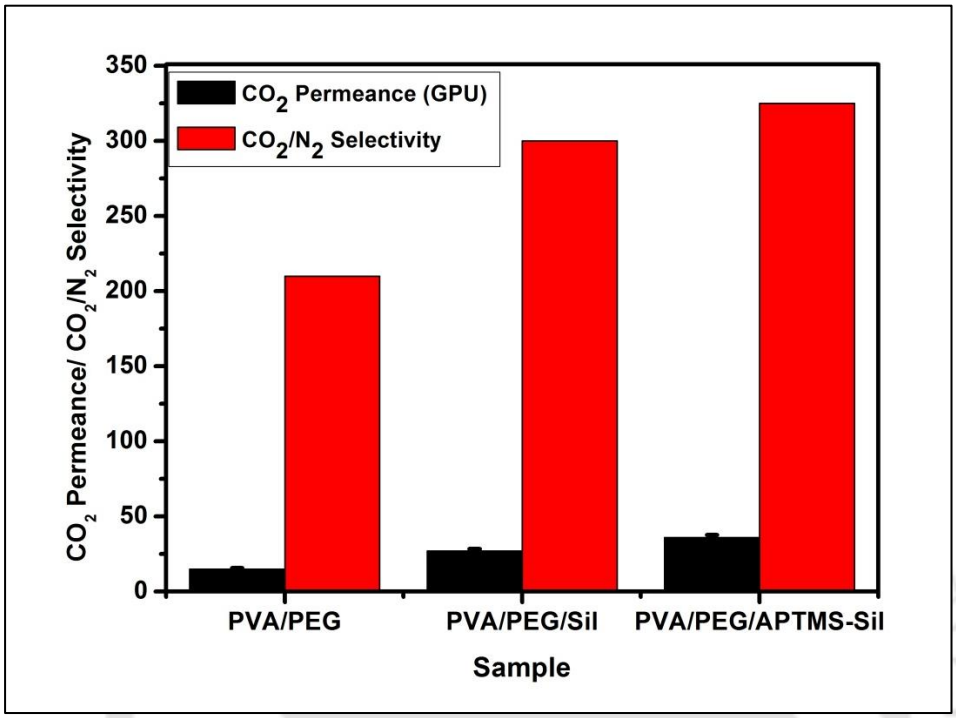

Figure 4.9 Effect of CO_2 permeance (GPU) and CO_2/N_2 selectivity on PVA/PEG, PVA/PEG/Sil and PVA/PEG/APTMS-Sil at temperature=100 °C, feed/ sweep water flow rate= 0.03/0.04 ml/min, and feed/sweep side pressure= 2.5/1.2 atm, respectively

4.7. Robeson's curve

The experimental results in this work exceeded the Robeson's upper bound barrier with exceptional CO_2 separation (Figure 4.10). Thus it can be concluded that addition of silica filler and its subsequent amine modification aggravates the CO_2 separation performance with better results pertaining to CO_2 permeability and CO_2/N_2 selectivity.

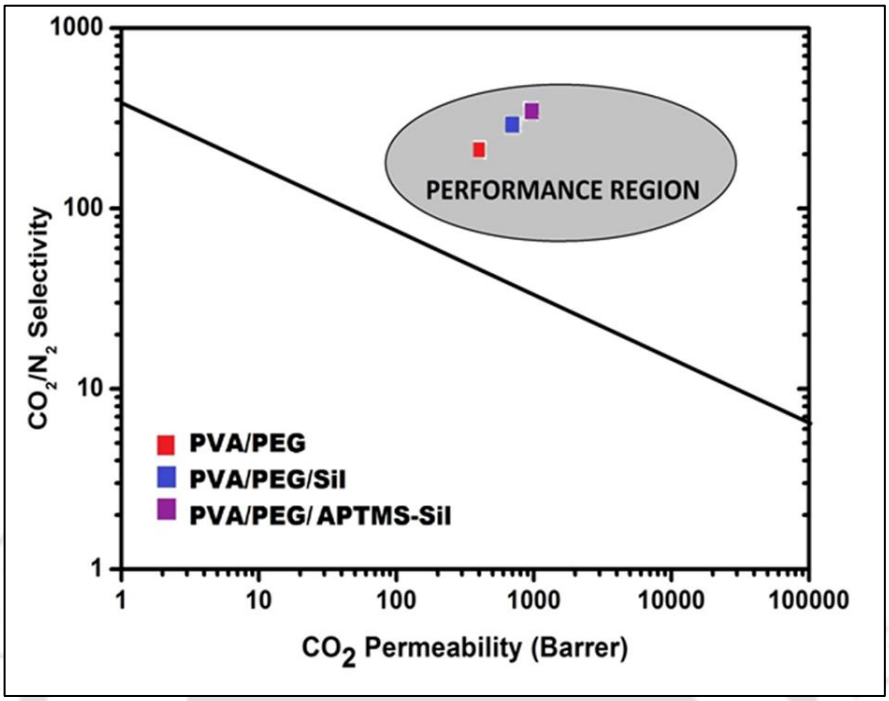

Figure 4.10 Robeson's upper bound curve of PVA/PEG, PVA/PEG/Sil and PVA/PEG/APTMS-Sil membrane

4.8. Conclusions

This study reports the formation of silica nanoparticle and its subsequent amine modification by 3-aminopropyltrimethoxysilane (APTMS) coupling agent. FESEM study established the increased surface roughness of the membrane with incorporation of APTMS-Sil thereby enhancing the reaction surface area aiding in the CO_2 permeability. Also, the tensile strength of PVA/PEG/APTMS-Sil film showed an increment by 115 % compared to PVA/PEG film as confirmed by UTM analysis. The successful impregnation of APTMS amine into the silica nanoparticle was further confirmed by ninhydrin assay and XPS analysis. The integrated positive effect of the amine carriers and the surface functionalization of nanoparticles imparts enhancement in the CO_2 permeance and CO_2/N_2 selectivity. The CO_2 permeance and CO_2/N_2 selectivity of

PVA/PEG/APTMS-Sil membrane obtained optimal results of 36 GPU and 325 for temperature of 100 °C, water flow rate of 0.03/0.04 ml/min (feed/sweep) surpassing the Robeson's curve. These results showed a remarkable boost in CO_2 permeance (GPU) and CO_2/N_2 selectivity by 141 % and 55 % when compared to PVA/PEG membrane. Thus, the superior gas separation properties of PVA/PEG/APTMS functionalized silica mixed matrix membrane could provide a striking opportunity for its utilization in large-scale CO_2 capture solution.

References

[1] M. Wang, Z. Wang, S. Zhao, J. Wang and S. Wang, Recent advances on mixed matrix membranes for CO_2 separation, Chin. J. Chem. Eng. 25(11) (2017) 1581-1597.

[2] B. Prasad and B. Mandal, Moisture responsive and CO_2 selective biopolymer membrane containing silk fibroin as a green carrier for facilitated transport of CO_2, J. Membr. Sci. 550 (2018) 416-426.

[3] J. Hu, J.H. Cai, H. Ren, Y. Wei, Z. Xu, H. Liu and Y. Hu, Mixed matrix membrane hollow fibers of $Cu_3(BTC)_2$ MOF and polyimide for gas separation and adsorption, Ind. Eng. Chem. Res. 49(24) (2010) 12605-12612.

[4] T.S. Chung, L.Y. Jiang, L. Yi and S. Kulprathipanja, Mixed matrix membranes (MMMs) comprising organic polymers with dispersed inorganic fillers for gas separation, Prog. Polym. Sci. 32 (2007) 483–507.

[5] M. Vinoba, M. Bhagiyalakshmi, Y. Alqaheem, A.A. Alomair, A. Perez and M.S. Rana, Recent progress of fillers in mixed matrix membranes for CO_2 separation: A review, Sep. Purif. Technol. 188 (2017) 431-450.

[6] B. Ghalei, A.P. Isfahani, S. Nilouyal, E. Vakili and M.K. Salooki, Effect of polyvinyl alcohol modified silica particles on the physical and gas separation properties of the polyurethane mixed matrix membranes, Silicon. (2018).

[7] A. Mondal and B. Mandal, Novel CO_2-selective cross-linked poly (vinyl alcohol)/ polyvinylpyrrolidone blend membrane containing amine carrier for CO_2–N_2 separation: synthesis, characterization, and gas permeation study, Ind. Eng. Chem. Res. 53(51) (2014) 19736-19746.

[8] L. Dong, M. Chen, J. Li, D. Shi, W. Dong, X. Li and Y. Bai, Metal-organic framework-graphene oxide composites: A facile method to highly improve the CO_2 separation performance of mixed matrix membranes, J. Membr. Sci. 520 (2016) 801-811.

[9] M. Isanejad and T. Mohammadi, Effect of amine modification on morphology and performance of poly (ether-block-amide)/fumed silica nanocomposite membranes for CO_2/CH_4 separation, Mater. Chem. Phys. 205 (2018) 303-314.

[10] S.B. Hamouda and S. Roudesli, Transport properties of PVA/PEI/PEG composite membranes: sorption and permeation characterizations, Cent. Eur. J. Chem. 6(4) (2008) 634-640.

[11] M. Barooah and B. Mandal, Enhanced CO_2 separation performance by PVA/PEG/silica mixed matrix membrane, J. Appl. Polym. Sci. 46481 (2018) 1-12.

[12] H. Pingan, J. Mengjun, Z. Yanyan and H. Ling, A silica/PVA adhesive hybrid material with high transparency, thermostability and mechanical strength, RSC Adv. 7 (2017) 2450-2459.

[13] J. Li, J. Suo and R. Deng, Structure, mechanical, and swelling behaviours of poly (vinyl alcohol)/SiO_2 hybrid membranes, J. Reinf. Plast. Compos. 29 (2010) 618–629.

[14] J. Kim and Y. Lee, Gas permeation properties of poly (amide-6-b-ethylene oxide)–silica hybrid membranes, J. Membr. Sci. 193 (2001) 209-225

[15] H. Cong and B. Yu, Aminosilane cross-linked PEG/PEPEG/PPEPG membranes for CO_2/N_2 and CO_2/H_2 separation, Ind. Eng. Chem. Res. 49 (19) (2010) 9363–9369.

[16] S. Hasebe, S. Aoyama, M. Tanaka and H. Kawakami, CO_2 separation of polymer membranes containing silica nanoparticles with gas permeable nano-space, J. Membr. Sci. 536 (2017) 148−155.

[17] G. Xomeritakis, C.Y. Tsai and C.J. Brinker, Microporous sol–gel derived aminosilicate membrane for enhanced carbon dioxide separation, Sep. Purif. Technol. 42 (2005) 249-257.

[18] S. Suzuki, S.B. Messaoud, A. Takagaki, T. Sugawara, R. Kikuchi and S.T. Oyama, Development of inorganic–organic hybrid membranes for carbon dioxide/methane separation, J. Membr. Sci. 471 (2014) 402-411

[19] K.S. Jang, H.J. Kim, J. Johnson, W.g. Kim, W.J. Koros and C.W. Jones, Modified mesoporous silica gas separation membranes on polymeric hollow fibers, Chem. Mater. 23 (2011) 3025-3028

[20] S.B. Messaoud, A. Takagaki, T. Sugawara, R. Kikuchi and S.T. Oyama, Alkylamine–silica hybrid membranes for carbon dioxide/methane separation, J. Membr. Sci. 477 (2015) 161-171.

[21] J. Abdi, M. Vossoughi, N.M. Mahmoodi and I. Alemzadeh, Synthesis of amine-modified zeolitic imidazolate framework-8, ultrasound-assisted dye removal and modelling, Ultrason. Sonochem. 39 (2017) 550-564.

[22] Y. Sakamoto, K. Nagata, K. Yogo and K. Yamada, Preparation and CO_2 separation properties of amine-modified mesoporous silica membranes, Micropor. Mesopor. Mater. 101 (2007) 303-311.

[23] H.J. Kim, W. Chaikittisilp, K.S. Jang, S.A. Didas, J.R. Johnson, W.J. Koros, S. Nair and C.W. Jones. Aziridine-functionalized mesoporous silica membranes on polymeric hollow fibers: synthesis and single-component CO_2 and N_2 permeation properties, Ind. Eng. Chem. Res. 54 (2014) 4407-4413

[24] M. Zargar, Y. Hartanto, B. Jin and S. Dai, Polyethyleneimine modified silica nanoparticles enhance interfacial interactions and desalination performance of thin film nanocomposite membranes, J. Membr. Sci. 541 (2017) 19-28.

[25] S.C. Shen, W.K. Ng, L. Chia, Y.C. Dong and R.B.H. Tan, Sonochemical synthesis of (3-aminopropyl) triethoxysilane-modified monodispersed silica nanoparticles for protein immobilization, Mater. Res. Bull. 46 (2011) 1665-1669.

[26] M. Ostwal, R.P. Singh, S.F. Dec, M.T. Lusk and J.D. Way, Aminopropyltriethoxysilane functionalized inorganic membranes for high temperature CO_2/N_2 separation, J. Membr. Sci. 369 (2011) 139-147

[27] E.P.F. Nhavene, G.F. Andrade, J.A.Q.A. Faria, D.A. Gomes and E.M.B.de Sousa, Biodegradable polymers grafted onto multifunctional mesoporous silica nanoparticles for gene delivery, Chem Eng. 2 (2018) 24.

[28] T. Sakpal, A. Kumar, S. Kamble and R. Kumar, Carbon dioxide capture using amine functionalized silica gel, Indian J. Chem. 51A (2012) 1214-1222.

[29] H. Luo, J. Lu, S. Ren, G. Fang and G. Jiang, Studies of polyvinyl alcohol/alkali lignin/silica composite foam material (PLCFM), Bioresources. 10(3) (2015) 5961-5973.

[30] E.S. Cantu, R. Cueto, J. Koch and P.S. Russo, Synthesis and rapid characterization of amine-functionalized silica, Langmuir. 28 (2012) 5562−5569.

[31] S.H. Araghi and M.H. Entezari, Amino-functionalized silica magnetite nanoparticles for the simultaneous removal of pollutants from aqueous solution, Applied Surf. Sci. 333 (2015) 68–77.

[32] L.F. de Oliveira, K. Bouchmella, A.S. Picco, L.B. Capeletti, K.A. Gonçalves, J.H. Z. dos Santos, J. Kobarge and M.B. Cardoso, Tailored silica nanoparticles surface to increase drug load and enhance bactericidal response, J. Braz. Chem. Soc. 28(9) (2017) 1715-1724

[33] H.T. Lu, Synthesis and characterization of amino functionalized silica nanoparticles, Colloid J. 75(3) (2013) 311–318.

[34] K. Choi, S. Lee, J.O. Park, J.A. Park, S.H. Cho, S.Y. Lee, J.H. Lee and J.W. Choi, Chromium removal from aqueous solution by a PEI-silica nanocomposite, Sci. Rep. (2018) 8:1438.

[35] W. Qin, F. Vautard, P. Askeland, J. Yu and L. Drzal, Modifying the carbon fiber–epoxy matrix interphase with silicon dioxide nanoparticles, RSC Adv. 5 (2015) 2457-2465.

[36] M. Barooah and B. Mandal, Synthesis, characterization and CO_2 separation performance of novel PVA/PG/ZIF-8 mixed matrix membrane, J. Membr. Sci. 572 (2019) 198-209.

[37] B. Prasad and B. Mandal, Graphene-incorporated biopolymeric mixed-matrix membrane for enhanced CO_2 separation by regulating the support pore filling, ACS Appl. Mater. Interfaces. 10 (2018) 27810−27820.

[38] B. Prasad and B. Mandal, Moisture responsive and CO_2 selective biopolymer membrane containing silk fibroin as a green carrier for facilitated transport of CO_2, J. Membr. Sci. 550 (2018) 416-426.

[39] M. Jia, Y. Feng, J. Qiu, X.F. Zhang and J. Yao, Amine-functionalized MOFs@GO as filler in mixed matrix membrane for selective CO_2 separation, Sep. Purif. Technol. 213 (2019) 63-69.

[40] A. Mondal, and B. Mandal, CO_2 separation using thermally stable crosslinked poly (vinyl alcohol) membrane blended with polyvinylpyrrolidone/ polyethyleneimine/ tetraethylenepentamine, J. Membr. Sci. 460 (2014) 126-138

[41] A. Mondal, M. Barooah and B. Mandal, Effect of single and blended amine carriers on CO_2 separation from CO_2/N_2 mixtures using crosslinked thin-film poly (vinyl alcohol) composite membrane, Int. J. Greenh. Gas. Con. 39 (2015) 27–38

CHAPTER 5

Synthesis and Characterization of Novel PVA/PG and PVA/PG/ZIF-8 Membrane for CO_2/N_2 Separation

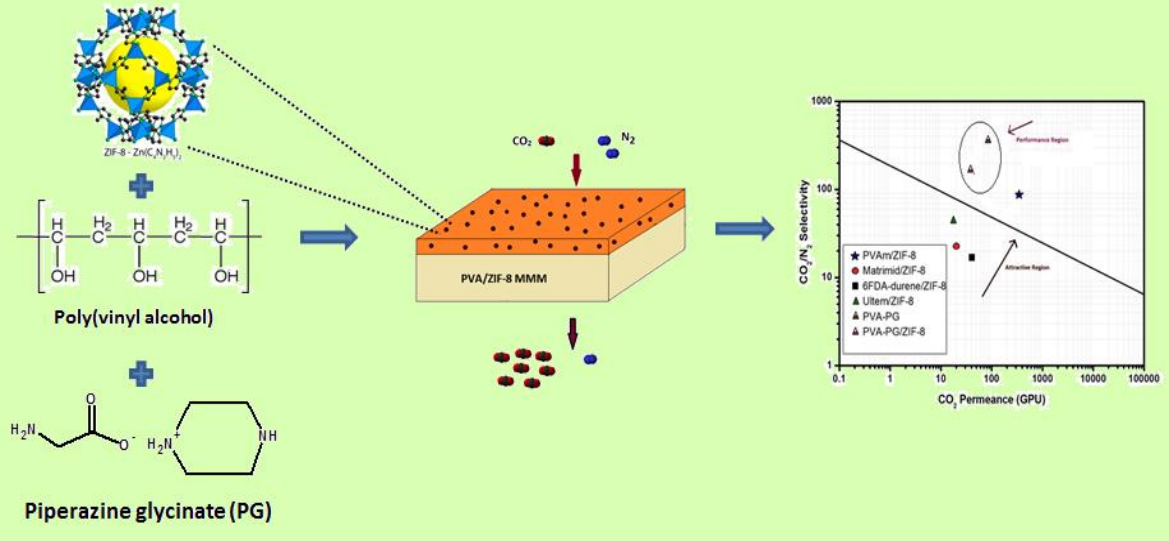

Graphical abstract of PVA/PG/ZIF-8 mixed matrix membrane synthesis and the Robeson's upper curve

CHAPTER 5

Synthesis and Characterization of Novel PVA/PG and PVA/PG/ZIF-8 Membrane for CO_2/N_2 Separation

This chapter aims at investigating zeolitic imidazolate framework-8 (ZIF-8) metal-organic framework (MOF) as filler material for CO_2 separation. The synthesised ZIF-8 MOF (regular pore size ~0.35 nm) embedded into the poly (vinyl alcohol) (PVA)/ piperazine glycinate (PG) solution were cast on the PES support to impart mechanical stability to the membrane. The ZIF-8 could serve as a potential molecular sieving material. Its partial organic nature when combined with the organic PVA/PG polymer matrix could pave the way for the formation of intrinsically compatible defect-free novel MMM for effective CO_2 separation. Detailed characterization techniques revealed the thermal and mechanical property enhancement with incorporation of ZIF-8 filler into this novel combination. The PVA/PG/ZIF-8 membrane could thereby be considered as a potential pathway for industrial CO_2 separation studies. This work is scientifically published in the journal, ***"Journal of Membrane Science".***

5.1. Introduction

Polymer membranes which usually follow solution-diffusion mechanism are subject to trade-off limitation between gas permeability and selectivity usually called the Robeson's upper bound limitation. To overcome these constraints, amino groups which are introduced into the membrane improves the CO_2 permeation by following the facilitated transport mechanism. However, in most cases, the lack of mobility in fixed site carriers leads to lower CO_2 permeability compared to mobile carriers. Amines such as alkalines and amino acid salts have been utilized as mobile carriers in CO_2 facilitated transport membrane. Among them, the amino acid salts have advantages of high diffusivity and negligible volatility [1]. Due to the fast reaction kinetics and high CO_2 absorption capacity, amino acid salts have been intensively studied as CO_2 absorbents [2]. Ho et al. [3] studied the effects of different amino acid salts on membrane transport performance and found that piperazine glycinate (PG) amino acid salt as mobile carrier performed better compared to potassium glycinate and lithium glycinate salts. Also, the

high-performance of MMM is greatly influenced by the polymer-filler interface compatibility in the absence of which non-selective voids at the interface is obtained. This leads to comparatively higher diffusion of larger gas molecules thereby leading to steep decline in overall selectivity. Thus, the good affinity between filler and polymer material plays a major role in the formation of desired defect-free MMMs [4-5]. Among the common fillers [6-16], metal-organic framework (MOF) is hugely preferred over others for MMM fabrication. This class of hybrid organic-inorganic crystalline nanoporous framework offers high porosity, adjustable pore size, specific surface area and convenient synthesis process. When compared to zeolites, silica, or other porous materials, MOFs offer advantages of large surface area making it an attractive candidate for gas separation. In addition, the highly tunable physical and chemical characteristic makes it a desirable filler material in MMMs [18-21]. Zeolitic imidazolate framework (ZIFs), a subclass of MOFs consisting of transition metal ions (e.g., Zn, Co) linked by imidazolate ligands to form tetrahedral frameworks resembling zeolite topologies exhibit high thermal and chemical stability along with permanent porosity. ZIF-8 has a sodalite (SOD) structure connected with a large pore size of 11.6 Å and small pore size of 3.4 Å [22]. The ZIFs with the nanoporous structure could effectively serve as a potential molecular sieving material for separation of gas molecules with small kinetic diameters (such as CO_2, H_2) along with gas storage facility [23]. Also, the partial organic nature of the imidazolate linkers in ZIF-8 when combined with the organic polymer matrix improves the interfacial compatibility between the two phases [24, 25]. Thus we envisage that the formation of intrinsically compatible defect-free polymer/ZIF-8 MMM without any complex membrane modification technique will present a potential route for effective CO_2 separation. Literature has reported an extensive application of ZIF-8 fillers for CO_2 adsorption capacities and also its performance as fillers in MMMs for gas separation [26]. Different polymers such as 6FDA-durene diamine, polyvinyl amine (PVA_m), PIM-1 embedded with ZIF-8 particle have been reported. However, the noteworthy combination of polyvinyl alcohol (PVA) and ZIF-8 has not yet been explored for CO_2 gas separation studies. Song et al. [27] studied the Matrimid /ZIF-8 membrane and reported CO_2 permeability at different ZIF-8 loading. It was observed that

with the increase in ZIF-8 loading to 20 wt %, the CO_2 permeance increased 2 folds compared to polymer membrane. Also, an increment in the N_2 permeance and overall selectivity was observed. Nafisi and Hagg [28] reported 6FDA-durene diamine/ ZIF-8 membrane with improvement in CO_2 permeance by 50 % with the incorporation of 30 wt % ZIF-8 into 6FDA-durene diamine matrix. Zhao et al. [29] studied the separation performance of PVA_m/ ZIF-8 membranes and reported CO_2 permeance as high as 297 GPU along with a selectivity of 83. Chen and Ho [30] reported PVA_m / piperazine glycinate (PG) membranes with CO_2 permeance as high as 1100 GPU and CO_2/N_2 selectivity of more than 140 at a flue gas temperature of 57 $^{\circ}$C and 17 % water vapor with a low active layer thickness of 100-200 nm. Bushell et al. [31] studied the separation performance of PIM-1/ ZIF-8 membrane. Increased CO_2/CH_4 selectivity along with decreased CO_2 permeance was observed by incorporating 28 vol % ZIF-8 into PIM-1. Zhang et al. [32] successfully incorporated ZIF-8 into polyimide and achieved high-performance propylene/propane separation. Very recently, Kwon et al. [33] studies showed improved propylene/propane separation by growing ZIF-67 on ZIF-8 seed layers. Amirilargani et al. [34] reported poly (vinyl alcohol)/ zeolitic imidazolate frameworks (ZIF-8) mixed matrix membranes and studied the pervaporation property of isopropanol. The characterization analysis showed improved thermal, mechanical and morphological results with the addition of ZIF-8 loading into the PVA polymer matrix. Thus, the combination of the film forming ability of PVA along with the excellent molecular sieving properties of the ZIF-8 to form defect-free PVA/ZIF-8 membrane is expected to provide a new, innovative approach for improved CO_2 gas separation studies. In this study, crosslinked poly (vinyl alcohol) of high molecular weight was used as the base polymer. To the aqueous polymer solution, the synthesized piperazine glycinate (PG) amino acid salt (Figure 5.1a) solution was added in a fixed stoichiometric amount. The PG salts act as mobile carrier incorporating facilitated transport mechanism and leading to a considerable enhancement in CO_2 transport as compared to pure PVA membrane films. The PVA/PG membrane was further doped with ZIF-8 nano-fillers (Figure 5.1b) and the changes in the separation results analysed. We envisage that the inclusion of ZIF-8 nanoparticles interrupts the PVA/PG blend polymer chain packing thus increasing the free volume and diffusion pathway for gas penetrants resulting in the

upsurge in the CO_2 permeance. Also, the molecular sieving property of the ZIF-8 particle is expected to separate the smaller CO_2 gas molecules through its interior cavity thereby leading to the increment in CO_2/N_2 selectivity. Literature has reported PVA_m/ZIF-8 membrane and found good results for CO_2 transport. However, this work is an attempt to synthesize facilitated transport novel membrane in a more economical way by considering low-cost materials and tailoring it into high-performance mixed matrix membranes. The novelty of the present work is in the incorporation of ZIF-8 filler into the PVA/PG membrane, the combination of which has not been reported for gas separation studies till date. The thermal and mechanical property enhancement with the addition of ZIF-8 fillers and piperazine glycinate salt (PG) carriers was thoroughly analysed and discussed. The PVA/PG/ZIF-8 membrane thereby is considered to provide CO_2-facilitated transport pathway for high CO_2 separation performance.

5.2. Materials

Poly (vinyl alcohol) (99 mol % hydrolyzed powder, M_w = 130,000), and 2-methylimidazole (Hmim) [$C_4H_6N_2$] were purchased from Sigma-Aldrich, USA. Formaldehyde solution (37 wt % in H_2O), glycine (Assay> 99 %), piperazine (99 %), zinc nitrate hexahydrate [$Zn(NO_3)_2.6H_2O$], and methanol were obtained from Merck, India. All chemicals were used without any further purification. Poly (ether sulfone) (PES) supports (thickness: 150 μm and pore size: 0.03 μm) were provided by Sterlitech USA. Binary feed gas (20 % CO_2 and 80 % N_2) mixtures used for the gas permeation analysis was supplied by Vadilal Pvt. Ltd., India.

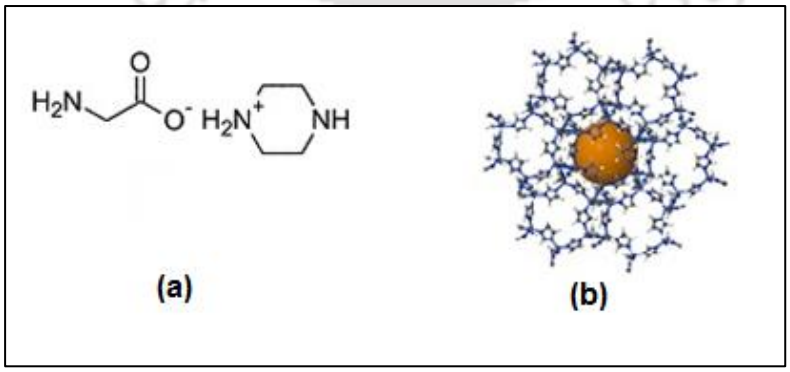

Figure 5.1 Structural formulas of (a) Piperazine glycinate (PG), and (b) ZIF-8 nanocrystal

5.3. Experimental

5.3.1. Synthesis of piperazine glycinate salt

The piperazine glycinate salt solution was synthesized by a method reported by Chen and Ho [30]. Stoichiometric amount of aqueous glycinate solution was prepared by continuous stirring at ambient condition for 2 h. Thereafter, calculated amount of piperazine was added to the glycine solution leading to the formation of amino acid salts. The piperazine and glycinate salt was further mixed together and stirred continuously for another 2 h until a homogeneous PG mobile carrier solution was formed which was utilized for the MMM preparation.

5.3.2. Synthesis of crosslinked PVA/PG membrane

The PVA polymer solution was prepared as mentioned [35-37]. Here in, the dopant solution was cast onto porous poly (ether sulfone) support (average pore size: 0.03 µm). The PVA aqueous solution (10 wt % solid weight) was prepared by continuously stirring at a temperature of 90 C maintained constant via oil bath. The PVA solution was in-situ crosslinked with formaldehyde at a ratio already optimized through our previous studies. Thereafter, the prepared PG salt solution was added fixed in the weight ratio of 70 and 30 to form the final crosslinked PVA/PG polymer solution. The prepared solutions at high viscosity (~ 1200 cp) were then centrifuged (10000 rpm, 30 min) to remove any air bubble or undissolved particle. The final centrifuged solution was then cast onto the porous PES support kept over glass plate. The thickness of the polymer film was maintained by a micrometre adjustable film applicator (GARDCO, Paul N. Gardner, USA). The approximate dry coating thickness was assumed based on the equation:

$$l_2 \times r_2 = 0.5 \times c_1 \times r_1 \times l_{gap} \qquad (5.1)$$

where l_2 is the dry thickness of the coated PVA/PG membrane, r_2 the dry membrane density, c_1 the total solid weight concentration of the coating solution, r_1 the coating solution density, and l_{gap} the gap setting of the coating knife. The dense selective layer thickness obtained by the above equation is comparable to the results obtained by litematic digimatic measuring unit (Make: Mitutoyo, Model: VL-50) with an accuracy of

about ± 0.5µm, and FESEM images. The membrane was dried overnight in a laminar flow chamber under ambient condition followed by heating in the oven at 120 °C for 10 hours. The thickness of the active layers was calculated to be around 4 µm. The membrane effective area was considered to be 8.5 cm^2.

5.3.3. Synthesis of ZIF-8 nanocrystal

ZIF-8 was synthesized following the procedure explained by Cravillon et al. [38]. A fixed amount of precursor, Zn $(NO_3)_2.6H_2O$ (2.933 gm) was added to 200 ml of methanol to form zinc nitrate solution. The ligand solution was prepared by adding 6.48 gm of 2-methylimidazole (Hmim) into 200 ml of methanol. Both the solutions were then mixed and the resultant solution was stirred vigorously for 1 h. The final milky solution was allowed to rest for 12 h. It was then centrifuged at around 10,000 rpm for 35 min and finally washed three times with methanol. This step was repeated several times until the formation of ZIF-8 nanoparticles. The mechanism of ZIF-8 synthesis is depicted in Figure 5.2.

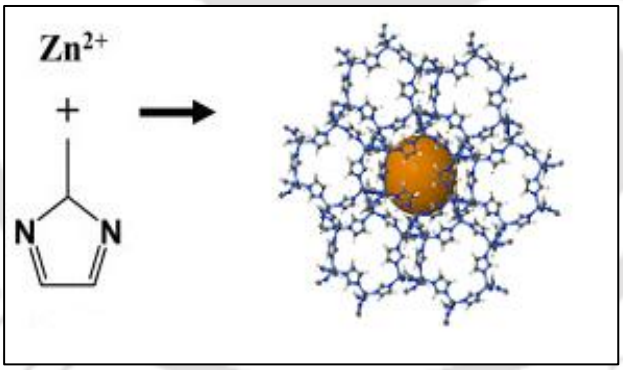

Figure 5.2 Mechanism of ZIF-8 synthesis

5.3.4. Synthesis of crosslinked PVA/PG/ZIF-8 membrane

The MMM sample with ZIF-8 particle loading of 5 wt % was denoted by PVA/PG/ZIF-8. The final centrifuged solutions were cast onto the porous PES support. The membrane was dried overnight in a laminar flow chamber under ambient condition followed by heating in the oven at 120 °C for 10 h. The thickness was maintained by a micrometer adjustable film applicator (GARDCO, Paul N. Gardner, USA) calculated to be ~4 µm.

5.4. Membrane characterization

The thermal effect of the polymer film was studied using TGA analysis (TGA4000, Perkin-Elmer, USA). Heat treatment was carried out from 25 °C to 900 °C at the rate of 10 °C/min under N_2 environment. The glass transition temperature (T_g) was determined by subjecting the sample to double heating-cooling system using 1/400 STARe system (METTLER TOLEDO, Switzerland). The functional groups present in the ZIF-8 nanoparticle and the synthesized active layer were confirmed from the ATR-FTIR (SHIMADZU, IRAffinity 1, and Japan) with wavenumber in the range of 4000 to 400 cm^{-1}, 40 scans per sample and 4 cm^{-1} resolution. The ZIF-8 particles are added with KBr pellets for sample analysis. XRD analysis was performed using Bruke D8, for 2θ angles between 10^o and 60^o with Cu Kα radiation (30 kV-40 mA). The samples for BET were degassed for 24 h followed by the analysis. The internal surface area was determined by BET method and the micropore volume by the t-plot method. The surface property was investigated by AFM, Innova, Bruker. It was processed using Windows-Scanning-x-Microscope (WSxM) software at a scan rate of 0.7 Hz (tapping mode). The top and cross-sectional image confirms the surface morphology and distribution of the ZIF-8 particles in the membrane by FESEM, ZEISS, USA and EDX analysis. The samples were first fractured in liquid nitrogen for ease of analysis, fixed on a stub with a carbon tape and then sputter coated with gold prior to imaging. XPS was conducted using Thermo Scientific Escalab Xi^+ XPS spectrometer for quantitative and qualitative nalysis of surface chemical state. The X-ray source was mono-chromated Al Kα radiation of pot size 900 µm. The analysis pressure was maintained at 7×10^{-9} mBar and the data was recorded using Avantage v5.984 software.

5.5. Results and discussion

5.5.1. Thermogravimetric analysis (TGA)

Thermal stability of ZIF-8 nanoparticle, and dense selective PVA/PG, and PVA/PG-ZIF-8 (ZIF-8 loading 5 wt %) layer was investigated using thermo-gravimetric analysis as shown in Figure 5.3. The weight loss of ZIF-8 filler, PVA/PG and PVA/PG/ZIF-8 and its effect on the thermal stability and phase transition was analysed. The samples showed three distinct stages of weight loss. For synthesized ZIF-8 particles, a long plateau was observed in the temperature range of 300-550 °C, indicating excellent thermal stability to 550 °C of the synthesized ZIF-8 particles. ZIF-8 showed no significant weight drop to 250 °C indicating hydrophobic pores [39]. At 250 °C, a negligible weight loss of 5 wt % referred to the removal of the moisture physically absorbed during the synthesis process. From 500-600 °C, the weight loss of around 10 wt % was due to the solvent loss and loss of moisture entrapped in the ZIF-8 nanocrystal. For PVA/PG and PVA/PG/ZIF-8 membrane, the initial weight loss below 150 °C is due to the loss of moisture captured from the atmosphere during membrane synthesis along with other volatile matters. The weight loss in the second stage from 210-360 °C is due to the depletion of hydroxyl groups and free amine groups from the polymer matrix. It was observed that the weight loss in case of PVA/PG/ZIF-8 membrane is significantly less (30 %) when compared to the pure PVA/PG membrane (60 %). This can confirm good interaction between the polymer and ZIF-8 filler. The increase in polymer chain stiffness and backbone rigidity with addition of ZIF-8 leads to an increment in the overall thermal behaviour [40, 41]. The final weight loss at 405 °C is attributed to the breakdown of the C-C polymer backbone. The residual weight loss was 19.8 % for PVA/PG/ZIF-8 membrane which reduced to 8.1 % for PVA/PG membrane. Thus it can be inferred that the PVA/PG/ZIF-8 membrane showed better thermal stability compared to PVA/PG membrane. Also, the stable performance of the membranes to 150 °C as shown by TGA curve reinstates the thermal stability of membrane for CO_2 separation performance study for a temperature range of 25-90 °C.

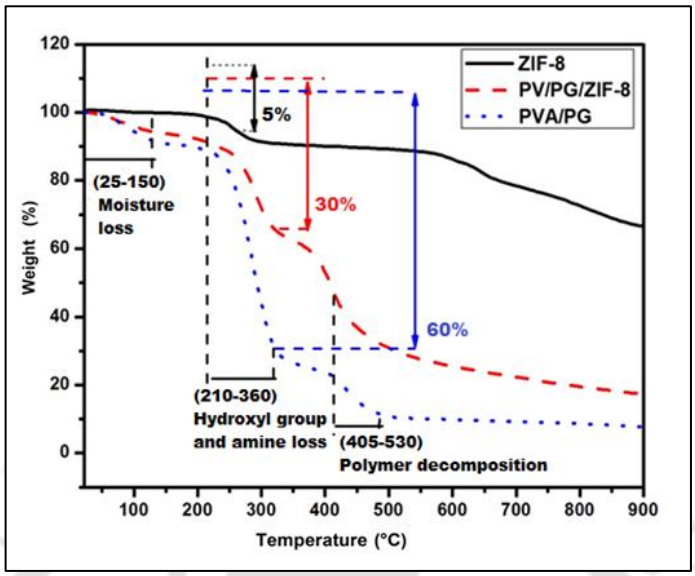

Figure 5.3 TGA curve of ZIF-8, PVA/PG and PVA/PG/ZIF-8 membrane

5.5.2. Fourier transform infrared spectroscopy analysis (FTIR)

The FTIR characterization of the synthesized ZIF-8 filler, PVA/PG and PVA/PG/ZIF-8 membrane was depicted in Figure 5.4. The peaks of the synthesized ZIF-8 filler were similar to the reported data [42-44]. The synthesized material exhibited the adsorption bands of the functional group of imidazole units. The peaks for ZIF-8 were derived from the ligands of 2-methylimidazole. The sharp peak at 3620 cm^{-1} is due to O−H bond indicative of the presence of water molecule in the crystal. The absorption band at 3180 cm^{-1} and 2920 cm^{-1} was ascribed to the aromatic and aliphatic C−H stretch of the imidazole. The C=N stretch mode was observed by the peak at 1630 cm^{-1}. The wavenumber region of 1450–900 cm^{-1} exhibited various bands assigned to the in-plane bending of the imidazole ring. The bands below 800 cm^{-1} were ascribed to the out-of-plane bending of the rings. The functional groups present in the PVA/PG and PVA/PG/ZIF-8 membranes were investigated. The broad peak around 3350 cm^{-1} and 3280cm^{-1} indicated the presence of hydrogen-bonded hydroxyl groups (O-H) in the membrane and the shift in the peak indicated the presence of amino group with the N-H stretch. The peak at 2970 cm^{-1} refers to the presence of the alkyl groups. The intensity around 1670 cm^{-1} refers to the (C=C) stretching and at 1500 cm^{-1} to the (C-H) bending, respectively. The vibrational bands observed at around 1670 cm^{-1} and 1360 cm^{-1}

attributes to the CH_2 bending [45]. The peak at 1150 cm^{-1} was assigned to C-O stretching vibration. The FTIR spectra of PVA/PG/ZIF-8 film confirmed the presence of both ZIF-8 nanoparticles and PVA film. The peak intensity of O-H bond increased with a slight shift thereby confirming interaction with the ZIF-8 particles for PVA/PG/ZIF-8 membrane. The new peak at 1650 cm^{-1} confirms to the N-H bending for PVA/PG/ZIF-8 membrane thereby confirming the interaction of PG amine with ZIF-8. Peak around 500 cm^{-1} confirmed the formation of Zn-N bond present in the ZIF-8 nanoparticle. The vibrations observed below 800 cm^{-1} and 1350-900 cm^{-1} were assigned to out of plane bending and the in-plane bending of the imidazolate ring thereby confirming the interaction with the functional groups of ZIF-8 particle [46, 47].

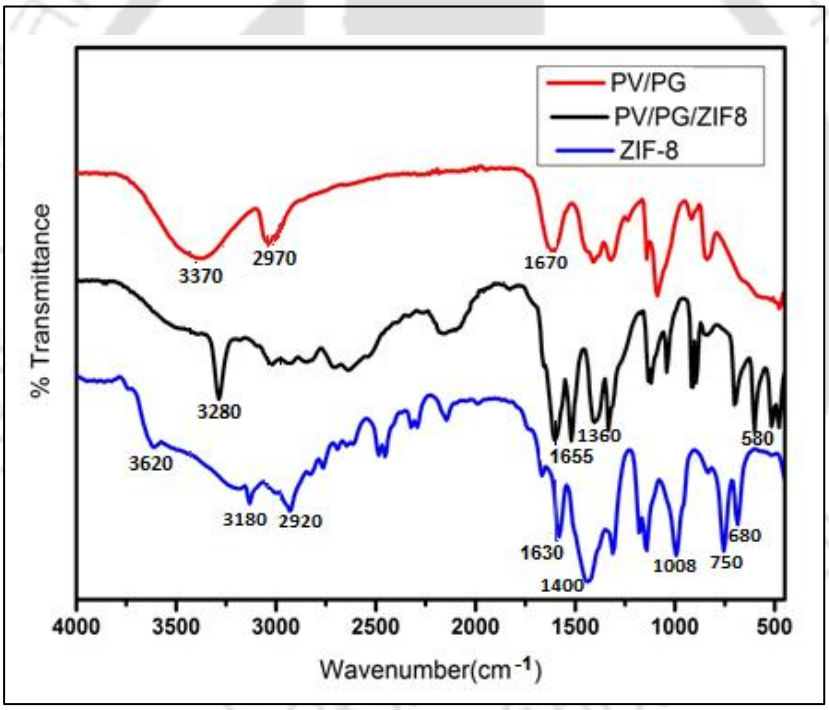

Figure 5.4 FTIR curve of ZIF-8, PVA/PG and PVA/PG/ZIF-8 membrane

5.5.3. X-ray diffraction analysis (XRD)

The crystalline structure of as-synthesized ZIF-8 powder, PVA/PG and PVA/PG/ZIF-8 membrane was investigated by XRD analysis as demonstrated in Figure 5.5. It was observed that the position and intensity of the diffraction peaks were in agreement with the reported data as mentioned in the literature [46-48]. The XRD value of ZIF-8 nanoparticle depicts strong peak at 2θ angle of 10.3° (002), 12.6° (112), 14.8° (022),

16.2° (013), 18^{o} (222), 24.6^{o} (233), 26.9^{o} (134) peaks respectively. This validates the successful formation of the ZIF-8 particles. The broad peak observed at 2θ of 19.8^{o} corresponding to (101) plane for PVA/PG and PVA/PG/ZIF-8 membrane confirms the semi-crystalline structure of the membrane film. The slight relocation of the peak to the right in case of PVA/PG/ZIF-8 membrane indicates the reduction in PVA chain distance thereby indicating close interaction of the polymer-filler material.

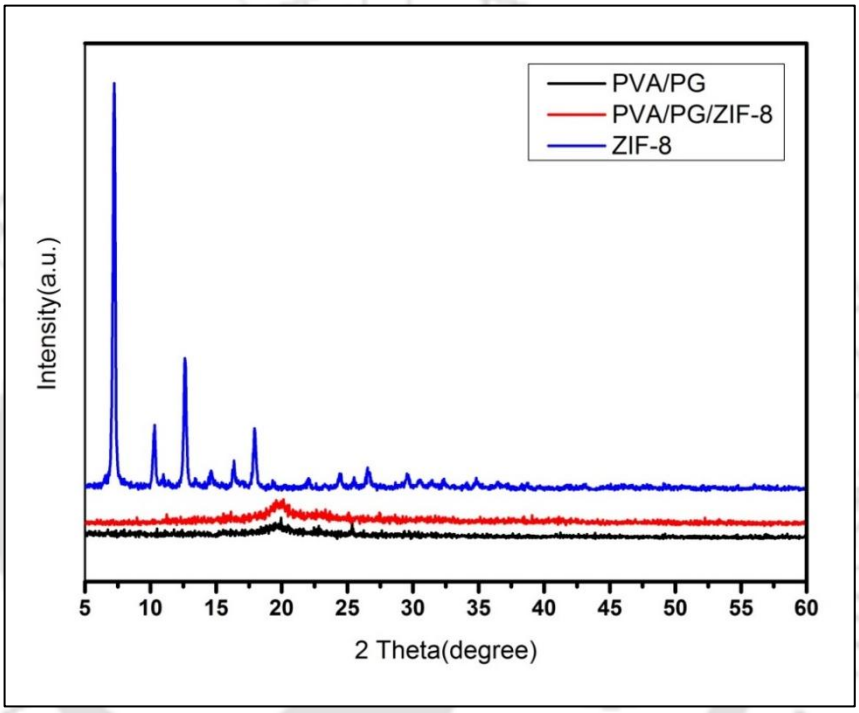

Figure 5.5 XRD curve of ZIF-8, PVA/PG and PVA/PG/ZIF-8 membrane

5.5.4. Field emission transmission electron microscopy analysis (FETEM)

The FETEM image of the ZIF-8 filler and the PVA/PG/ZIF-8 mixed matrix membrane at different ZIF-8 loading (5 wt % and 10 wt %) was depicted in Figure 5.6 (a-d). Figure 5.6(a) and (c) confirmed homogeneous dispersion of ZIF-8 in solution as well as membrane at 5 wt % loading. With increase in loading to 10 wt %, some crowding was observed as confirmed by Figure 5.6(b) and (d). The synthesized ZIF-8 exhibited uniform particle size of ~100 nm of polyhedral shape thereby confirming the formation of ZIF-8 particles.

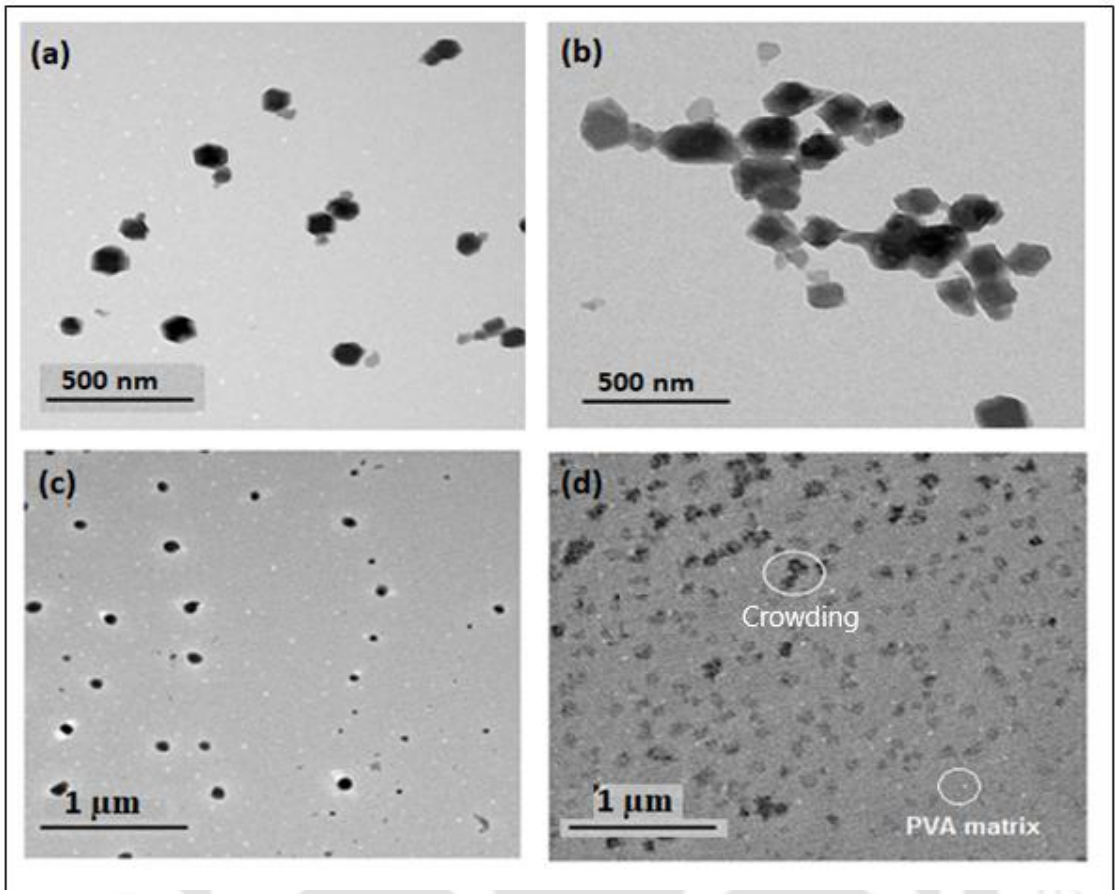

Figure 5.6 FETEM image of the ZIF-8 filler at loading of 5 wt % (a) and 10 wt % (b), and the PVA/PG/ZIF-8 mixed matrix membrane at ZIF-8 loading of 5 wt % (c) and 10 wt % (d)

5.5.5. Field emission scanning electron microscope analysis (FESEM)

The FESEM analysis of the top and cross-sectional image of the synthesized membranes was shown in Figure 5.7(a-d). The top surface image of pure PVA/PG membrane confirms a smooth topography of the active layer. For PVA/PG/ZIF-8 membrane, homogeneous dispersion of ZIF-8 in the matrix is observed thereby confirming the exceptional compatibility and interaction between the polymer-filler interface. The cross-sectional view for both PVA/PG and PVA/PG/ZIF-8 membrane confirmed the formation of active dense layer of thickness 4µm on the PES support. Also, no leakage of polymer

solution was observed thereby having no effect on the overall resistance offered by the membrane.

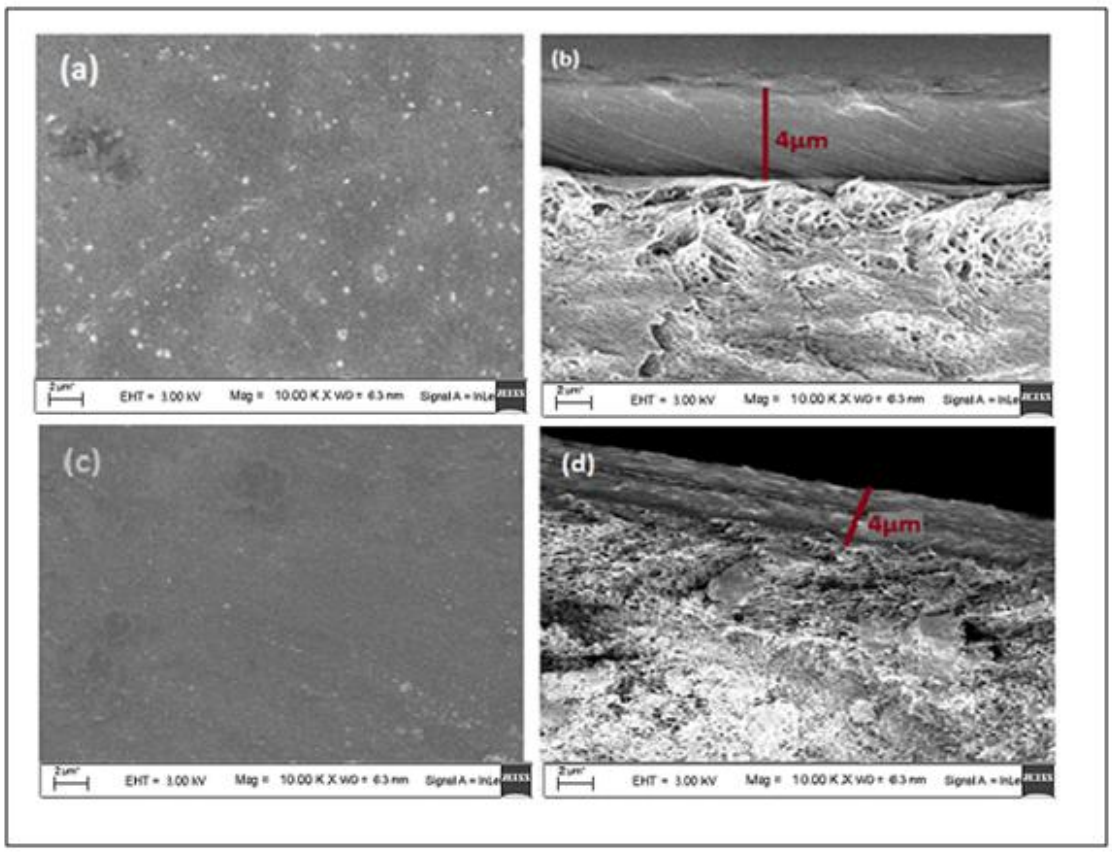

Figure 5.7 FESEM image of top surface and cross-sectional image (a, b) PVA/PG/ZIF-8 membrane and (c, d) PVA/PG membrane

5.5.6. X-ray photoelectron spectroscopy analysis (XPS)

The XPS analysis of the PVA/PG/ZIF-8 film was performed at a temperature of 24 ºC. The survey scan (Figure 5.8) of XPS spectrum of the PVA/PG/ZIF-8 film sample showed the existence of C 1s, N 1s, O 1s and Zn 2p peaks thereby confirming the successful formation and integration of ZIF-8 MOF in the membrane sample.

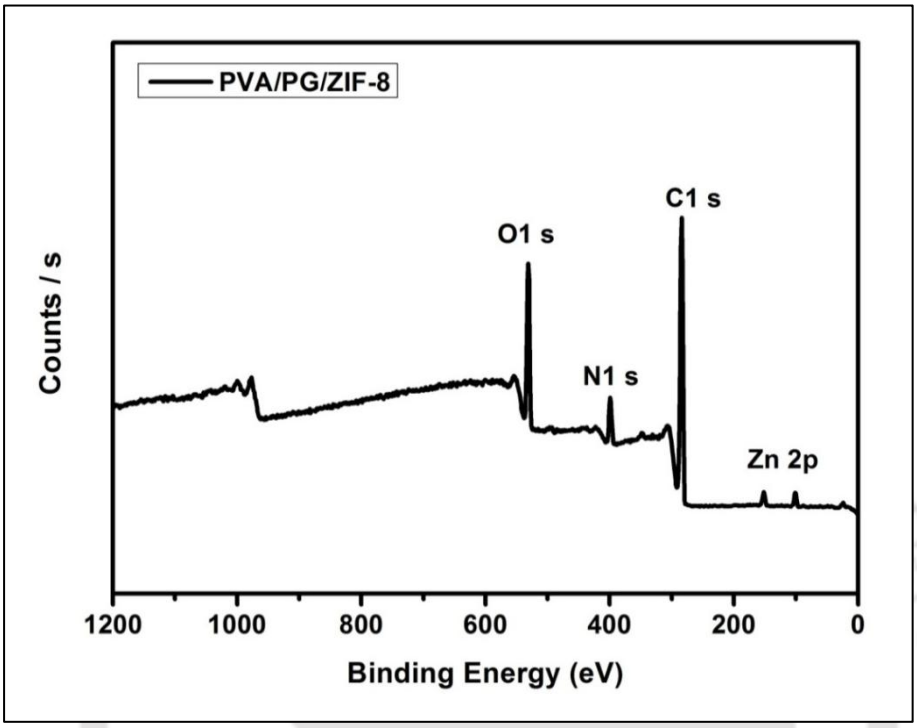

Figure 5.8 The XPS data profile survey scan of PVA/PG/ZIF-8 membrane

5.6. CO_2 separation performance study of the membrane

The binary gas mixture has been analysed for variation in temperature (60-110 ºC) and sweep side water flow rate (0.01-0.075 ml/min).

5.6.1. Effect of temperature on separation performance

The performance of PVA/PG and PVA/PG-ZIF-8 membrane for temperature variation (range: 60 to 110 °C) was investigated in Figure 5.9 (a, b). The feed/sweep side pressure, feed/sweep side water flow rates was maintained at 2.5 atm and 1.2 atm, 0.03 and 0.05 ml/min, respectively. It was observed that the CO_2 permeance for both PVA/PG and PVA/PG/ZIF-8 membrane showed constant improvement with increment in temperature to 80 °C with insignificant rise with further increase in temperature. At 95 °C, the

membranes showed optimal performance and the CO_2 permeance and CO_2/N_2 selectivity for PVA/PG membrane was found to be 45 GPU and 210 which increased to a significant 82 GPU and 370 for PVA/PG/ZIF-8 membrane. This can be attributed to the increase in the rate of reaction of CO_2 and amine with increasing temperature and moisture content governed solely by the facilitated transport mechanism. However, at a lower temperature, both solution-diffusion mechanism and facilitated transport mechanism plays a substantial role in the CO_2 separation ability [49]. The reduction in the water retention capacity at higher temperature (up to 110 °C) leads to a restriction in the facilitated transport mechanism. However, for PVA/PG/ZIF-8 membrane, steep increment in the CO_2 permeance and the CO_2/N_2 selectivity is observed at higher temperature. This could be due to the fact that for mixed matrix membrane exhibiting molecular sieving effect, the gas transport is governed by solution-diffusion mechanism along with facilitated transport mechanism. CO_2 gas transport occurs through solubility due to the interaction between the gas molecule and polymer matrix. The small pore size of ZIF-8 (3.4Å) allows the passage of smaller CO_2 gas molecules (3.3Å) and restricting the passage of larger gas molecules (N_2) thereby leading to an increment in the CO_2 permeance [50, 51]. The N_2 gas transport on the other hand is governed basically by diffusivity whereby the gas diffuses through the free volume in the polymer matrix. Also, nitrogen diffusion coefficient is expected to be less affected by the incorporation of ZIF-8 than CO_2 diffusion coefficient mainly due to the restricted geometry of nitrogen molecules thereby impeding the diffusion inside the ZIF-8 pores [25]. Thus considering the overall facilitated transport and molecular sieving effect, an impressive increment in CO_2 permeance of 82 GPU and CO_2/N_2 selectivity of 370 at 95 °C for PVA/PG/ZIF-8 membrane was observed. At temperature > 105 °C, reduction in the membrane flexibility and increase in its stiffness impedes the easy passage of CO_2 gas molecules and hence the CO_2-carrier reaction rate leads to no significant increment in the CO_2 permeance and CO_2/N_2 selectivity. The N_2 gas transport which follows the solution-diffusion mechanism is not affected by this phenomenon. It only showed a marginal, very slow rate of increase in the N_2 permeance with temperature. The CO_2 permeance and CO_2/N_2 selectivity

increased by 82.2 % and 76.2 % for PVA/PG/ZIF-8 membrane compared to PVA/PG membrane.

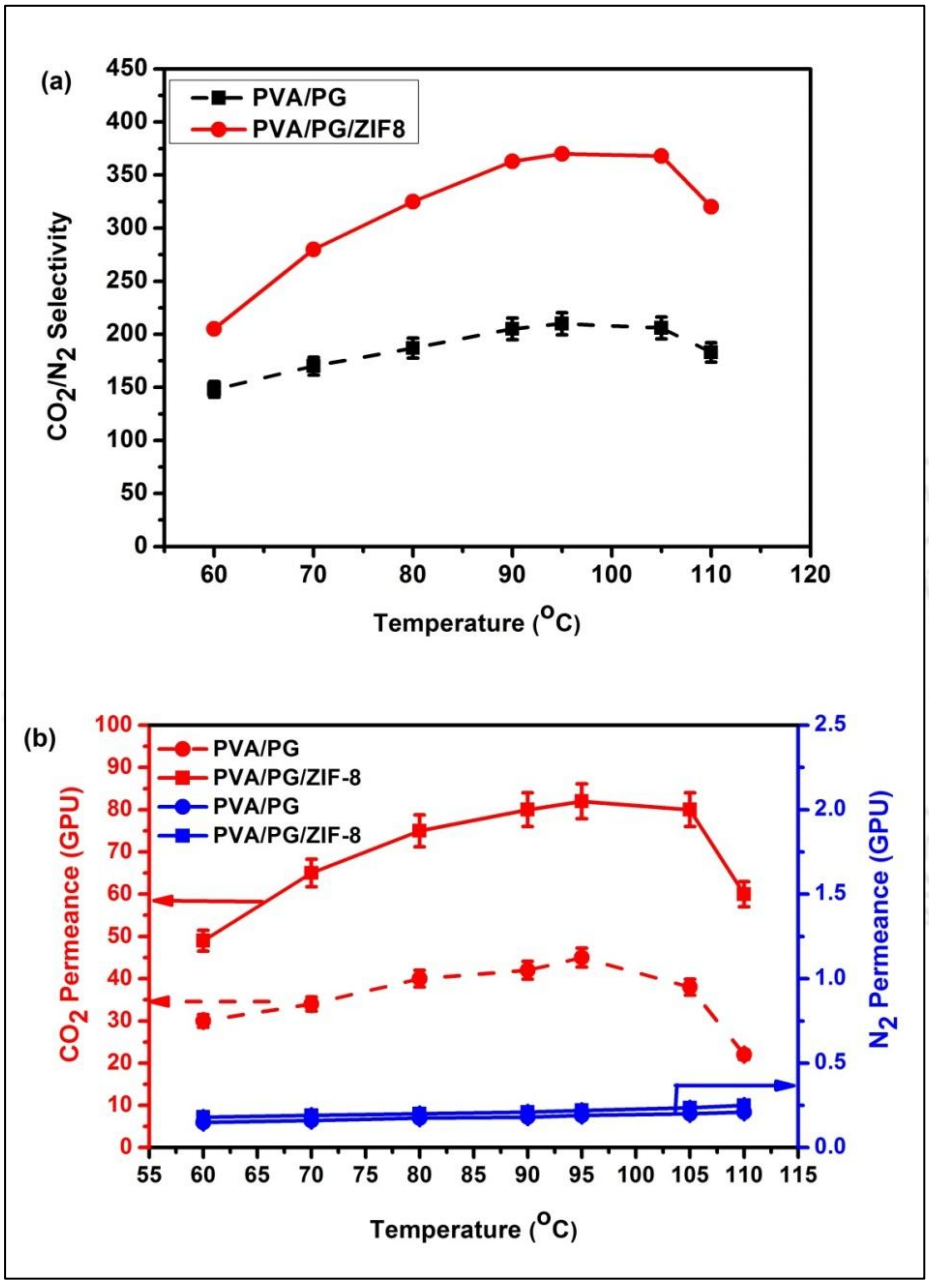

Figure 5.9 Effect of temperature on (a) CO_2/N_2 selectivity (b) CO_2 and N_2 Permeance (GPU) for PVA/PG and PVA/PG/ZIF-8 membrane at feed absolute pressure = 2.5 atm, sweep absolute pressure = 1.2 atm, and water flow rates = 0.03/0.05 ml/min (feed/sweep)

5.6.2. Effect of sweep side water flow rate on separation performance

The effect of sweep side water flow rate (ml/min) on CO_2/N_2 selectivity, CO_2 and N_2 permeance (GPU) has been reported in Figure 5.10(a, b). The sweep water flow rate was varied from 0 to 0.075 ml/min. The feed water flow rate, temperature and feed/sweep absolute pressure was fixed at 0.03 ml/min, 100 °C, 2.5/1.2 atm, respectively. At no water condition, the CO_2 permeance and CO_2/N_2 selectivity showed inferior results for both the membranes. However, with supply of moisture content, the water retention capacity of the membrane increases thereby permitting the separation through facilitation transport mechanism. The reversible reaction between CO_2 and amine was accelerated leading to the formation of more CO_2-carrier complex with increasing water flow rate. Thus the CO_2/N_2 selectivity and CO_2 permeance (GPU) showed superior performance with increase in sweep side water flow rate. At higher sweep side water flow rate, the CO_2 permeance and CO_2/N_2 selectivity showed insignificant change and saturated at this condition. The swelling increased the inter-chain spacing of the polymer network. This allowed more N_2 molecules to pass through it [51-54]. The CO_2 permeance and CO_2/N_2 selectivity showed ~ 22 fold, ~ 18 fold and ~ 27 fold, ~ 28 fold improvements for PVA/PG and PVA/PG/ZIF-8 membrane, respectively when the water flow rate (sweep) was varied from 0 to 0.075 ml/min.

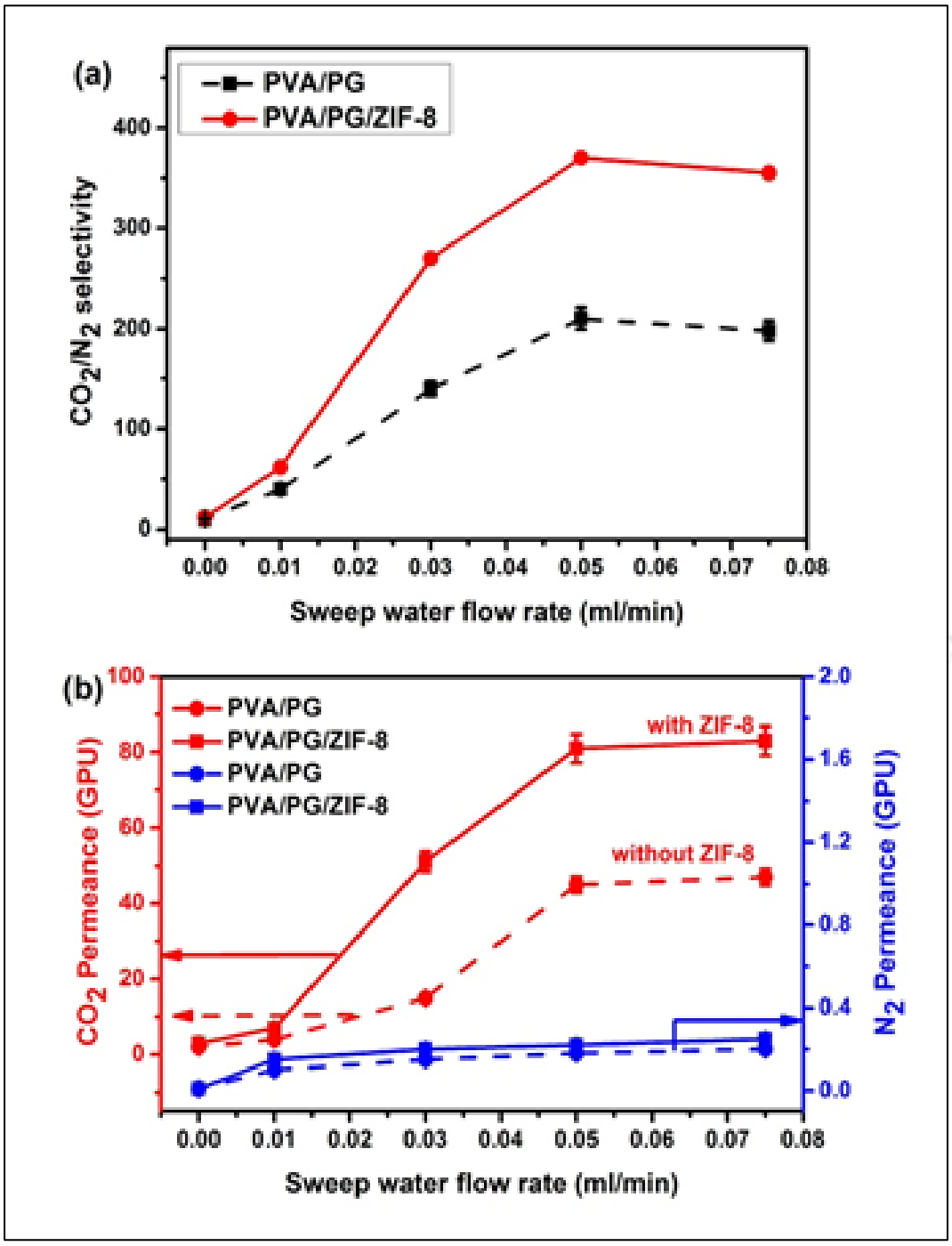

Figure 5.10 Effect of sweep side water flow rate on (a) CO_2/N_2 selectivity (b) CO_2 and N_2 permeance (GPU) for PVA/PG and PVA/PG/ZIF-8 membrane at 100 °C, sweep absolute pressure = 1.2 atm, and feed water flow rate = 0.03 ml/min

The bar diagram shows the comparative enhancement in selectivity and permeance (GPU) results as depicted in Figure 5.11. The CO_2 permeance (GPU) and CO_2/N_2 selectivity showed a significant 82.2 % and 76.2 % increment for PVA/PG/ZIF-8 membrane when compared to pure PVA/PG membrane. Thus it establishes that the addition of ZIF-8 filler into the polymeric matrix leads to a remarkable augmentation in CO_2 gas performance. The CO_2 permeability (Barrer) and CO_2/N_2 selectivity for different membrane materials are reported in Table 5.1. Comparison with the reported values in literature showed that the PVA/PG and PVA/PG/ZIF-8 membrane exhibited higher values of CO_2 permeability and CO_2/N_2 selectivity [57-62]. However, the stability issue and poor mechanical property at high humidity condition involved in PVA_m polymer makes our result comparative and liable to be utilized for further scale up [57].

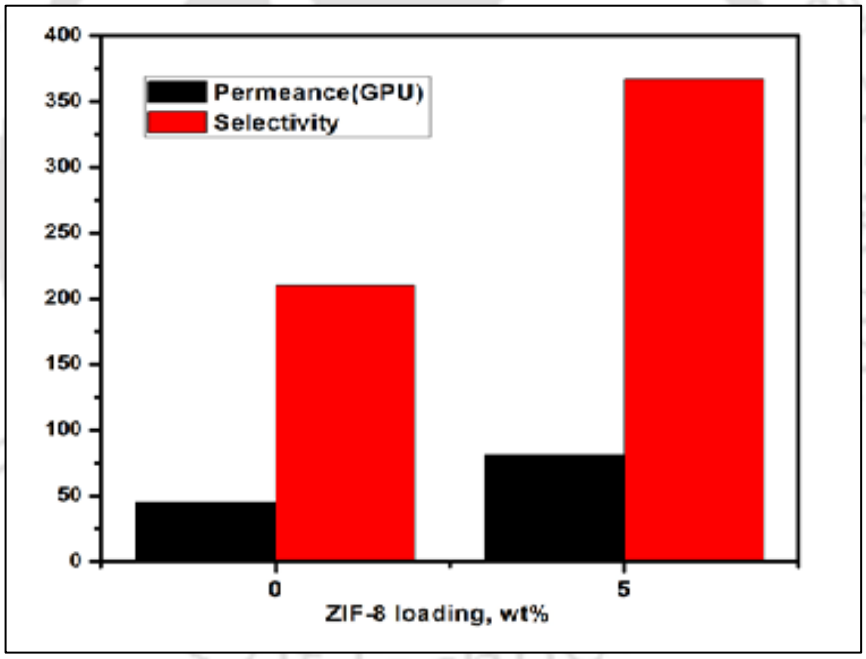

Figure 5.11 Bar diagram for CO_2 permeance (GPU) and CO_2/N_2 selectivity for pure PVA/PG membrane and PVA/PG/ZIF-8 membrane

Table 5.1 CO_2 permeability (Barrer) and CO_2/N_2 selectivity results for different membrane material

Polymer	CO_2 permeability (Barrer)	CO_2/N_2 selectivity	Thickness (μm)	Reference
Ultem/ZIF-8	11.1	28-44	63-92	[25]
Matrimid/ZIF-8	20	23	40-70	[27]
6FDA-durene/ZIF-8	1593	25	40-60	[28]
Polyvinyl amine(PVA_m)/ ZIF-8(9.1-23.1 wt %)	~100	72-83	0.38	[29]
Pebax1657[bmim][Tf_2N] @ZIF-8	104.9	83.9	70-90	[50]
PSf/ZIF-8(16 wt %)	11.8	11.5	90	[59]
PMPS/ ZIF-8(4.5 wt %)	827	7	20	[60]
SEBS/ZIF-8 (30 wt %)	454	10.6-12.0	-	[61]
PI/ZIF-8 (7-30 wt %)	560-1437	12-20	-	[62]
Crosslinked PVA/PG membrane (No filler)	180	210	4	This work
Crosslinked PVA/PG/ZIF-8 membrane ZIF-8 (5 wt %)	328	370		This work

5.7. Robeson's curve

The permeation results obtained experimentally in this work were plotted in the famous Robeson's upper bound curve. The present work has been compared with literature reported on different polymer/ZIF-8 MMMs for CO_2/N_2 gas separation. The PVA/PG membrane and PVA/PG/ZIF-8 membrane exhibited high values of CO_2 permeability and CO_2/N_2 selectivity well surpassing Robeson's upper bound limit as compared to the reported values in the literature (Figure 5.12).

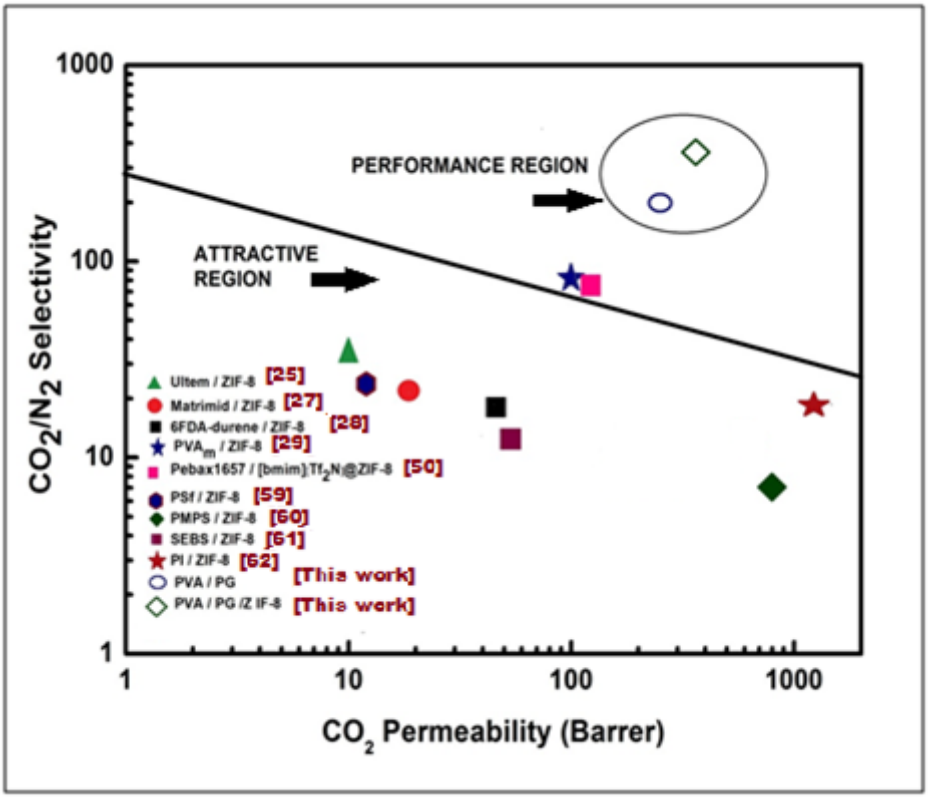

Figure 5.12 Robeson upper bound relationship of CO_2 permeability (Barrer) and CO_2/N_2 selectivity of high performing MMMs and comparison with the present work performed

5.8. Conclusions

High-performance defect-free, thin PVA/PG MMMs (active layer thickness ~4µm) with different ZIF-8 loadings were synthesized on PES support by solution casting method. The ZIF-8 nanoparticles were synthesized with a uniform size range of 100 nm. The good compatibility between the PVA polymer and ZIF-8 filler was confirmed via characterization techniques. TGA analysis of ZIF-8 nanoparticle showed excellent thermal stability to 550 °C with negligible weight loss. This ability had enhanced the thermal property in PVA/PG/ZIF-8 membrane when compared to PVA/PG membrane. The FTIR profile validated the interaction of amine and ZIF-8 in the membrane. FESEM study confirmed the homogeneous dispersion of the fillers in the polymer matrix. AFM studies revealed the increase in the rough surface of the membrane with increase in the ZIF-8 loading. The compatibility of ZIF-8 filler in the PVA/PG matrix resulted in enhancement of CO_2 permeance and CO_2/N_2 selectivity. The results depicted that PVA/PG membrane loaded with 5 wt % ZIF-8 showed a CO_2 permeance of 82 GPU and CO_2/N_2 selectivity of 370 which was 82.2 % and 76.2 % higher when compared to pure PVA/PG membrane. Thus ZIF-8 doped PVA mixed matrix membrane serves as a potential candidate for industrial gas separation studies. Both PVA/PG and PVA/PG/ZIF-8 membrane showed impressive gas separation properties very well surpassing the results reported in the literature. Also, the membrane was tested over time and was found to have no changes. Thus, it can be very well concluded that the thermal and chemical stability as confirmed by TGA and XPS analysis suggests potential application for CO_2 separation from flue gas.

References

[1] Z. Dai, J. Deng, L. Ansaloni, S. Janakiram and L. Deng, Thin-film-composite hollow fiber membranes containing amino acid salts as mobile carriers for CO_2 separation, J. Membr. Sci. 578 (2019) 61-68.

[2] M. Teramoto, K. Nakai, N. Ohnishi, Q. Huang, T. Watari and H. Matsuyama, Facilitated transport of carbon dioxide through supported liquid membranes of aqueous amine solutions, Ind. Eng. Chem. Res. 35(2) (1996) 538-545.

[3] Y. Chen, L. Zhao, B. Wang, P. Dutta and W.S.W. Ho, Amine-containing polymer/ zeolite Y composite membranes for CO_2/N_2 separation, J. Membr. Sci. 497 (2016) 21–28.

[4] J. Liao, Z. Wang, C. Gao, M. Wang, K. Yan, X. Xie, S. Zhao, J. Wang and S. Wang, A high performance PVA_m–HT membrane containing high-speed facilitated transport channels for CO_2 separation, J. Mater. Chem. A. 3 (2015) 16746-16761.

[5] S. Wang, X. Li, H. Wu, Z. Tian, Q. Xin, G. He, D. Peng, S. Chen, Y. Yin and Z. Jiang, Advances in high permeability polymer-based membrane materials for CO_2 separations, Energy Environ. Sci. 9 (2016) 1863-1890.

[6] C.I. Chaidou, G. Pantoleontos, D.E. Koutsonikolas, S.P. Kaldis and G.P. Sakellaropoulos, Gas separation properties of polyimide-zeolite mixed matrix membranes, Sep. Sci. Technol. 47 (2012) 950–962.

[7] M. Hussain and A. Konig, Mixed matrix membrane for gas separation: polydimethylsiloxane filled with zeolite, Chem. Eng. Technol. 35 (2012) 561–569.

[8] M. Barooah and B. Mandal, Enhanced CO_2 separation performance by PVA/PEG/silica mixed matrix membrane, J. Appl. Polym. Sci. 46481 (2018) 1-12.

[9] S. Kim, E. Marand, J. Ida and V.V. Guliants, Polysulfone and mesoporous molecular sieve MCM-48 mixed matrix membranes for gas separation, Chem. Mater. 18(5) (2006) 1149–1155.

[10] S.M. Sanip, A.F. Ismail, P.S. Goh, M.N.A. Norrdin, T. Soga, M. Tanemura and H. Yasuhiko, Carbon nanotubes based mixed matrix membrane for gas separation, Adv. Mater. Res. 364 (2012) 272-277.

[11] H. Sun, T. Wang, Y. Xu, W. Gao, P. Li and Q. J. Niu, Fabrication of polyimide and functionalized multi-walled carbon nanotubes mixed matrix membranes by in-situ polymerization for CO_2 separation, Sep. Purif. Technol. 177 (2017) 327-336.

[12] X. Li, L. Ma, H. Zhang, S. Wang, Z. Jiang, R. Guo, H. Wu, X.Z. Cao, J. Yang and B. Wang, Synergistic effect of combining carbon nanotubes and graphene oxide in mixed matrix membranes for efficient CO_2 separation, J. Membr. Sci. 479 (2015) 1-10.

[13] D.Q. Vu, W.J. Koros and S.J. Miller, Mixed matrix membranes using carbon molecular sieves: I. Preparation and experimental results, J. Membr. Sci. 211 (2003) 311–334.

[14] D. Qadir, H. Mukhtar, L.K. Keong, Synthesis and characterization of polyethersulfone/carbon molecular sieve based mixed matrix membranes for water treatment application, Procedia Engg. 148 (2016) 588 – 593.

[15] G. Dong, J. Hou, J. Wang, Y. Zhang, V. Chen and J. Liu, Enhanced CO_2/N_2 separation by porous reduced graphene oxide/pebax mixed matrix membranes, J. Membr. Sci. 520 (2016) 860–868.

[16] N. Jusoh, Y.F. Yeong, W.L. Cheong, K K. Lau and A.M. Shariff, Facile fabrication of mixed matrix membranes containing 6FDA-durene polyimide and ZIF-8 nanofillers for CO_2 capture, J. Ind. Eng. Chem. 44 (2016) 164-173.

[17] M. Wang, Z. Wang, S. Zhao, J. Wang and S. Wang, Recent advances on mixed matrix membranes for CO_2 separation, Chin. J. Chem. Eng. 25(11) (2017) 1581-1597.

[18] M.S. Denny Jr, J.C. Moreton, L. Benz and S.M. Cohen, Metal-organic frameworks for membrane-based separations, Nat. Rev. Mater. 1 (2016) 16078.

[19] C.A. Trickett, A. Helal, B.A. Al Maythalony, Z. H. Yamani, K. E. Cordova and O. M. Yagh, The chemistry of metal–organic frameworks for CO_2 capture, regeneration and conversion, Nat. Rev. Mater. 2 (2017) 17045.

[20] L. Dong, M. Chen, J. Li, D. Shi, W. Dong, X. Li and Y. Bai, Metal-organic framework-graphene oxide composites: A facile method to highly improve the CO_2 separation performance of mixed matrix membranes, J. Membr. Sci. 520 (2016) 801-811.

[21] N.N.R. Ahmad, C.P. Leo, A.W. Mohammad and A.L. Ahmad, Modification of gas selective SAPO zeolites using imidazolium ionic liquid to develop polysulfone mixed matrix membrane for CO_2 gas separation, Micropor. Mesopor. Mater. 244 (2017) 21-30.

[22] M. Gholami, T. Mohammadi, S. Mosleh and M. Hemmati, CO_2/CH_4 separation using mixed matrix membrane-based polyurethane incorporated with ZIF-8 nanoparticles, Chem. Pap. 71 (2017) 1839-1853.

[23] H.J. Jo, C.Y. Soo, G. Dong, Y.S. Do, H.H. Wang, M.J. Lee, J.R. Quay, M.K. Murphy and Y.M. Lee, Thermally rearranged poly (benzoxazole-co-imide) membranes with superior mechanical strength for gas separation obtained by tuning chain rigidity, Macromolecules. 48 (2015) 2194-2202.

[24] H. Wang and H. Dai, Strongly coupled inorganic–nano-carbon hybrid materials for energy storage, Chem. Soc. Rev. 42 (2013) 3088-3113.

[25] D. Eiras, Y. Labreche and L.A. Pessan, Ultem/ZIF-8 mixed matrix membranes for gas separation: transport and physical properties, Mater. Res. 19(1) (2016) 220-228.

[26] M. Vinoba, M. Bhagiyalakshmi, Y. Alqaheem, A.A. Alomair, A. Perez and M.S. Rana, Recent progress of fillers in mixed matrix membranes for CO_2 separation: A review, Sep. Purif. Technol. 188 (2017) 431-450.

[27] Q. Song, S.K. Nataraj, M.V. Roussenova, J.C. Tan, D.J. Hughes, W. Li, P. Bourgoin, M. A. Alam, A.K. Cheetham, S.A. Al Muhtaseb and E. Sivaniah, Zeolitic imidazolate framework (ZIF-8) based polymer nanocomposite membranes for gas separation, Energy Environ. Sci. 5(8) (2012**)** 8359−8369.

[28] V. Nafisi and M.B. Hagg, Gas separation properties of ZIF-8/6FDA-durene diamine mixed matrix membrane, Sep. Purif. Technol. 128 (2014) 31−38.

[29] S. Zhao, X. Cao, Z. Ma, Z. Wang, Z. Qiao, J. Wang and S. Wang, Mixed-matrix membranes for CO_2/N_2 separation comprising a poly(vinylamine) matrix and metal–organic frameworks, Ind. Eng. Chem. Res. 54 (2015**)** 5139-5148.

[30] Y. Chen and W.S.W. Ho, High-molecular-weight polyvinylamine/piperazine glycinate membranes for CO_2 capture from flue gas, J. Membr. Sci. 514 (2016) 376-384.

[31] A.F. Bushell, M.P. Attfield, C.R. Mason, P.M. Budd, Y. Yampolskii, L. Starannikova, A. Rebrov, F. Bazzarelli, P. Bernardo, J.C. Jansen, M. Lanč, K. Friess, V. Shantarovich, V. Gustov and V. Isaeva, Gas permeation parameters of mixed matrix membranes based on the polymer of intrinsic microporosity PIM-1 and the zeolitic imidazolate framework ZIF-8, J. Membr. Sci. 427 (2012) 48-62.

[32] C. Zhang, Y. Dai, J.R. Johnson, O. Karvan and W.J. Koros, High performance ZIF-8/6FDA-DAM mixed matrix membrane for propylene/propane separations, J. Membr. Sci. 389 (2012) 34-42.

[33] H.T. Kwon, H.K. Jeong, A.S. Lee, H.S. An and J.S. Lee, Heteroepitaxially grown zeolitic imidazolate framework membranes with unprecedented propylene/Propane Separation Performances, J. Am. Chem. Soc. 137(38) (2015) 12304-12311.

[34] M. Amirilargani and B. Sadatnia, Poly (vinyl alcohol)/zeolitic imidazolate frameworks (ZIF-8) mixed matrix membranes for pervaporation dehydration of isopropanol, J. Membr. Sci. 469 (2014) 1-10.

[35] A. Mondal, M. Barooah and B. Mandal, Effect of single and blended amine carriers on CO_2 separation from CO_2/N_2 mixtures using crosslinked thin-film poly (vinyl alcohol) composite membrane, Int. J. Greenh. Gas Con. 39 (2015) 27-38.

[36] A. Mondal and B. Mandal, CO_2 separation using thermally stable crosslinked poly (vinyl alcohol) membrane blended with polyvinylpyrrolidone/ polyethyleneimine/ tetraethylenepentamine, J. Membr. Sci. 460 (2014) 126-138.

[37] A. Mondal and B. Mandal, Synthesis and characterization of crosslinked poly (vinyl alcohol)/ poly (allylamine)/ 2-amino-2-hydroxymethyl-1,3-propanediol/ polysulfone composite membrane for CO_2/N_2 separation, J. Membr. Sci. 446 (2013) 383-394.

[38] J. Cravillon, S. Munzer, S.J. Lohmeier, A. Feldhoff, K. Huber, and M. Wiebcke, Rapid room-temperature synthesis and characterization of nanocrystals of a prototypical zeolitic imidazolate framework, Chem. Mater. 21(8) (2009) 1410–1412.

[39] S. Shahid and K. Nijmeijer, Performance and plasticization behaviour of polymer–MOF membranes for gas separation at elevated pressures, J. Membr. Sci. 470 (2014) 166-177.

[40] G. Duong and Y.M. Lee, Microporous polymeric membranes inspired by adsorbent for gas separation, J. Mater. Chem. A. 5 (2017) 13294.

[41] H.B. Park, C.H. Jung, Y.M. Lee, A.J. Hill, S.J. Pas, S.T. Mudie, E. Van Wagner, B. D. Freeman and D. J. Cookson, Science. 318 (2007) 254-258.

[42] M.Z. Ahmad, V.M. Gil, V. Perfilov, P. Sysel and V. Fila, Investigation of a new co-polyimide, 6FDA-bisP and its ZIF-8 mixed matrix membranes for CO_2/CH_4 separation, Sep. Purif. Technol. 207 (2018) 523-534.

[43] S. Anastasiou, N. Bhoria, J. Pokhrel and G.N. Karanikolos, Metal organic framework mixed matrix membranes for CO_2 separation, SPE-183264-MS.

[44] L. Wang, M. Fang, J. Liu, J. He, L. Denng, J. Li and J. Lei, The influence of dispersed phases on polyamide/ZIF-8 nanofiltration membranes for dye removal from water, RSC Adv. 5 (2015) 50942-50954.

[45] H. Shin, W.S. Chin, S. Bae, J.H. Kim and J. Kim, High-performance thin PVC-POEM/ZIF-8 mixed matrix membranes on alumina supports for CO_2/CH_4 separation, J. Ind. Eng. Chem. 53 (2017) 127-133.

[46] X. Zhang, T. Zhang, Y. Wang, J. Li, C. Liu, N. Li and J. Liao, Mixed-matrix membranes based on Zn/Ni-ZIF-8-PEBA for high performance CO_2 separation, J. Membr. Sci. 560 (2018) 38-46.

[47] P.Y. Hsu, T.Y. Hu, S.R. Kumar, C.H. Chang, K.C.W. Wu, K.L. Tung and S.J. Lue, Highly zeolite-loaded polyvinyl alcohol composite membranes for alkaline fuel-cell electrolytes, Polymers. 10(1) (2018) 102.

[48] B. Prasad and B. Mandal, Moisture responsive and CO_2 selective biopolymer membrane containing silk fibroin as a green carrier for facilitated transport of CO_2, J. Membr. Sci. 550 (2018) 416-426.

[49] N. Jusoh, Y.F. Yeong, K.K. Lau and A.M. Shariff, Mixed matrix membranes comprising of ZIF-8 nanofillers for gas transport properties, Procedia Engg. 148 (2016) 1259-1265.

[50] A. Jomekian, B. Bazooyar, R. M. Behbahani, T. Mohammadi and A. Kargari, Ionic liquid-modified Pebax 1657 membrane filled by ZIF-8 particles for separation of CO_2 from CH_4, N_2 and H_2, J. Membr. Sci. 524 (2017) 652-662.

[51] R. Yegani, H. Hirozawa, M. Teramoto, H. Himei, O. Okada, T. Takigawa, N. Ohmura, N. Matsumiya and H. Matsuyama, Selective separation of CO_2 by using novel facilitated transport membrane at elevated temperatures and pressures, J. Membr. Sci. 291 (2007) 157-164.

[52] S. Luanwuthi, A. Krittayavathananon, P. Srimuk and M. Sawangphruk, In situ synthesis of permselective zeolitic imidazolate framework-8/graphene oxide composites: rotating disk electrode and Langmuir adsorption isotherm, RSC Adv. 5 (2015) 46617.

[53] Y. Ding, Y. Xua, B. Ding, Z. Li, F. Xie, F. Zhang, H. Wang, J. Liu and X. Wang, Structure induced selective adsorption performance of ZIF-8 nanocrystals in water, Colloids Surf. A. 520 (2017) 661-667

[54] S. Yu, S. Li, S. Huang, Z. Zeng, S. Cui and Y. Liu, Covalently bonded zeolitic imidazolate frameworks and polymers with enhanced compatibility in thin film nanocomposite membranes for gas separation, J. Membr. Sci. 540 (2017) 155-164.

[55] L.M. Robeson, The upper bound revisited, J. Membr. Sci. 320 (2008) 390-400.

[56] D. Venturi, L. Ansaloni and M.G. Baschetti, Nanocellulose based facilitated transport membranes for CO_2 separation, Chem. Eng. Trans. 522 (2016).

[57] Y. Dai, J.R. Johnson, O. Karvan, D.S. Sholl and W.J. Koros, Ultem®/ZIF-8 mixed matrix hollow fiber membranes for CO_2/N_2 separations, J. Membr. Sci. 401 (2012) 76−82.

[58] H. Li, L. Tuo, K. Yang, H.K. Jeong, Y. Dai, G. He and W. Zhao, Simultaneous enhancement of mechanical properties and CO_2 selectivity of ZIF-8 mixed matrix membranes: Interfacial toughening effect of ionic liquid, J. Membr. Sci. 511 (2016) 130–142.

[59] S. Anastasiou, N. Bhoria, J. Pokhrel, K.S.K. Reddy, C. Srinivasakannan, K. Wang and G.N. Karanikolos, Metal-organic framework/graphene oxide composite fillers in mixed matrix membranes for CO_2 separation, Mater. Chem. Phys. 212 (2018) 513-522.

[60] L. Diestel, X.L. Liu, Y.S. Li, W.S. Yang and J. Caro, Comparative permeation studies on three supported membranes: pure ZIF-8, pure polymethylphenylsiloxane, and mixed matrix membranes, Micropor. Mesopor. Mater. 189 (2014) 210–215.

[61] W.S. Chi, S. Hwang, S.J. Lee, S. Park, Y.S. Bae, D.Y. Ryu, J.H. Kim and J. Kim, Mixed matrix membranes consisting of SEBS block copolymers and size-controlled ZIF-8 nanoparticles for CO_2 capture, J. Membr. Sci. 495 (2015) 479–488.

[62] Z. Wang, D. Wang, S. Zhang, L. Hu and J. Jin, Interfacial design of mixed matrix membranes for improved gas separation performance, Adv. Mater. (2016) 3399–3405.

CHAPTER 6

Effect of Amino-Functionalized ZIF-8 Incorporated Mixed Matrix Membrane for Enhanced CO_2 Separation

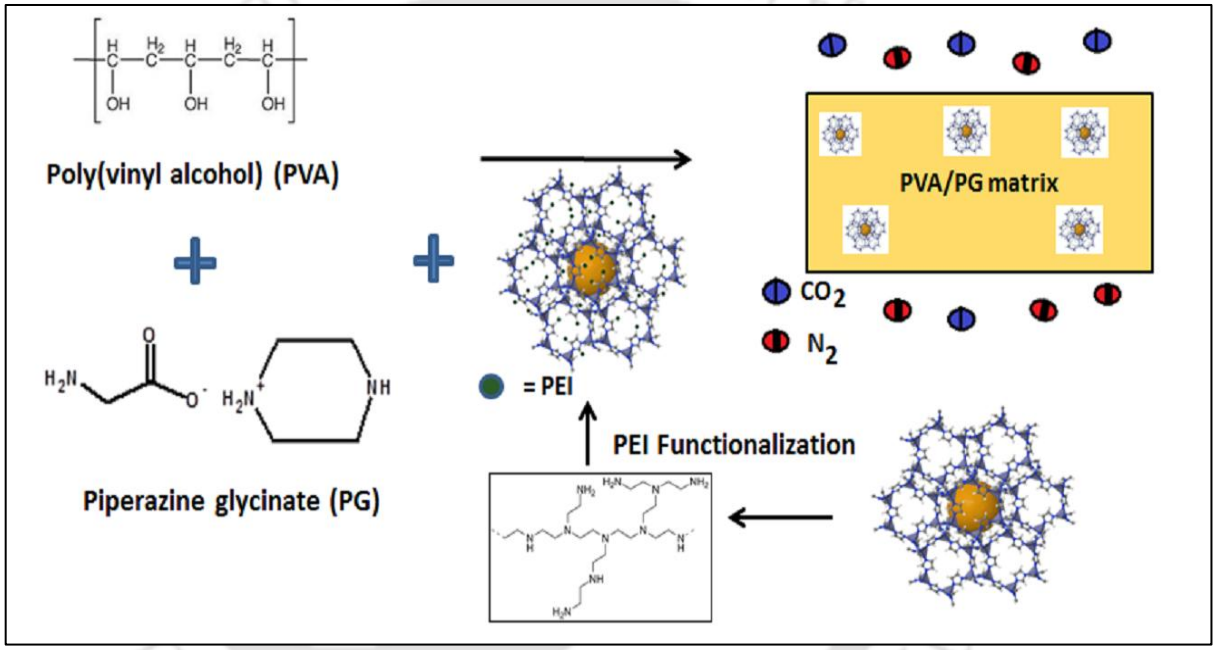

Graphical abstract PEI amino-functionalization of ZIF-8 and PVA/PG/ZIF-8@PEI mixed matrix membrane

CHAPTER 6

Effect of Amino-Functionalized ZIF-8 Incorporated Mixed Matrix Membrane for Enhanced CO_2 Separation

This chapter encompasses the preparation of mixed matrix membrane (MMM) by incorporating zeolitic imidazolate framework (ZIF-8) MOF surface functionalized with polyethyleneimine (PEI) amino-functional moieties into the PVA/PG matrix. In Chapter 5, the novelty and stability improvement of PVA/PG/ZIF-8 membrane for CO_2 separation has been discussed in detail. To further improve the polymer-particle compatibility and CO_2 transport performance, the ZIF-8 MOF is surface amino-functionalized with polyethyleneimine (PEI). Detailed material characterization by XPS and ninhydrin assay confirmed the successful grafting of the amino group on the silica surface. We thus envision that this work will invigorate a potential and cost effective route for large-scale CO_2 capture studies.

6.1. Introduction

ZIF-8 MOFs, a relatively new class of highly crystalline porous hybrid material consisting of metal cluster bound to organic ligands have molecular sieving properties that aids in gas separation application. It integrates the desirable high surface area and pore size tunability of MOFs and the structural diversity of zeolites thereby showing great potential in gas separation studies [1, 2]. The organic moiety of ZIF-8 provides better compatibility with polymer matrix and hence preferred over other inorganic particles as filler material. Also, it possesses unique characteristics of large surface area, porosity, highly tailorable organic framework, regulated pore structure and tunable pore sizes [3-5]. However, the fabrication of defect-free, thin selective layer MOF based membrane with large surface area still remains a challenge due to its compatibility issue with organic matrix and formation of voids in the interfaces and hence undergoes steps such as grafting and surface modification to improve the MOF properties.

A versatile approach to improve the MOF efficiency and gas separation performance is by substrate modification with various functional moieties [6]. Amino groups like 3-

aminopropyltrimethoxysilane (APTMS) have been reported for performance enhancement of MOF MMMs. The amine-modified MOF incorporated into MMM exhibited enhanced performance and novel properties compared with their pristine counterparts. The presence of amino groups in the MOF surface provides available nitrogen sites and strong affinity towards CO_2 molecules thereby facilitating the CO_2 uptake [7, 8]. One such technique of functionalization includes the post-synthetic modification (PSM) approach wherein the pre-formed MOF undergoes chemical modification. Zhang et al. [9] reported improvement in CO_2 adsorption with ZIF-8 modification with ethylene diamine (ED). Cho et al. [10] reported post synthetic amine-functionalized ZIF-8 modification as potential platform for the ZIF-based materials designed with specific functional group. Vankelecom et al. [11] reported that the covalent bond between matrimid and amino group of MOFs (NH_2-UiO-66) MMMs enhanced the interfacial compatibility showing remarkable improved effects on the gas performance. Yahya et al. [12] reported that the amino-impregnated ZIF-8 resulted in a significant 199.6 % increment in the CO_2 adsorption capacity when compared to ZIF-8 alone. Yu at al. [13] studied the enhancement in compatibility with the addition of amine-modified ZIF-8 (NH_2-ZIF-8) and polyamide matrix thereby leading to high separation performance for CO_2/N_2, CO_2/NO and CO_2/He gas pair which surpassed the Robeson's upper bound.

Polyethyleneimine (PEI), a sterically hindered amine is a promising functionalization agent due to its high amine density and available primary amine sites on the chain ends. The PEI amine is expected to access both the interior and exterior of ZIF-8 crystal, thereby functionalizing it at both ends. However, very limited literature has been reported on the MOF functionalization with PEI. Xian et al. [14] reported enhanced CO_2 capacities and selectivity by 6.2 and 27 times with PEI loading on ZIF-8 as compared to unmodified ZIF-8. In the presence of water vapour, only one amine group in PEI react with the CO_2 molecules thereby promoting more CO_2 molecules to be adsorbed and hence are preferable as functionalization agent. Poly (vinyl alcohol) (PVA), on the other hand, a base polymer has excellent film forming ability, fabrication simplicity along with excellent amine compatibility [15-17]. Also, amino acid salts as mobile carriers have

advantages of high diffusivity, fast reaction kinetics, high CO_2 absorption capacity and negligible volatility over other fixed amine carriers. The piperazine glycinate (PG) amino acid salts as mobile carrier enhances the mobility of CO_2-carrier reaction pathway [18, 19]. ZIF-8 as filler in MMMs is expected to interrupt the polymer chain packing thus increasing the free volume and diffusion pathway for gas penetrants thus resulting in increased CO_2 permeability [20, 21]. Also, the molecular sieving effect of ZIF-8 particle separates the smaller CO_2 gas molecules through its interior cavity leading to improved permselectivity [22].

A novel PVA/PG/ZIF-8 mixed matrix membrane exhibiting high CO_2 separation performance along with enhanced mechanical properties has been discussed in detail in Chapter 5 [42]. Further improvement in the membrane compatibility and separation performance is envisioned to be achieved with incorporation of PEI amino functional moieties into the surface of ZIF-8 nanoparticle. The novel combination of PVA/PG blend and PEI-functionalized ZIF-8 into a unique mixed matrix membrane could thus pave the path for efficient CO_2 separation. Also the role of uniformly distributed amine-modified ZIF-8 on the overall thermal and mechanical property of the membrane has been critically analysed.

6.2. Materials

Poly (vinyl alcohol) (99 mol % hydrolyzed powder, Mw = 130,000), and 2-methylimidazole (Hmim) [C_4 H_6 N_2], polyethyleneimine (average M_W = 25,000) were procured from Sigma-Aldrich, USA. Formaldehyde solution (37 wt % in H_2O), glycine (Assay> 99 %), piperazine (99 %), zinc nitrate hexahydrate [Zn $(NO_3)_2.6H_2O$], and methanol were purchased from Merck, India. The chemicals were used without any further purification. Poly (ether sulfone) (PES) support with thickness of 150 μm and pore size of 0.03 μm were acquired from Sterlitech USA. Binary feed gas (20 % CO_2 and 80 % N_2) mixture for gas permeation analysis was supplied by Vadilal Pvt. Ltd., India.

6.3. Experimental

6.3.1. Synthesis of ZIF-8@PEI nanocrystal

ZIF-8 nanocrystals were synthesized as explained [23]. The PEI modified ZIF-8 nanoparticle was prepared by the room-temperature rapid synthesis method [14]. The ZIF-8 nanoparticle was first activated by overnight drying at 150 °C for 8-10 h. A stoichiometric amount of polyethyleneimine (PEI) was dissolved in methanol solution and gradually activated ZIF-8 was added. The mixture was refluxed at 110 °C for 20 h. The solution was then centrifuged (10,000 rpm, 20 min) and finally washed with methanol several times for removal of excess unreacted reagents and finally dried at 50 °C. The schematic representation of PEI amine-functionalized ZIF-8 nanocrystal is shown in Figure 6.1.

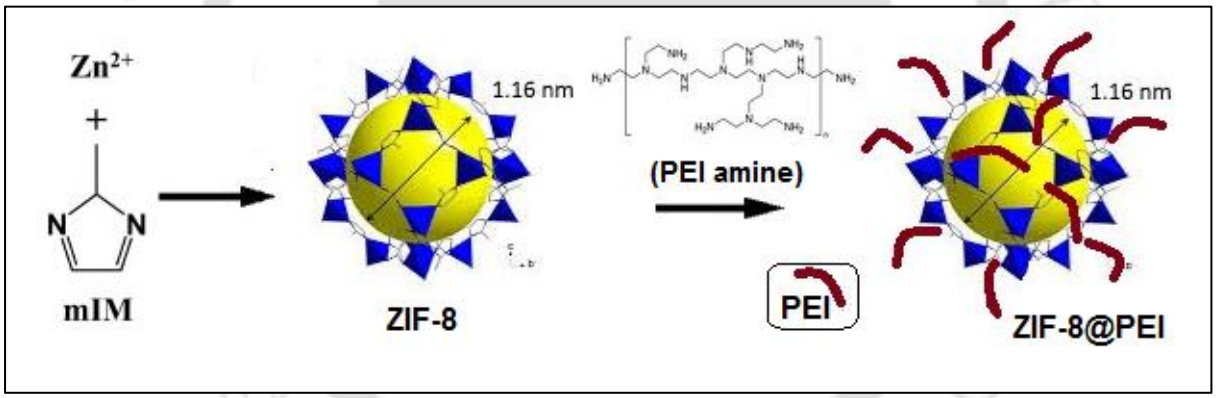

Figure 6.1 Schematic representation of PEI amine functionalized ZIF-8 (ZIF-8@PEI)

6.3.2. Synthesis of PVA/PG/ZIF-8@PEI mixed matrix membrane

For the synthesis of PVA/PG/ZIF-8@PEI membrane, the cross-linking agent, weight ratio of amine was considered in a ratio as fixed [23]. The prepared solution was kept at high viscosity (~ 1200 cp) to ensure no penetration of the coating solution on the porous substrate. It was further centrifuged (10000 rpm, 30 min) to remove any air bubble or undissolved particles. The final centrifuged solution was cast on to the porous PES support (average pore size: 0.03µm) kept over glass plate. The thickness of the polymer film was maintained by a micrometer adjustable film applicator (GARDCO, Paul N. Gardner, USA). The dense selective layer thickness result is comparable to that obtained by litematic digimatic measuring unit (Make: Mitutoyo, Model: VL-50) with an accuracy of about ± 0.5µm, and FESEM images. The average thickness of the active layer was calculated to be ~4 µm. The membrane was dried overnight in a laminar flow chamber under ambient condition followed by heating in the oven at 120 °C for 10 h.

6.4. Membrane characterization

The thermal effect of the polymer film was studied using TGA analysis (TGA4000, Perkin-Elmer, USA). Heat treatment was carried out from 25 °C to 900 °C at the rate of 10 °C/min under N_2 environment. The functional groups were confirmed from the ATR-FTIR (SHIMADZU, IRAffinity 1, and Japan) with wavenumber in the range of 4000 to 400 cm^{-1}, 40 scans per sample and 4 cm^{-1} resolutions. The ZIF-8 particles were added with KBr pellets for FTIR sample analysis. XRD analysis was performed using Bruke D8, for 2θ angles between 10º and 60° with Cu Kα radiation (30 kV-40 mA). The top and cross-sectional image established the surface morphology and distribution of ZIF-8 particles in the membrane by FETEM and FESEM, ZEISS, USA. The samples were first fractured in liquid nitrogen for ease of analysis. Thereafter, it was fixed on a stub with a carbon tape and then sputter coated with gold prior to imaging. The samples for BET were degassed for 24 h followed by analysis. The internal surface area was determined by Bruner-Emmett-Teller (BET) method. X-ray Photoelectron Spectroscopy (XPS) was conducted using Thermo Scientific Escalab Xi^+ XPS spectrometer with mono-chromated Al Kα radiation as the X-ray source of pot size 900 µm. The analysis pressure was maintained at 7×10^{-9} mBar and the data was recorded using Avantage v5.984 software.

6.5. Results and discussion

6.5.1. Thermogravimetric analysis (TGA)

Thermogravimetric analysis (Figure 6.2) of PVA/PG/ZIF-8 and PVA/PG/ZIF-8@PEI film investigated the influence of ZIF-8 and ZIF-8@PEI inclusion in the thermal stability of MMM. The excellent ZIF-8 particle intrinsic thermal behaviour and its close interaction with the polymer matrix enhanced the MMM thermal stability to ranges high enough for gas separation performance. The synthesized ZIF-8 nanocrystals exhibited excellent thermal stability (~550 °C) as already reported [23]. It is consistent with the data reported in literature [24]. Both the membranes showed three distinctive weight loss steps. The initial weight loss < 150 °C was attributed to the depletion of absorbed water molecules captured during the synthesis procedure. The second weight loss (210-360 °C) corresponds to the reduction in –OH and $–NH_2$ groups in the polymer matrix. The amine-modified ZIF-8 (ZIF-8@PEI) mixed matrix membrane (PVA/PG/ZIF-8@PEI) showed slightly lower weight loss (~25 %) than PVA/PG/ZIF-8 membrane (~30 %). This could be attributed to enhanced interaction between the amine-modified ZIF-8 and polymer matrix [24]. For both samples, the organic framework collapsed at temperature > 405 °C corresponding to the decomposition of the polymer backbone and imidazolate linker of the carbon species. The residual weight loss for PVA/PG/ZIF-8@PEI membrane (~23.7 %) reduced when compared to PVA/PG/ZIF-8 membrane (~19.3 %). Thus it can be inferred that the ZIF-8@PEI particle further improved the thermal stability of membrane when compared to unfunctionalized ZIF-8 particle.

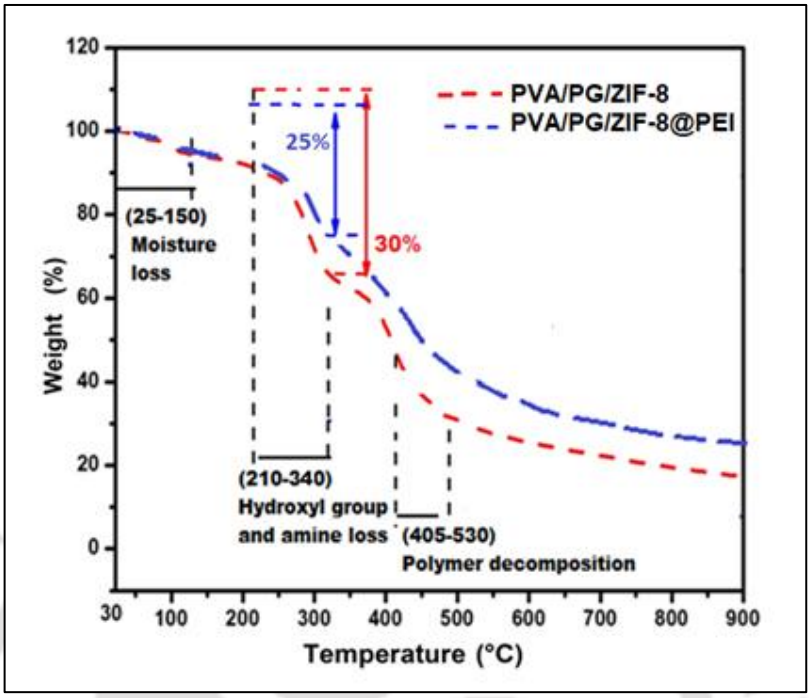

Figure 6.2 TGA curve of PVA/PG/ZIF-8 and PVA/PG/ZIF-8@PEI membrane

6.5.2. Fourier transform infrared spectroscopy (FTIR)

The FTIR study was conducted on the PVA/ZIF-8 and PVA/ZIF-8@PEI film to confirm the integration of PEI amino groups on to the ZIF-8 nanocrystal (Figure 6.3). For the PVA/ZIF-8@PEI membrane, the sharp peak intensity at 3280 cm^{-1} correspond to the symmetric vibration of the $–NH_2$ group. The formation of new peak at ~1645 cm^{-1} for PVA/ZIF-8@PEI membrane is ascribed to the presence of amino group. The absorption band at 920 and 850 cm^{-1} correspond to the N-H bending and wagging vibration. These new peaks thereby confirm the presence of amino groups and hence the successful attachment of PEI amino functionalities on the surface of ZIF-8 nanocrystals.

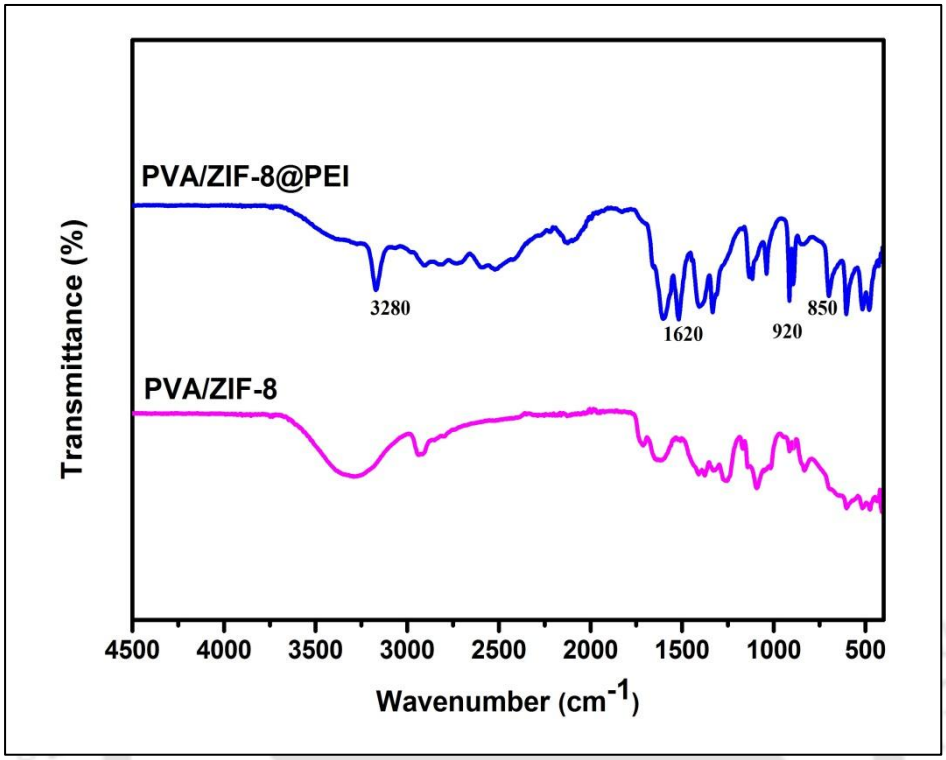

Figure 6.3 FTIR curve of PVA/ZIF-8 and PVA/ZIF-8@PEI membrane

6.5.3. Field emission transmission electron microscopy analysis (FETEM)

The FETEM image of the ZIF-8 and ZIF-8@PEI filler in PVA/PG membrane with ZIF-8 loading of ~5 wt % was depicted in Figure 6.4(a, b). The ZIF- and ZIF-8@PEI particles showed homogeneous dispersion in the polymer matrix and polyhedral-like shape. Uniform particle size with average particle diameter of ~100 nm was observed thereby confirming no change in the ZIF-8 particle morphology with amine-functionalization [25].

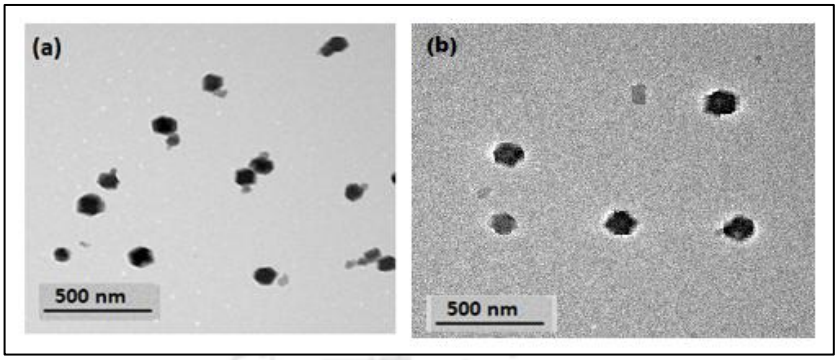

Figure 6.4 FETEM analysis of (a) ZIF-8 and (b) ZIF-8@PEI nanocrystal

6.5.4. Field emission scanning electron microscopy analysis (FESEM)

The FESEM analysis showed the top surface morphologies of PVA/PG/ZIF-8 and PVA/PG/ZIF-8@PEI membrane (Figure 6.5(a, b)). The top surface image of both the membranes established the homogeneous dispersion of ZIF-8 and amine modified ZIF-8 in the polymer matrix. The formation of distinct and uniform dense active layer confirmed no leakage of polymer solution into the porous substrate and formation of defect-free membrane [25, 26]. No visible voids were observed indicating good adhesion between the matrix and ZIF-8 and ZIF-8@PEI nanocrystals.

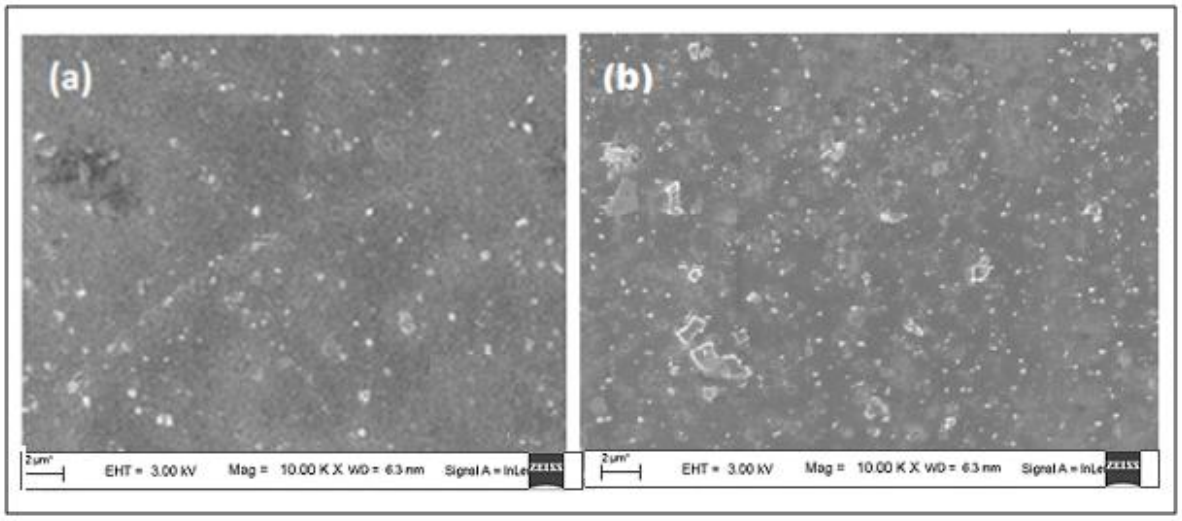

Figure 6.5 FESEM of top surface morphology of (a) PVA/PG/ZIF-8 and (b) PVA/PG/ZIF-8@PEI membrane

6.5.5. Surface area analysis

The BET analysis confirms high specific area of 1083 m^2/gm for synthesized ZIF-8 particle which reduced for ZIF-8@PEI powder (850 m^2/gm) (Figure 6.6 and Table 6.1). The polyethyleneimine (PEI) accessed the interior of ZIF-8 crystal and functionalized both the interior and exterior of the material. The partial pore blocking by the amine groups is expected to result in decrement in BET surface area. These phenomena could be contributed to the interaction of the polyethylenemine (PEI) amine with ZIF-8.

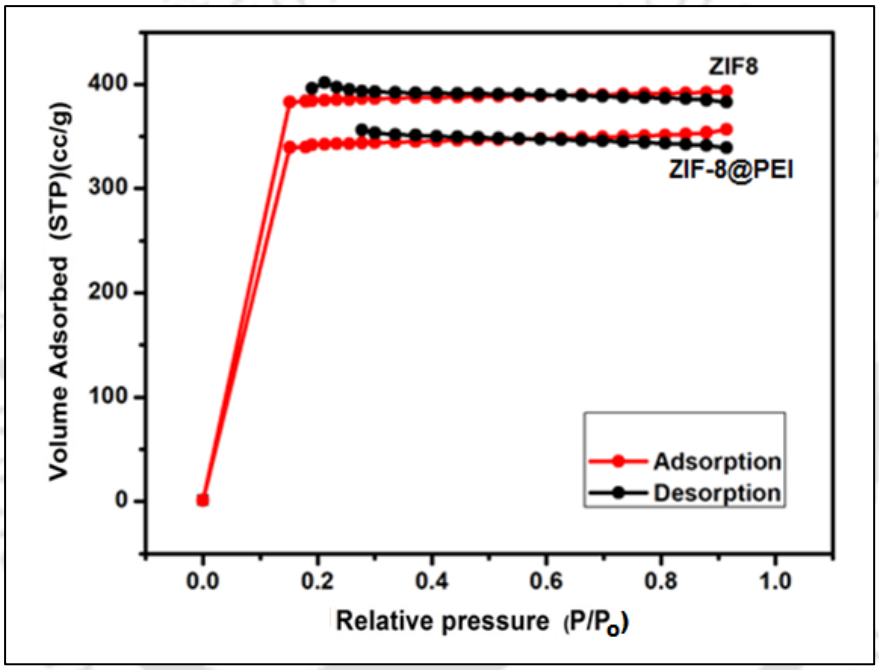

Figure 6.6 N_2 adsorption-desorption isotherm of ZIF-8 and ZIF-8@PEI

Table 6.1 BET surface area and total pore volume of the synthesized ZIF-8 and ZIF-8@PEI nanoparticles

Sample	BET surface area (m^2/gm)	Total pore volume (cm^3/gm)
ZIF-8	1083	0.58
ZIF-8@PEI	855	0.45

6.5.6. Mechanical strength analysis

The tensile strength of PVA/PG, PVA/PG/ZIF-8 and PVA/PG/ZIF-8@PEI film was determined by the stress-strain curve as shown in Figure 6.7. The mechanical stability increased with incorporation of ZIF-8 which further increased with amino-modification of ZIF-8 into the polymer material. This positive effect could be attributed to the strong interfacial interaction between ZIF-8 and the PVA matrix thereby leading to better tensile strength compared to pristine PVA/PG matrix.

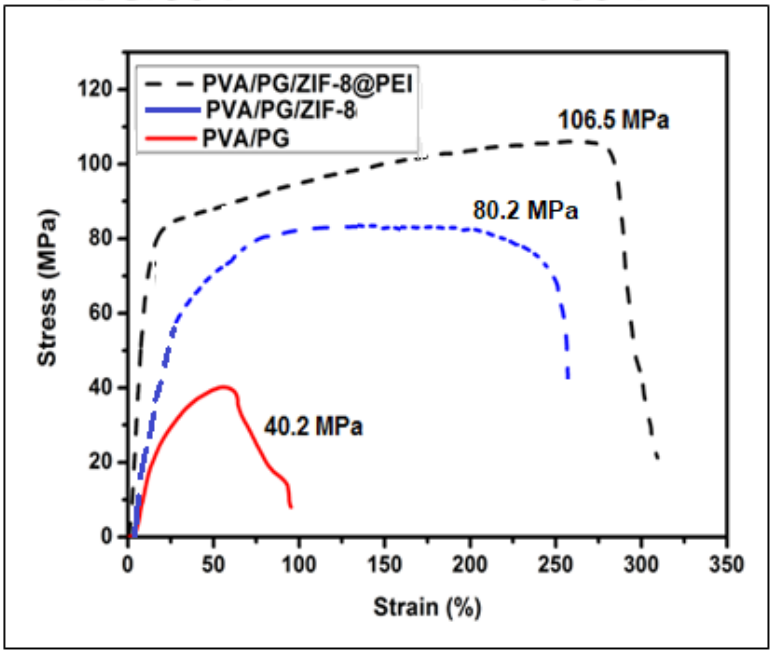

Figure 6.7 Typical stress-strain curve of PVA/PG, PVA/PG/ZIF-8 and PVA/PG/ZIF-8@PEI membrane

6.5.7. Ninhydrin assay

The standard Kaiser test with ninhydrin solution was performed to investigate the presence of PEI amine and confirm the surface amine-modification of the ZIF-8 nanoparticle [27-30]. About 1 mL of ninhydrin solution was added to fixed amount of PEI amine-modified ZIF-8 (ZIF-8@PEI) which was sonicated for ~30 mins followed by heating at 80-90 °C for 20 min. A purple-blue Ruhemann's complex was formed due to the reaction between ninhydrin solution and amino groups attached to the surface of ZIF-8. Thus the test established the successful attachment of PEI amine to the surface of the ZIF-8 filler.

6.5.8. X-ray photoelectron spectroscopy analysis (XPS)

The survey scan XPS analysis of PVA/ZIF-8 and PVA/ZIF-8@PEI film was shown in Figure 6.8(a). The survey scan of both samples confirmed the existence of C 1s, N 1s, O 1s and Zn 2p peaks corresponding to binding energies of 285 eV, 400 eV, 532 eV and 152 eV, respectively. The deconvulated N 1s peak (Figure 6.8(d)) represented a new peak at ~ 401.5 eV indicative of the amide bond formed between amine-modified ZIF-8 (ZIF-8@PEI) and the poly (vinyl alcohol) (PVA). The formation of new peak established the successful incorporation of PEI amino group onto the ZIF-8 surface [13].

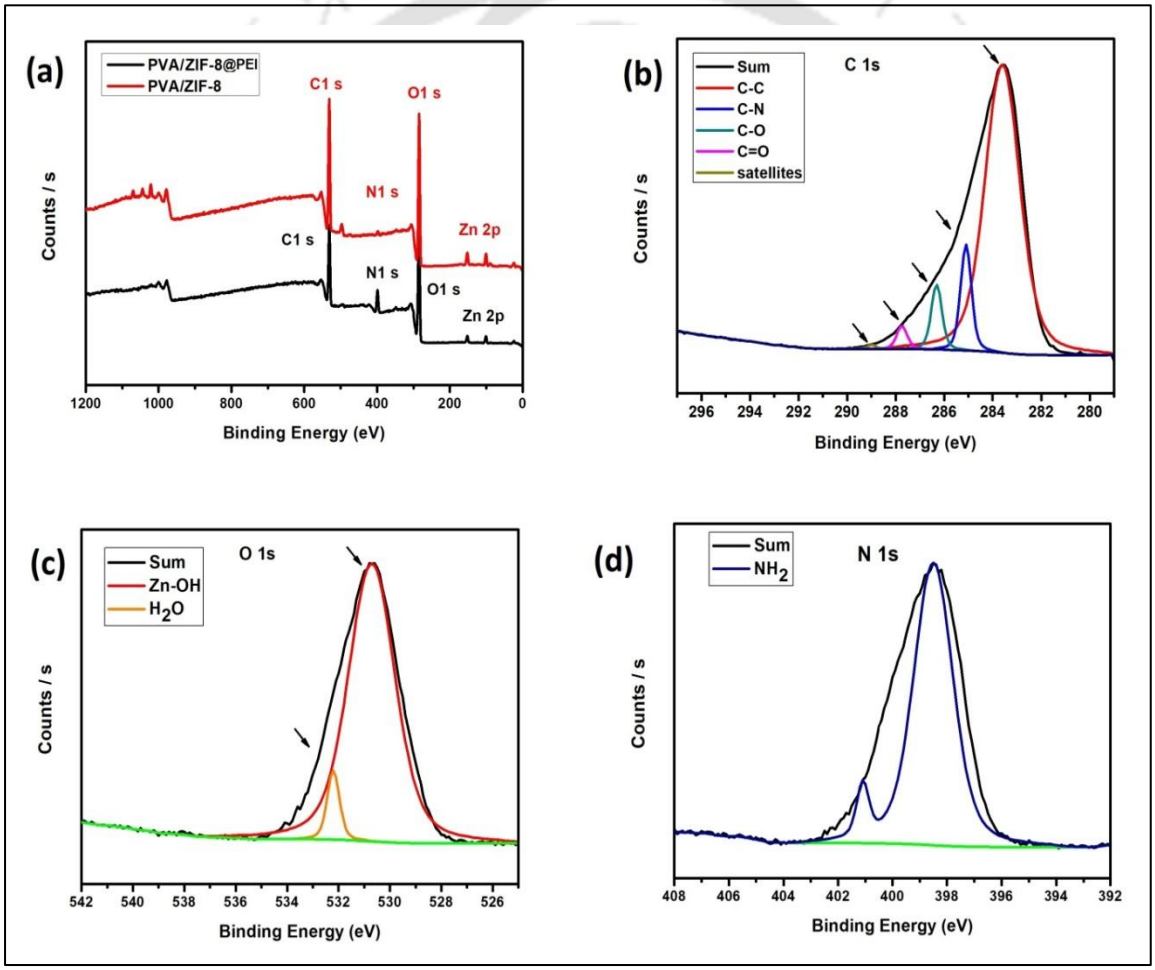

Figure 6.8 The XPS data profile of (a) survey scan of PVA/ZIF-8 and PVA/ZIF-8@PEI, de-convoluted (b) C 1s peak, (c) O 1s peak and (d) N 1s peak of PVA/ZIF-8@PEI sample

6.6. CO_2 separation performance study of membrane

The effect of CO_2 permeance (GPU) and CO_2/N_2 selectivity was analysed for amine-modified ZIF-8 MOF embedded into the PVA/PG matrix by mixed gas permeation analysis. The CO_2 separation performance was analysed for temperature (60-110 °C), and water flow rate change of sweep side (0-0.075 ml/min). Binary feed gas mixture and sweep gas (Argon (Ar)) was considered for mixed gas permeation study.

6.6.1. Effect of temperature on CO_2 performance

The effect of temperature plays a crucial role in determining the long-term application of membrane for gas separation. As observed in Figure 6.9(a), the CO_2 permeance and CO_2/N_2 selectivity showed a gradual increase with temperature. The increment in CO_2 permeance was evidently visible up to 100 ºC after which it showed a decline. This could be contributed by the amalgamated effect of the following conditions: increased CO_2 solubility and diffusivity, enhanced CO_2-amine reaction rate contributed by the mobile carrier along with the additional amines attached to ZIF-8 nanocrystal and also by the molecular sieving ability of the desired gas molecules through the pores of the ZIF-8 nanocrystals [56]. Compared to CO_2 diffusivity, the diffusion ability of N_2 gas molecules through the ZIF-8 pore is largely restricted by its geometrical constraint. The increased CO_2 solubility contributed by the interaction between the CO_2 molecule and polymer matrix along with its high diffusivity leads to an uptrend in the gas transport performance. These effects along with the facilitated transport and molecular sieving effect thus contribute to impressive CO_2 permeance and CO_2/N_2 selectivity results of 109 GPU and 385. These results were obtained for optimum conditions at temperature of 100 ºC, feed and sweep side absolute pressure of 2.5 atm and 1.2 atm and feed and sweep side water flow rates of 0.03 ml/min and 0.05 ml/min, respectively.

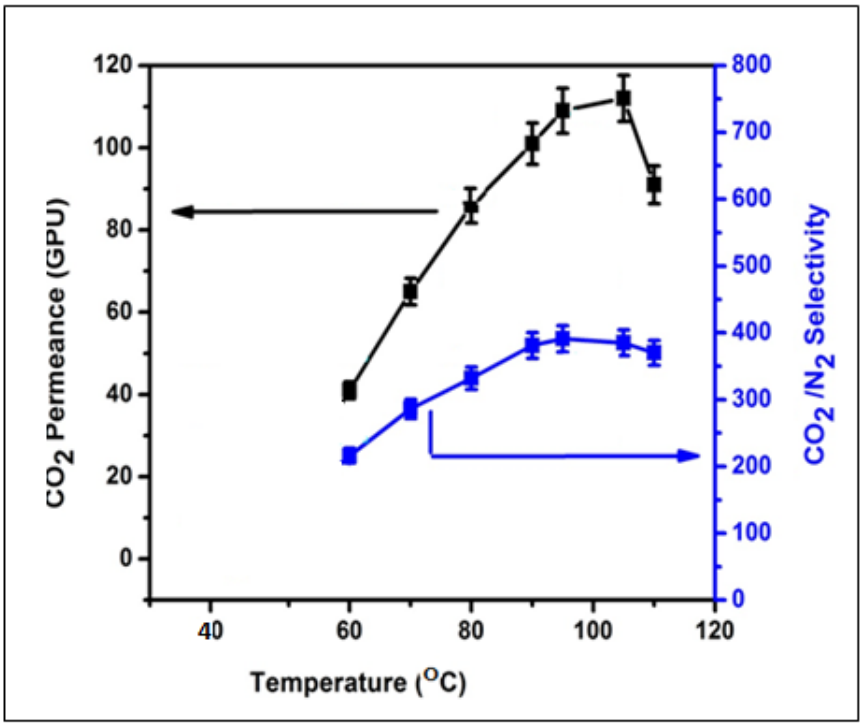

Figure 6.9(a) Effect of temperature on CO_2 permeance (GPU) and CO_2/N_2 selectivity at feed absolute pressure = 2.5 atm, sweep absolute pressure = 1.2 atm, sweep/feed water flow ratio = 1.67

6.6.2. Effect of sweep water flow rate on CO_2 performance

The change in CO_2 permeance and CO_2/N_2 selectivity with variation in sweep water flow rate was analysed as shown in Figure 6.9(b). As has been confirmed by zwitterion mechanism, the CO_2-amine reversible reaction is facilitated only in the presence of moisture. Augmentations in CO_2 transport performance occurred when the water flow rate in the sweep side surpassed the feed side water flow rate. Thus, it was observed that the CO_2 permeance and CO_2/N_2 selectivity showed noticeable and substantial rise with the introduction of moisture content into the membrane. The swelling inside the membrane increased the fractional free volume allowing more gas molecules to pass through the membrane leading to high CO_2 gas permeance along with CO_2/N_2 selectivity. However, at sweep water flow rate exceeding 0.05 ml/min, the CO_2 permeance showed no significant change. The increased fractional free volume at higher

flow rate (> 0.05 ml/min) allows the larger N_2 molecules to pass through thereby slightly impeding the CO_2/N_2 selectivity results at sweep water flow rate > 0.05 ml/min.

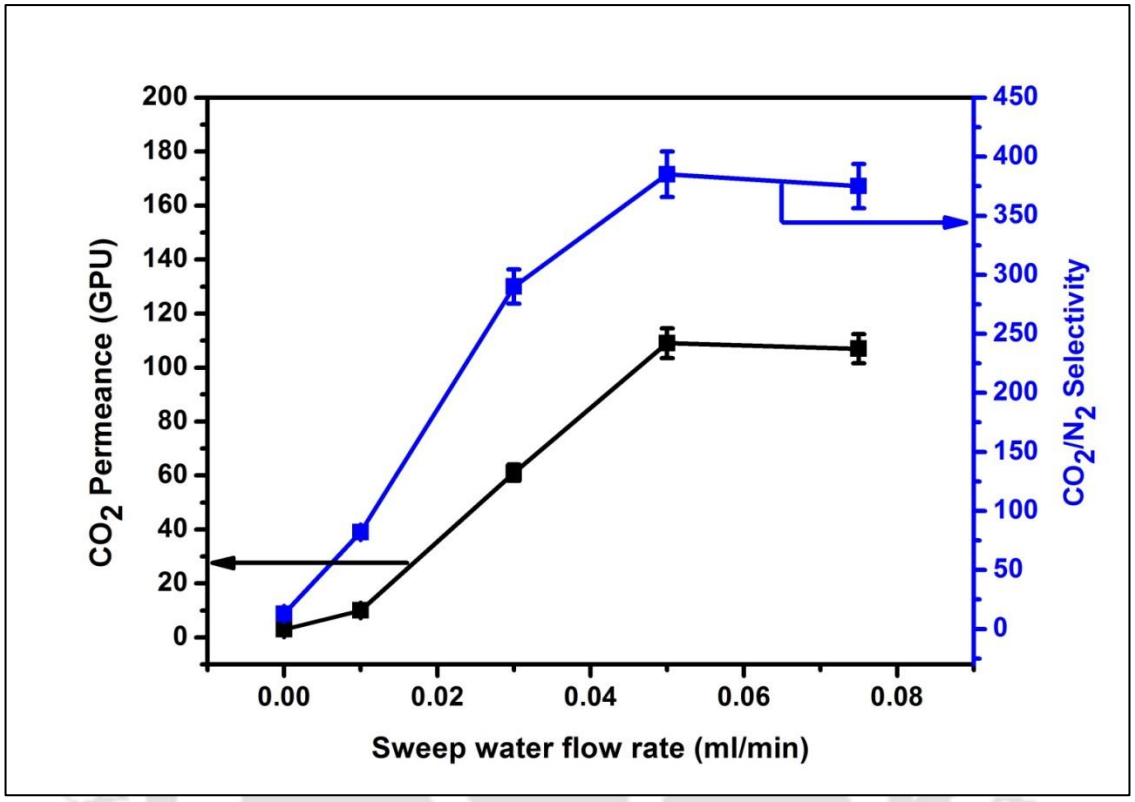

Figure 6.9(b) Effect of sweep water flow rate (ml/min) on CO_2 permeance (GPU) and CO_2/N_2 selectivity at temperature of 100 ºC, feed and sweep absolute pressure of 2.5 and 1.2 atm

The effect of PVA/PG, PVA/PG/ZIF-8 and PVA/PG/ZIF-8@PEI membrane sample on the CO_2 permeance (GPU) and CO_2/N_2 selectivity has been depicted (Figure 6.10).

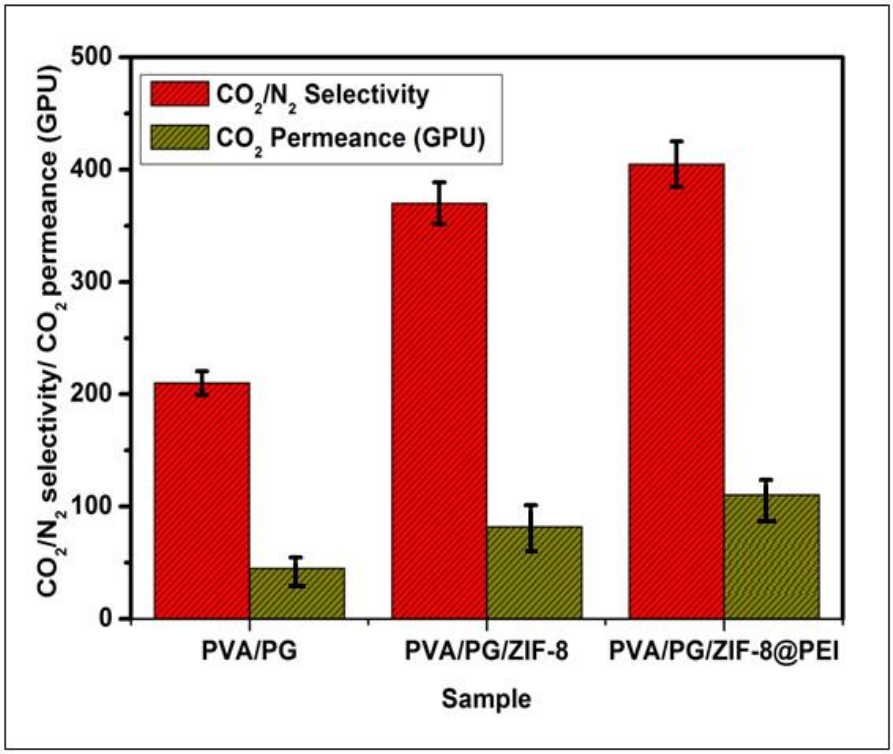

Figure 6.10 Effect of CO_2 permeance (GPU) and CO_2/N_2 selectivity on PVA/PG, PVA/PG/ZIF-8 and PVA/PG/ZIF-8@PEI sample at temperature=100 °C, feed/ sweep water flow rate= 0.03/0.05 ml/min, and feed/sweep side pressure= 2.5/1.2 atm, respectively

6.7. Robeson's curve

The permeation results obtained experimentally in this work well surpassed Robeson's upper bound curve (Figure 6.11). This result discussed the effect of amine impregnation on ZIF-8 filler on the CO_2 performance and mechanical property of the membrane.

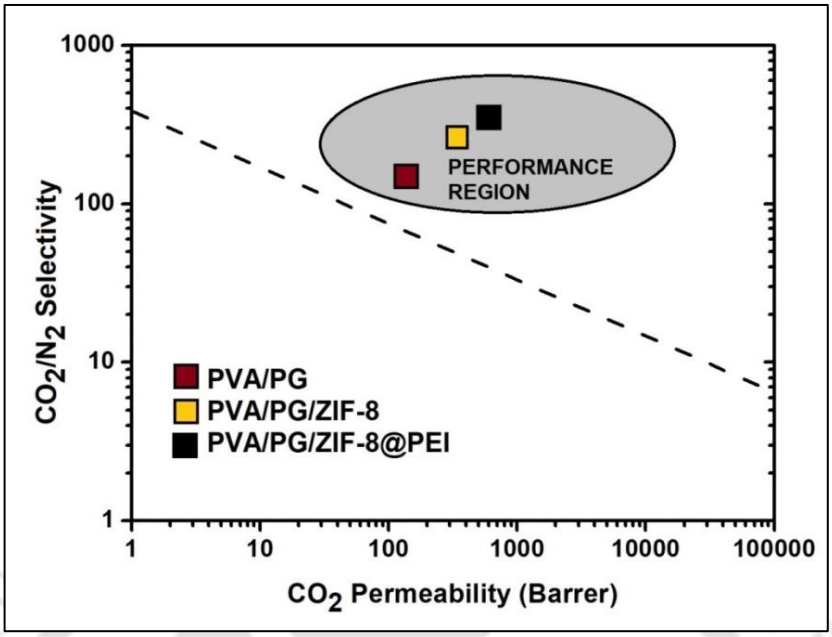

Figure 6.11 Robeson's upper bound curve of PVA/PG, PVA/PG/ZIF-8 and PVA/PG/ZIF-8@PEI membrane

6.8. Conclusions

ZIF-8 MOFs were surface functionalized with polyethylenimine (PEI) amine-moieties and its effect on the CO_2 permeance (GPU) and CO_2/N_2 selectivity was analysed. High-performance defect-free, thin PVA/PG MMMs (active layer thickness ~4µm) with ZIF-8@PEI loading were synthesized on PES support by solution casting method. The amine-functionalized ZIF-8 material (ZIF-8@PEI) showed improved tensile strength and uniform distribution in the PVA/PG matrix with negligible change in the membrane morphology (uniform size ~100 nm). The thermal stability improved with the addition of ZIF-8 which further increased with PEI functionalized ZIF-8 (ZIF-8@PEI). This ensured good interaction and compatibility between the PVA matrix and ZIF-8 filler. The FTIR and XPS analysis confirmed the successful interaction of PEI amine into ZIF-8 nanocrystal. The decline in the BET surface area confirmed the filling of the nanofiller pore with the PEI amine and hence its subsequent interaction between the amine and the

ZIF-8 pore. For a temperature of 100 °C, feed/sweep water flow rate of 0.03/0.05 ml/min and feed/sweep side pressure of 2.5/1.2 atm, respectively, the PVA/PG/ZIF-8@PEI membrane showed CO_2/N_2 selectivity and CO_2 permeance results of 385 and 109 GPU. The CO_2/N_2 selectivity and CO_2 permeance showed 4.05 % and 33 % increment when compared to PVA/PG/ZIF-8 membrane and by 83.4 % and 142.2 % when compared to PVA/PG membrane. This result could be attributed to the molecular sieving properties of the amino-functionalized ZIF-8 and the presence of amino groups in the ZIF-8 filler thereby facilitating the reversible CO_2-amine reaction. The amine groups enhanced the overall CO_2-philicity thereby increasing the CO_2 permeance along with selectivity. This was further confirmed by Robeson's curve wherein the PVA/PG, PVA/PG/ZIF-8 and PVA/PG/ZIF-8@PEI films showed impressive gas separation surpassing the Robeson's upper bound limitation. Thus, it could be well established that this membrane could serve as prospective material for large-scale CO_2 separation from flue gas.

References

[1] P. Krokidas, S. Moncho, E.N. Brothers, M. Castier and I.G. Economou, Tailoring the gas separation efficiency of metal organic framework ZIF-8 through metal substitution: a computational study, Phys. Chem. Chem. Phys. 20 (2018) 4879-4892.

[2] K. Tao, C. Kong and L. Chen, High performance ZIF-8 molecular sieve membrane on hollow ceramic fiber via crystallizing-rubbing seed deposition, Chem. Eng. J. 334 (2018) 1749-1753.

[3] G. Yuan, H. Tu, J. Liu, C. Zhao, J. Liao, Y. Yang, J. Yang and N. Liu, A novel ion-imprinted polymer induced by the glycylglycine modified metal-organic framework for the selective removal of Co (II) from aqueous solutions, Chem. Eng. J. 333 (2018) 280-288.

[4] M.S. Denny Jr, J.C. Moreton, L. Benz and S.M. Cohen, Metal-organic frameworks for membrane-based separations, Nat. Rev. Mater. 1 (2016) 16078.

[5] H. Gong, C.Y. Chuah, Y. Yang and T.H. Bae, High performance composite membranes comprising Zn (pyrz) $_2$ (SiF_6) nanocrystals for CO_2/CH_4 separation, J. Ind. Eng. Chem. 60 (2018) 279-285.

[6] N.A.H.M. Nordin, A. F. Ismail, N. Misdan and N.A.M. Nazri, Modified ZIF-8 mixed matrix membrane for CO_2/CH_4 separation, AIP Conference Proceedings. 1891 (2017) 02009.

[7] B. Ghalei, K. Sakurai, Y. Kinoshita, K. Wakimoto, A.mP. Isfahani, K. Song, K. Doitomi, S. Furukawa, H. Hirao, H. Kusuda, S. Kitagawa and E. Sivaniah, Enhanced selectivity in mixed matrix membranes for CO_2 capture through efficient dispersion of amine-functionalized MOF nanoparticles, Nat. Energy. 2 (2017) 17086.

[8] C. Wang, D. Liu and W. Lin, Metal-organic frameworks as a tunable platform for designing functional molecular materials, J. Am. Chem. Soc. 135(36) (2013) 13222-13234.

[9] Z. Zhang, S. Xian, Q. Xia, H. Wang, Z. Li and J. Li, Enhancement of CO_2 adsorption and CO_2/N_2 selectivity on ZIF-8 via postsynthetic modification, separations: Materials, Devices, and Processes. 59(6) (2013) 2195-2206.

[10] K.Y. Cho, H. An, X.H. Do, K. Choi, H.G. Yoon, H.K. Jeong, J.S. Lee and K.Y. Baek, Synthesis of amine-functionalized ZIF-8 with 3-amino-1,2,4-triazole by post synthetic modification for efficient CO_2–selective adsorbents and beyond, J. Mater. Chem. A. 6 (2018) 18912-18919.

[11] M.W. Anjum, F. Vermoortele, A.L. Khan, B. Bueken, D. De. Vos and I. Vankelecom, Modulated UiO-66 based mixed matrix membranes for CO_2 separation, ACS Appl. Mater. Interfaces. 7 (45) (2015) 25193–25201.

[12] N.H. Yahya, Y.F. Yeong and L.S. Lai, Synthesis of amino-impregnated ZIF-8 for CO_2 adsorption, IOP Conf. Series: Mater. Sci. Eng. 226 (2017) 012164.

[13] S. Yu, S. Li, S. Huang, Z. Zeng, S. Cui and Y. Liu, Covalently bonded zeolitic imidazolate frameworks and polymers with enhanced compatibility in thin film nanocomposite membranes for gas separation, J. Membr. Sci. 540 (2017) 155–164.

[14] S. Xian, F. Xu, C. Ma, Y. Wu, Q. Xia, H. Wang and Z. Li, Vapor-enhanced CO_2 adsorption mechanism of composite PEI@ZIF-8 modified by polyethyleneimine for CO_2/N_2 separation, Chem. Eng. J. 280 (2015) 363-369.

[15] A. Mondal, M. Barooah and B. Mandal, Effect of single and blended amine carriers on CO_2 separation from CO_2/N_2 mixtures using crosslinked thin-film poly(vinyl alcohol) composite membrane, Int. J. Greenh. Gas Con. 39 (2015) 27-38.

[16] L. Ansaloni, Y. Zhao, B.T. Jung, K. Ramasubramanian, M.G. Baschetti and W.S.W. Ho, Facilitated transport membranes containing amino-functionalized multi-walled carbon nanotubes for high-pressure CO_2 separations, J. Membr. Sci. 490 (2015) 18-28.

[17] G. Guerrero, D. Venturi, T. Peters, N. Rival, C. Denonville, C. Simon, P.P. Henriksen and M.B. Hagg, Influence of functionalized nanoparticles on the

CO_2/N_2 separation properties of PVA-based gas separation membranes, Energy Procedia. 114 (2017) 627-635.

[18] Y. Chen and W.S.W. Ho, High-molecular-weight polyvinylamine/piperazine glycinate membranes for CO_2 capture from flue gas, J. Membr. Sci. 514 (2016) 376-384.

[19] M.E. Hamzehie and H. Najibi. Experimental and theoretical study of carbon dioxide solubility in aqueous solution of potassium glycinate blended with piperazine as new absorbents, J. CO_2 Utilization. 16 (2016) 64-77.

[20] A.F. Bushell, M.P. Attfield, C.R. Mason, P.M. Budd, Y. Yampolskii, L. Starannikova, A. Rebrov, F. Bazzarelli, P. Bernardo, J.C. Jansen, M. Lanč, K. Friess, V. Shantarovich, V. Gustov and V. Isaeva, Gas permeation parameters of mixed matrix membranes based on the polymer of intrinsic microporosity PIM-1 and the zeolitic imidazolate framework ZIF-8, J. Membr. Sci. 427 (2012) 48-62.

[21] C. Zhang, Y. Dai, J.R. Johnson, O. Karvan and W.J. Koros, High performance ZIF-8/6FDA-DAM mixed matrix membrane for propylene/propane separations, J. Membr. Sci. 389 (2012) 34-42.

[22] M.Z. Ahmad, V.M. Gil, V. Perfilov, P. Sysel and V. Fila, Investigation of a new co-polyimide, 6FDA-bisP and its ZIF-8 mixed matrix membranes for CO_2/CH_4 separation, Sep. Purif. Technol. 207 (2018) 523-534.

[23] M. Barooah and B. Mandal, Synthesis, characterization and CO_2 separation performance of novel PVA/PG/ZIF-8 mixed matrix membrane, J. Membr. Sci. 572 (2019) 198-209.

[24] H. Shin, W.S. Chin, S. Bae, J.H. Kim and J. Kim, High-performance thin PVC-POEM/ZIF-8 mixed matrix membranes on alumina supports for CO_2/CH_4 separation, J. Ind. Eng. Chem. 53 (2017) 127-133.

[25] M. Wu, X. Guo, F. Zhao and B. Zeng, A Poly(ethyleneglycol) Functionalized ZIF-8 membrane prepared by coordination-based post-synthetic strategy for the enhanced adsorption of phenolic endocrine disruptors from water, Scientific Reports. 8912 (2017).

[26] B. Prasad and B. Mandal, Graphene-incorporated biopolymeric mixed-matrix membrane for enhanced CO_2 separation by regulating the support pore filling, ACS Appl. Mater. Interfaces. 10(33) (2018) 27810-27820.

[27] E.S. Cantu, R. Cueto, J. Koch and P.S. Russo, Synthesis and rapid characterization of amine-functionalized silica, Langmuir. 28 (2012) 5562−5569.

[28] S.H. Araghi and M.H. Entezari, Amino-functionalized silica magnetite nanoparticles for the simultaneous removal of pollutants from aqueous solution, Appl. Surf. Sci. 333 (2015) 68–77.

[29] L.F. de Oliveira, K. Bouchmella, A.S. Picco, L.B. Capeletti, K.A. Gonçalves, J.H.Z. dos. Santos, J. Kobarge and M.B. Cardoso, Tailored silica nanoparticles surface to increase drug load and enhance bactericidal response, J. Braz. Chem. Soc. 28(9) (2017) 1715-1724.

[30] H.T. Lu, Synthesis and characterization of amino functionalized silica nanoparticles, Colloid J. 75(3) (2013) 311–318

[31] X. Zhang, T. Zhang, Y. Wang, J. Li, C. Liu, N. Li and J. Liao, Mixed-matrix membranes based on Zn/Ni-ZIF-8-PEBA for high performance CO_2 separation, J. Membr. Sci. 560 (2018) 38-46.

[32] C. Wang, D. Liu and W. Lin, Metal-organic frameworks as a tunable platform for designing functional molecular materials, J. Am. Chem. Soc. 135(36) (2013) 13222-13234.

CHAPTER 7

Overall Conclusions and Recommendation for Future Work

CHAPTER 7

Overall Conclusions and Recommendation for Future Work

This chapter summarizes the salient achievements and major conclusions based on the investigations carried out in the present study. It also highlights the major recommendations for future work in the relevant field.

7.1. Major conclusions

This work has been studied systematically to understand the gas transport behaviour and applicability of CO_2-selective membrane. The experimental results provide a good data base for rational design of membrane process. The results obtained in this work suggest that CO_2-selective polymer and mixed matrix membranes have a very good potential for industrial large-scale CO_2 separation from flue gas.

The major conclusions are summarized below:

- Novel crosslinked PVA membrane with PEG as blend polymer, PEI and TETA amine as carriers and hydrophilic SiO_2 nanoparticles synthesized by in situ sol-gel technique were prepared by solution casting methodology. The dispersion and interaction of the filler into polymer matrix were confirmed by TGA, FTIR, XRD, FETEM and FESEM analysis. FESEM analysis of the synthesized membranes established the homogeneous dispersion of the filler in the polymer matrix. The increased compatibility between the polymer-filler group and the thermal and mechanical behaviour of the membrane. Compared to pristine PVA/PEG membrane, PVA/PEG/Sil membrane with 3 wt % silica loading showed pronounced improvement in CO_2 transport performance with 78 % and 36 % improvement in CO_2 permeance and CO_2/N_2 selectivity for fixed conditions pertaining to sweep side water flow rate of 0.04 ml/min and 100 °C temperature.

- The silica prepared by Stober's process was amino-functionalized with 3-aminopropyltrimethoxysilane (APTMS) coupling agent to form the amino-functionalized silica (APTMS-Sil). This was further added to the PVA/PEG matrix to form a novel PVA/PEG/APTMS-Sil mixed matrix membrane. Detailed characterization studies revealed the impact of amine-functionalization on the mechanical strength of the membrane. The successful impregnation on to the silica surface were confirmed by XPS analysis and ninhydrin assay. The transport properties of the binary gas mixture (CO_2/N_2) for PVA/PEG/APTMS-Sil membrane for temperature and sweep water flow rate variation revealed enhancement in selectivity and permeance with silica functionalization. The PVA/PEG/APTMS-Sil membrane exhibited optimal CO_2 permeance of 36 GPU and CO_2/N_2 selectivity of 325 at sweep water flow rate of 0.04 ml/min and temperature of 100 °C. The performance beyond the Robeson's curve opens up possibility of the material as a prospective contender for large-scale carbon capture studies.

- Zeolitic imidazolate framework-8 (ZIF-8) having regular pore size (~0.35 nm) were synthesized and embedded into the poly (vinyl alcohol) (PVA)/ piperazine glycinate (PG) polymer solution coated on to polyethersulfone (PES) support and utilized for CO_2/N_2 separation studies. Detailed characterization studies and the effect of temperature and sweep water flow rate on the membrane performance were evaluated. The excellent compatibility of ZIF-8 filler in the PVA/PG matrix resulted in enhancement of CO_2 permeance and CO_2/N_2 selectivity. The results depicted that PVA/PG membrane loaded with 5 wt % ZIF-8 (PVA/PG/ZIF-8) showed high CO_2 permeance of 82 GPU and CO_2/N_2 selectivity of 370 which was 82.2 % and 76.2 % higher compared to pristine crosslinked PVA/PG membrane. Thus ZIF-8 doped PVA mixed matrix membrane serves as a potential candidate for industrial gas separation studies.
- Zeolitic imidazolate framework (ZIF-8) MOF surface functionalized with polyethyleneimine (PEI) amine-functional moieties was prepared for successful fabrication of robust high-performance PVA/PG/ZIF-8@PEI mixed matrix membrane. Detailed characterization studies and the effect of sweep water flow rate and temperature for the binary gas mixture (CO_2/N_2) was analysed. The

PVA/PG/ZIF-8@PEI membrane exhibited CO_2 permeance of 109 GPU and CO_2/N_2 selectivity of 385 which showed an appreciable 142.2 % and 83.4 % increment compared to PVA/PG membrane. The appreciable molecular sieving properties of the fine-tuned amino-functionalized ZIF-8 allowing selective passage of gas molecules and the amino groups in the highly branched polyethyleneimine (PEI) facilitating the CO_2-amine reaction mechanism demonstrated a potential and novel mixed matrix membrane for CO_2 separation.

This study was undertaken to improve the CO_2 separation performance by employing facilitated transport polymeric and mixed matrix membranes. Poly (vinyl alcohol) (PVA) was chosen as the base polymer based on its suitability for gas separation. To achieve high separation efficiency, three different approaches was considered. The first approach consisted of considering various combinations of amines such as PEI, TETA, PG salt by engaging into the PVA polymer blend. It was observed that the PEI, TETA and PG addition initiated the CO_2 facilitated transport with impressive performance. In the second approach, with encouraging results obtained using the polymer facilitated transport membrane, inorganic fillers such as silica and ZIF-8 MOF were utilized and embedded into the membranes. The prepared novel PVA/PEG/Silica and PVA/PG/ZIF-8 membrane improved the membrane properties and showed outstanding results with increment in CO_2 permeance and CO_2/N_2 selectivity by many folds compared to its polymeric counterparts. This was achieved owing to the outstanding compatibility between the silica and ZIF-8 particle interface with the polymer backbone. The increased interaction between the polymer-particle interface increased its mechanical and thermal behavior along with its gas transport performance. In the third and final approach, to further increase the membrane compatibility and separation behavior, the silica and ZIF-8 particle were surface functionalized with PEI and APTMS amino-functional groups. Interesting results were achieved with encouraging improvement in the gas transport performance and membrane properties. This is attributed to the increased facilitated transport mechanism with the increment in the overall amine groups present in the polymer chain. All the membranes considered in this work showed good performance with results surpassing Robeson's upper bound limit as depicted in Figure 7.1. The

comparison table of CO_2 permeability and CO_2/N_2 selectivity results for different membrane material with the results obtained in this thesis work has been shown in Table 7.1.

The crosslinked PVA/PG with PEI amine-functionalized ZIF-8 (PVA/PG/ZIF-8@PEI) membrane showed optimum CO_2 permeance and CO_2/N_2 selectivity of 109 GPU and 385 for uniform active layer thickness of 4µm, respectively. Overall, it can thus be concluded that the work undertaken here forwards an innovative route for utilization of the test polymers for CO_2 separation with an effort to convert waste to wealth along with positive impact on energy and environment.

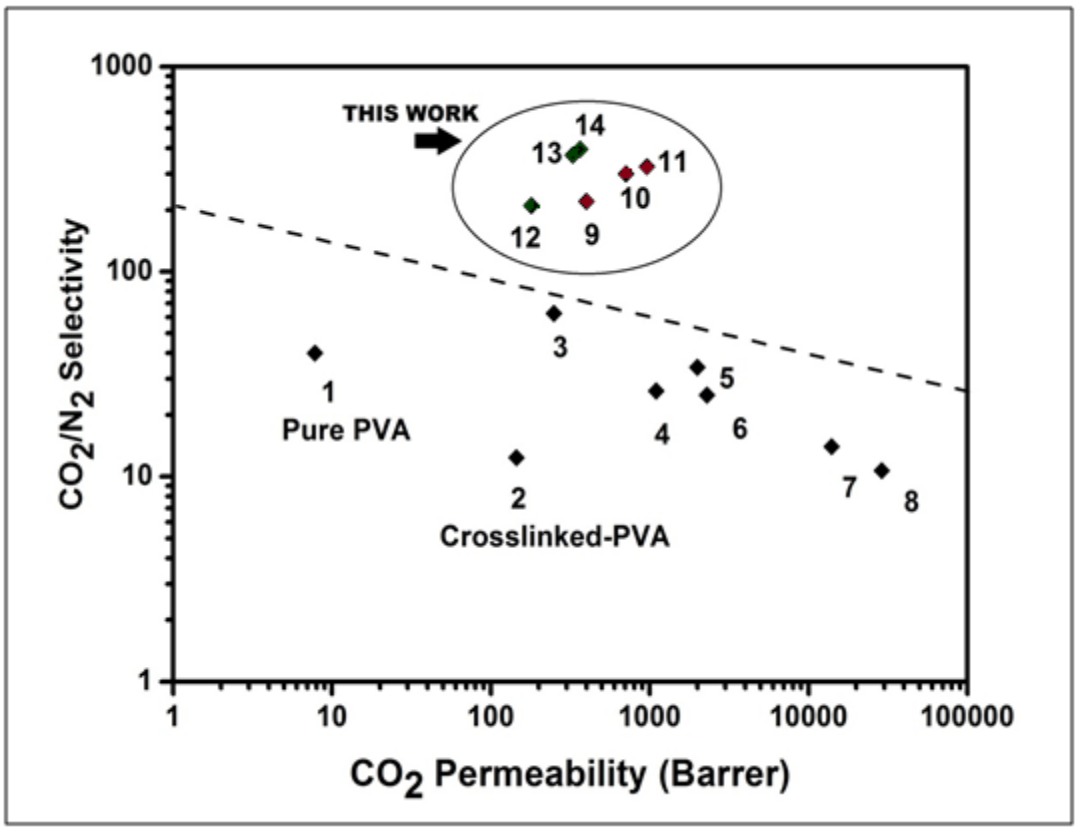

Figure 7.1 The upper bound relationship of CO_2 permeability (Barrer) and CO_2/N_2 selectivity of different polymeric membrane

Table 7.1 CO_2 permeability and CO_2/N_2 selectivity results for different membrane material

Composition in Figure 7.1	Polymer	CO_2 permeability (Barrer)	CO_2/N_2 selectivity	Ref
1	Pure PVA without carrier	7.8	40	[1]
2	Cross-linked PVA without carrier	145	12.4	
3	Poly[bis(2-(2-methoxyethoxy)ethoxy) phosphazene]	250	62.5	
4	PIM-7	1100	26.2	
5	Modified poly(dimethylsiloxane)	2000	34.2	[2]
6	PIM-1	2300	25	
7	Poly(trimethylgermylpropyne)	14000	14	
8	Poly(trimethylsilylpropyne)	29000	10.7	
9	**Crosslinked PVA/PEG membrane**	**400**	**220**	
10	**Crosslinked PVA/PEG/silica membrane**	**710**	**300**	
11	**Crosslinked PVA/PEG/APTMS-silica membrane**	**963**	**325**	**This Work**
12	**Crosslinked PVA/PG membrane**	**180**	**210**	
13	**Crosslinked PVA/PG/ZIF-8 membrane**	**328**	**370**	
14	**Crosslinked PVA/PG/ZIF-8@PEI membrane**	**436**	**385**	

7.2. Recommendations on future directions

This work presents a systematic and detailed investigation to understand the reactive membrane based separation characteristics with different amine carriers and inorganic fillers. There are certainly several areas which merit further research attention.

- Different filler materials and also ionic liquid could be explored into PVA based MMMs for study of CO_2 separation.
- Effect of impurities from industrial flue gases like SOx and NOx on the gas performance and stability of the membrane can be studied.
- Economic assessment of the synthesised membranes should be considered for scale-up for industrial application.
- Functionalization of the nanomaterials with different moieties could be explored to study the gas transport behaviour.
- The stability of the membranes has been tested for 18-20 days. The stability could be tested for even longer time period to be deemed useful for large-scale commercial application.
- Preparation of thinner membranes (< 4 μm) may be considered to achieve a high CO_2 permeance as it is needed for CO_2 capture from flue gas for reducing the capture cost.
- Equilibrium data to study the improvement in solubility and diffusivity could be included as future scope of study. Also, rigorous model may be developed for the successful design of the membrane transport process.

References

[1] Y. Cai, Z. Wang, C. Yi, Y. Bai, J. Wang and S. Wang, Gas transport property of polyallylamine-poly(vinyl alcohol)/polysulfone composite membranes, J. Membr. Sci. 310 (2008) 184-196.

[2] L.M. Robeson, The upper bound revisited, J. Membr. Sci. 320 (2008) 390- 400.

APPENDIX 1

Detailed Experimental Protocol Followed for Gas Permeation Measurement

A1.1 Experimental protocol

A.1.1.1 Membrane cell

The membrane module was custom made by stainless steel 316 in spherical shape. The module divided into two part: upper section is called the feed side and the lower section is called permeate side. A porous stainless steel membrane was used as a support for polymer composite membrane. The porous stainless steel support was kept at the permeate side of the membrane module. The polymer composite membrane was placed carefully on the top of the metal support. Finally, both parts of the module were sealed by two silicones O-rings with the help of six allen key socket head screw.

A.1.1.2 Feed gas control and regulatory system

The mixed gas supplied to the feed side of the membrane module consist of 20 % CO_2 and 80 % N_2. A two stage pressure regulator was used to control outlet pressure from the cylinder (1-25 bar). The feed gas then flows through the mass flow controller (MFC) at feed side whereby the gas flow rate is controlled. The outlet connection of the MFC (flow range: 0-250 ml/min, maximum pressure limit: 1000 psi) flows to the feed side of the membrane module through a humidifier. The pressure at the feed side of the membrane module was maintained by the back pressure regulator (0-20 bar) connected to the outlet of the feed side membrane module. Finally, the outlet of the back pressure regulator was connected to the G.C for composition analysis.

A.1.1.3 Permeate gas control and regulatory system

The permeate section supplies pure argon (Ar) gas as a carrier to the permeate side of the membrane module. Other connections of the permeate side were similar to the feed side with separate MFC (flow range: 0-250 ml/min, maximum pressure limit: 1000 psi).

A.1.1.4 HPLC pump

Two HPLC pumps were used to supply moisture to the feed and carrier gas. Automated program controller helps to maintain very low water flow rate (0.01-0.1 ml/min) against pressure.

A.1.1.5 Temperature controlled hot-air oven

The membrane module and two humidifiers were kept inside the oven through which the temperature of the system was maintained. Automated program controller was used to control temperature along with heating rate. Also it had been observed that the temperature fluctuation against set temperature was around ± 1 ºC.

A.1.1.6 Gas chromatograph with gas sampling valve (GSV)

During the permeation experiment, gas sampling valve was used for automatic sample gas injection with 100 micro liter sample loop. Initially the G.C was calibrated with five known concentration of CO_2 and N_2 gas mixture. (4 % CO_2 + 4 % N_2, balance Argon), (8 % CO_2 + 8 % N_2, balance Argon), (12 % CO_2 + 12 % N_2, balance Argon), (20 % CO_2, balance N_2) and (40 % CO_2, balance N_2) were used as calibration gas. The calibration gas purity list is shown in Appendix A3.3 (Table A3.1). The chromatograph was equipped with Thermal Conductivity Detector (TCD) and CP7430 capillary column (Agilent Technologies, Palo Alto, CA) which was the combination of two different capillary columns, one being the CP-Molsieve 5A and the other CP-PoraBOND Q. CP-PoraBOND Q (length = 25 m, I.D = 0.32 mm and df = 7 micron) is highly sensitive and accurate for the measurement of CO_2 concentration and CP-Molsieve 5A (length = 50 m, I.D = 0.53 mm and df = 50 micron) is capable for the separation of N_2 and Ar (argon). He (helium) was used for the G.C carrier gas.

A1.2 Permeation setup operational protocols

A.1.2.1 Inherent leak testing

The leak rate of the feed and permeate section observed by using transparent cellophane paper as a membrane and pressurizing the entire set-up for one day. The pressure increment in the two sections was then monitored for a day. Finally, the experiment was repeated with another cellophane paper to confirm the leak rate and the proper sealing of the membrane cell.

A.1.2.2 Operational protocols

The proper placement of the polymer composite membrane in the module is important to prevent membrane damage and accurately define the surface area of the membrane available for permeation. The module was carefully installed in the oven with the help of stainless steel gasket at room temperature (25 ^{o}C).

After the membrane installation, test was conducted to check for any membrane defects, such as stress fracture or pin-holes. For that reason, pressure at feed side was increased at a certain set point and kept for some time to observe the gas flow rate at permeate side. Then the temperature was slowly increased and the gas flow rate was observed at permeate side to check the membrane damage against temperature. The carrier gas (Ar) was injected at the permeate side of the module and the HPLC pump was then switched-on for both sides with particular water flow rates.

The experimental protocol can be divided into the following sections:

(1) Sample loading

- The membrane module is properly cleaned before placing the membrane in the module.
- The membrane is properly placed in the module and sealed with the help of O-rings and carefully installed inside the oven.

(2) Leak test

- After proper installation of the membrane, membrane defect such as stress fracture or pin-holes were checked by increasing pressure in the feed side and consecutively the gas flow rate at the permeate side was observed. If with pressure, the gas flow rate in the permeate side showed abnormal increase or the flow was also observed in the retentate side, then it could be established that the membrane showed leak and is not suitable for permeation study. Similar test was conducted to check the membrane behaviour with increase in temperature. Thereafter, the carrier gas (Ar) was injected and permeation analysis conducted.

APPENDIX 2

Generalized Calculation of Dry Membrane Compositions

A2.1 General calculation procedure

The amount of the materials considered for membrane formation can be calculated by the generalised formula given below:

Amount of PVA taken as basis = 2 gm

Mole of PVA taken = 2/44 = 0.045 mole

[Molecular weight of one repeating unit of PVA = 44 gm / mole]

Amount of (OH) groups of PVA reacting :

$$= 0.045 \times \text{wt\% of PVA} \times \text{mole\% of degree of crosslinking}$$

$$= 0.045 \times \frac{X}{100} \times \frac{N}{100} \text{ mole}$$

$$= 0.0000045 \times X \times N \text{ mole}$$

Amount of HCHO required:

$$= (0.0000045 \times X \times N) \times (\frac{30.03}{0.37}) \text{ gm}$$

[Molecular weight of HCHO = 30/0.03 gm/ mole and HCHO solution concentration = 37 wt %]

Weight of PVA increased after reaction:

$$= 0.045 \times \frac{N}{100} \times \frac{X}{100} \times (30.03\text{-}18) \text{ gm}$$

[Molecular weight of H_2O = 18 gm/ mole]

Membrane weight after reaction:

$$= [0.045 \times \frac{N}{100} \times \frac{X}{100} \times (30.03\text{-}18)] + 2 \text{ gm}$$

Total membrane weight increased after reaction:

$$= [(0.045 \times \frac{N}{100} \times \frac{X}{100} \times (30.03\text{-}18)) + 2] \times \frac{100}{X} \text{gm}$$

Now, Amount of KOH required:

$$= \{[(0.045 \times \frac{N}{100} \times \frac{X}{100} \times (30.03\text{-}18)) + 2] \times \frac{100}{X}\} \times (\frac{Z}{100}) \text{ gm}$$

Amount of amine required:

$$= \{[(0.045 \times \frac{N}{100} \times \frac{X}{100} \times (30.03\text{-}18)) + 2] \times \frac{100}{X}\} \times (\frac{M}{100}) \text{ gm}$$

Amount of PEG required:

$$= \{[(0.045 \times \frac{N}{100} \times \frac{X}{100} \times (30.03\text{-}18)) + 2] \times \frac{100}{X}\} \times (\frac{Y}{100}) \text{ gm}$$

APPENDIX 3

Gas Transport Parameters Calculation and Gas Chromatography Data

(The calculation procedure adapted here was originally taken from PhD thesis of Arijit Mondal, reference given at the end of the Appendix**)**

A3.1 Gas transport parameters (CO_2 and N_2 fluxes, CO_2 and N_2 permeability, CO_2/N_2 selectivity) calculation

η_R (mol/min) = retentate molar flux per unit area = $\frac{PV}{RT}$ (A3.1)

Where, Atmospheric pressure at which the retentate gas is emitting (P) = 1atm.

Volumetric flow rate of mixed gas at retentate side (V) = 30 cc/min = 30×10^{-6} m^3/min.

Temperature at ambient condition (ºK) = 298.15 °K

Universal gas constant (R) = 8.205746×10^{-5} m^3 atm/ mol ºK

$$\eta_R \text{ (mol/min)} = \frac{1 \times 30 \times 10^{-06}}{8.205746 \times 10^{-05} \times 298.15} = 1.21 \times 10^{-03} \text{ mole/min}$$

η_{Ar} (mol/min) = Carrier gas molar flux per unit area = $\frac{PV}{RT}$ (A3.2)

Atmospheric pressure at which the carrier gas is emitting (P) = 1 atm

Volumetric flow rate of carrier gas at permeate side (V) = 27 cc/min = 27×10^{-06} m^3/min.

Temperature at ambient condition (°K) = 298.15 °K

Universal gas constant (R) = 8.205746×10^{-5} m^3 atm/ mol ºK

$$\eta_{Ar}\,(mol/min) = \frac{1\times 27\times 10^{-06}}{8.205746\times 10^{-05}\times 298.15} = 1.09\times 10^{-03}\ mole/min$$

η_P (mol/min) = permeate molar flux per unit area =

$$[(CO_2 \text{ mole fraction} \times \frac{CO_2(P)_{G.C}}{CO_2(F)_{G.C}}) + (N_2 \text{ mole fraction} \times \frac{N_2(P)_{G.C}}{N_2(F)_{G.C}})] \times \frac{\text{Ar molar flux (mol/min)}}{[1 - (CO_2 \text{ mole fraction} \times \frac{CO_2(P)_{G.C}}{CO_2(F)_{G.C}}) - (N_2 \text{ mole fraction} \times \frac{N_2(P)_{G.C}}{N_2(F)_{G.C}})]} \quad (A3.3)$$

Where,

$CO_2(P)_{G.C}$ = CO_2 mole fraction at permeate side from G.C analysis (**Figure A3.1**)

$CO_2(F)_{G.C}$ = CO_2 mole fraction at feed side from G.C analysis (**Figure A3.1**)

$N_2(P)_{G.C}$ = N_2 mole fraction at permeate side from G.C analysis (**Figure A3.1**)

$N_2(F)_{G.C}$ = N_2 mole fraction at feed side from G.C analysis (**Figure A3.1**)

CO_2 mole fraction = 0.2

N_2 mole fraction = 0.8

Ar molar flow rate = 1.09×10^{-3} mol /min.

η_P (mol/min) = permeate molar flow rate = 3.1×10^{-5} mol/min.

P_{CO2} (R, psi) = CO_2 partial pressure at retentate side =

$$[BP_F + P_{Ambient} \times \frac{14.7}{101.325}] \times \frac{[\eta_R - 0.5 \times \eta_P] \times CO_2 \text{ mole fraction} \times [0.5 + 0.5 \times \frac{CO_2(R)_{G.C}}{CO_2(F)_{G.C}}}{[\eta_R - 0.5 \times \eta_P] + \frac{[0.5 \times H_2O_F] + [0.5 \times H_2O_{distribution} \times (H_2O_F + H_2O_s)}{18}} \quad (A3.4)$$

Where, BP_F = Back pressure (psig) at feed side of the membrane module = 22 psig

$P_{ambient}$ = Ambient pressure (kPa) = 101.6 kPa

$CO_2(R)_{G.C}$ = CO_2 concentration at retentate side from G.C analysis (**Figure A3.1**)

$CO_2(F)_{G.C}$ = CO_2 concentration at feed side from G.C analysis (**Figure A3.1**)

H_2O_F = Feed side water flow rate (ml/min) = 0.03 ml /min

H_2O_S = Sweep side water flow rate (ml/min) = 0.04 ml /min

$H_2O_{distribution}$ = Total water distribution (ml/min) =

$$\frac{\textit{Retentate side water knockout volume}}{\textit{Retentate side water knockout volume} + \textit{Sweep side water knockout volume}} = 0.24$$

η_R = Retentate molar flux per unit area (mol/min) = 1.21×10^{-03} mole / min

η_P = Permeate molar flux per unit area (mol/min) = 3.1×10^{-5} mol/min

CO_2 mole fraction = 0.2

P_{CO2} (R, psi) = CO_2 partial pressure at retentate side (psi) = 2.742 psi

P_{CO2} (P, psi) = CO_2 partial pressure at permeate side =

$$\frac{[BP_S + P_{Ambient} \times \frac{14.7}{101.325}]\times [\eta_{Ar} - 0.5 \times \eta_P] \times CO_2 \text{ mole fraction} \times [0.5 + 0.5 \times \frac{CO_2(P)_{G.C}}{CO_2(F)_{G.C}}}{[\eta_{Ar} + 0.5 \times \eta_P] + \frac{[0.5 \times H_2O_S] + [0.5 \times (1 - H_2O_{distribution}) \times (H_2O_F + H_2O_s)}{18}} \quad \text{(A3.5)}$$

Where,

BP_S = Back pressure (psig) at sweep side of the membrane module = 4 psig

$P_{ambient}$ = Ambient pressure (kPa) = 101.6 k Pa

$CO_2(P)_{G.C}$ = CO_2 concentration at permeate side from G.C analysis (**Figure A3.1**)

$CO_2(R)_{G.C}$ = CO_2 concentration at feed side from G.C analysis (**Figure A3.1**)

H_2O_F = Feed side water flow rate (ml/min) = 0.03 ml /min

H_2O_S = Sweep side water flow rate (ml/min) = 0.04 ml /min

$H_2O_{distribution}$ = Total water distribution (ml/min) = 0.24

η_{Ar} (Mole/min) = Carrier gas molar flux per unit area (mol/min) = 1.09×10^{-03} mole / min

η_P = Permeate molar flux per unit area (mol/min) = 3.1×10^{-5} mol/min

CO_2 mole fraction = 0.2

P_{CO2} (P, psi) = **CO_2 partial pressure at permeate side (psi) = 0.074 psi**

P_{N2} (R, psi) = N_2 partial pressure at retentate side =

$$\frac{[BP_F + P_{Ambient} \times \frac{14.7}{101.325}] \times [\eta_R - 0.5 \times \eta_P] \times N_2 \text{ mole fraction} \times [0.5 + 0.5 \times \frac{N_2(R)_{G.C}}{N_2(F)_{G.C}}]}{[\eta_R - 0.5 \times \eta_P] + \frac{[0.5 \times H_2O_F] + [0.5 \times H_2O_{distribution} \times (H_2O_F + H_2O_S)]}{18}} \quad \text{(A3.6)}$$

Where,

BP_F = Back pressure (psig) at feed side of the membrane module = 22 psig

$P_{ambient}$ = Ambient pressure (kPa) = 101.6kPa

N_2 (R) $_{G.C}$ = N_2 concentration at retentate side from G.C analysis (**Figure A3.1**)

N_2 (F) $_{G.C}$ = N_2 concentration at feed side from G.C analysis (**Figure A3.1**)

H_2O_F = Feed side water flow rate (ml/min) = 0.03 ml/min

H_2O_S = Sweep side water flow rate (ml/min) = 0.04 ml/min

$H_2O_{distribution}$ = Total water distribution (ml/min) = 0.24

η_R = Retentate molar flux per unit area (mol/min) = 1.21×10^{-03} mole / min

η_P = Permeate molar flux per unit area (mol/min) = 3.1×10^{-5} mol/min

N_2 mole fraction = 0.8

P_{N2}(R, psi) = **N_2 partial pressure at retentate side (psi) = 14.38 psi**

P_{N2} (P, psi) = N_2 partial pressure at permeate side =

$$\frac{\left[BP_S + P_{Ambient} \times \frac{14.7}{101.325}\right] \times [\eta_{Ar} + 0.5 \times \eta_P] \times N_2 \text{ mole fraction} \times \left[0.5 + 0.5 \times \frac{N_2(P)_{G.C}}{N_2(F)_{G.C}}\right]}{[\eta_{Ar} + 0.5 \times \eta_P] + \frac{[0.5 \times H_2O_S] + [0.5 \times (1 - H_2O_{distribution}) \times (H_2O_F + H_2O_S)}{18}} \quad \text{(A3.7)}$$

Where,

BP_S = Back pressure (psig) at sweep side of the membrane module = 4 psig

$P_{ambient}$ = Ambient pressure (kPa) = 101.6kPa

N_2 (P) $_{G.C}$ = N_2 concentration at permeate side from G.C analysis (**Figure A3.1**)

N_2 (F) $_{G.C}$ = N_2 concentration at feed side from G.C analysis (**Figure A3.1**)

H_2O_F = Feed side water flow rate (ml/min) = 0.03 ml/min

H_2O_S = Sweep side water flow rate (ml/min) = 0.04 ml/min

$H_2O_{distribution}$ = Total water distribution (ml/min) = 0.24

η_{Ar} = Argon molar flux per unit area (mol/min) = 1.09×10^{-03} mole / min

η_P = Permeate molar flux per unit area (mol/min) = 3.1×10^{-5} mol/min

N_2 mole fraction = 0.8

P_{N2} (P, psi) = **N_2 partial pressure at permeate side (psi) = 0.0028 psi**

V_{CO2} (cm^3/sec) = Permeate volumetric gas flow rate of CO_2 =

$$\frac{\eta_{Ar} \times CO_2\ (\mathrm{P})_{G.C} \times CO_2 \text{ mole fraction} \times 8.314 \times 273.15 \times 1000000}{CO_2(F)_{G.C} \times 101325 \times 60 \times [1-(CO_2 \text{ mole fraction} \times \frac{CO_2(P)_{G.C}}{CO_2(F)_{G.C}}) - (N_2 \text{ mole fraction} \times \frac{N_2(P)_{G.C}}{N_2(F)_{G.C}})]} \quad \text{(A3.8)}$$

$V_{CO_2}(cm^3/sec)$ = permeate volumetric gas flow rate of CO_2 = $1.12 \times 10^{-02} cm^3$/sec

V_{N2} (cm^3/sec) = permeate volumetric gas flow rate of N_2 =

$$\frac{\eta_{Ar} \times N_2\ (\mathrm{P})_{G.C} \times N_2 \text{ mole fraction} \times 8.314 \times 273.15 \times 1000000}{N_2(F)_{G.C} \times 101325 \times 60 \times [1-(CO_2 \text{ mole fraction} \times \frac{CO_2(P)_{G.C}}{CO_2(F)_{G.C}}) - (N_2 \text{ mole fraction} \times \frac{N_2(P)_{G.C}}{N_2(F)_{G.C}})]} \quad \text{(A3.9)}$$

$V_{N_2}(cm^3/sec)$ = permeate volumetric gas flow rate of N_2= 4.19×10^{-04} cm^3/sec

CO_2 Flux (10^{-06} cm^3 (STP)/cm^2sec), CO_2 Permeability (Barrer), CO_2 Permeance (GPU) and CO_2/N_2 Selectivity

$(\Delta p)_{CO2}$ at psi = partial pressure difference at psi = $p_{CO2}(R, psi)$ - p_{CO2} (P, psi)

$(\Delta p)_{CO_2}$ at psi = 2.67 psi

$(\Delta p)_{CO2}$ at cmHg = partial pressure difference at cmHg = $\frac{(\Delta p)_{CO2} \text{ at psi}}{14.7} \times 76$

$(\Delta p)_{CO_2}$ = 13.79 cm Hg

$$\textbf{CO}_2\ \textbf{flux (cm}^3\textbf{(STP)/cm}^2\textbf{s)} = \frac{\mathbf{V_{CO2}\ (cm^3/sec)}}{\mathbf{membrane\ area\ (cm^2)}} \quad \text{(A3.10)}$$

Where

V_{CO2} (cm^3/sec) = permeate volumetric gas flow rate of (cm^3/sec) = **$1.12 \times 10^{-02} cm^3$/sec**

Area of membrane = 49.5 cm^2

CO_2 flux = 226×10^{-6} in cm^3 (STP) / cm^2s

$$\textbf{CO}_2\textbf{ permeability } (10^{-10}\textbf{cm}^3\textbf{ (STP) cm /cm}^2\textbf{s cmHg}) = \frac{\textbf{V}_{CO2}\textbf{ (cm}^3\textbf{/sec)} \times \textbf{thickness (cm)}}{\textbf{Membrane area (cm}^2\textbf{)} \times (\Delta p)_{CO2}\textbf{ at cmHg}} \quad \text{(A3.11)}$$

Where,

V_{CO2} (cm^3/sec) = permeate volumetric gas flow rate of CO_2 = $\mathbf{1.12 \times 10^{-02} cm^3/sec}$

Area of membrane = 49.5 cm^2

Thickness = 0.0027 cm = 27 micron

$(\Delta p)_{CO_2}$ at cm Hg = 13.79 cm Hg

CO_2 Permeability = ~442 × 10^{-10} cm^3 (STP) cm/cm^2s cmHg = 442 Barrer

$$\textbf{CO}_2\textbf{ permeance (GPU)} = \frac{\textbf{CO}_2\textbf{ permeability}}{\textbf{Thickness}} = \frac{\mathbf{442}\ (\boldsymbol{Barrer})}{\mathbf{27}} = \sim \mathbf{16\ GPU}$$

1GPU=$10^{-6}$$cm^3$(STP)/$cm^2$s cmHg (A3.12)

$$\frac{\textbf{CO}_2}{\textbf{N}_2}\textbf{ Selectivity} = \frac{\dfrac{\textbf{CO}_2\textbf{(P)}_{\textbf{G.C}}}{\textbf{N}_2\textbf{(P)}_{\textbf{G.C}}}}{\dfrac{\textbf{CO}_2\textbf{(R)}_{\textbf{G.C}}}{\textbf{N}_2\textbf{(R)}_{\textbf{G.C}}}} = \frac{\dfrac{\mathbf{0.04}}{\mathbf{0.001}}}{\dfrac{\mathbf{0.1674}}{\mathbf{0.8338}}} = \mathbf{200} \quad \text{(A3.13)}$$

N_2 Flux (10^{-6} cm^3 (STP)/cm^2sec), N_2 Permeability (Barrer), N_2 Permeance (GPU) and CO_2/N_2 Selectivity

$(\Delta p)_{N2}$ at psi = partial pressure difference at psi = $p_{N2}(R, psi)$ - p_{N2} (P, psi)

$(\Delta p)_{N_2}$ (psi) = 14.37 psi

$(\Delta p)_{N2}$ at cmHg = partial pressure difference at cmHg = $\frac{(\Delta p)_{N2} \text{ at psi}}{14.7} \times 76$

$(\Delta p)_{N_2}$ = 74.36 cm Hg

$$\mathbf{N_2 \text{ flux } (cm^3(STP)/cm^2 s)} = \frac{\mathbf{V_{N2}\ (cm^3/sec)}}{\mathbf{\text{membrane area } (cm^2)}}$$

(A3.14)

V_{N_2} (cm^3/sec) = $4.19 \times 10^{-04} cm^3$/sec

Area of membrane = 49.5 cm^2

N_2 flux = ~ 8.13×10^{-6} cm^3 (STP) / cm^2s

$$\mathbf{N_2 \text{ permeability } (10^{-10} cm^3 \text{ (STP) cm/cm}^2\text{s cmHg})} = \frac{\mathbf{V_{N2}\ (cm^3/sec) \times \text{thickness (cm)}}}{\mathbf{\text{Membrane area } (cm^2) \times (\Delta p)_{N2} \text{ at cmHg}}} \quad \text{(A3.15)}$$

where

V_{N2} (cm^3/sec) = permeate volumetric gas flow rate of N_2 = $4.19 \times 10^{-04} cm^3$/sec

Area of membrane = 49.5 cm^2

Thickness = 0.0027 cm = 27 micron

$(\Delta p)_{N_2}$ at cm Hg = 74.36 cm Hg

N_2 Permeability = 3.0×10^{-10} cm^3 (STP) cm/cm^2s cmHg = 3 Barrer

$$\mathbf{N_2 \text{ permeance} = \frac{N_2 \text{ Permeability}}{\text{thickness}} = \frac{3}{27} = 0.11 \text{ GPU}} \quad \text{(A3.16)}$$

References

[1] A. Mondal, A. CO_2-Selective Thin-Film Polymer Composite Membranes: Improvement of Thermal Stability and Role of Amine Carriers. PhD Dissertation, *Indian Institute of Technology, Guwahati*, 2014.

[2] S. Barma, Amine functionalized ordered mesoporous silica materials and its applications towards adsorbent and membrane for CO_2 capture. PhD Dissertation, *Indian Institute of Technology, Guwahati*, 2015.

A3.2 Gas Chromatography Operating Protocol

Here, we have used Varian-450 G.C for all permeation experiments. The detail G.C operating protocols are mentioned below:

Injector programing: Heater (ON) at 120 °C

Time (min)	Split state	Split ratio
Initial	ON	1
0.00	ON	1
1.00	ON	1

Oven programing:

Column oven (ON) and Rear oven (ON) at 100 °C

Rate (°C/min)	Temperature (°C)	Time (min)	Total time (min)
initial	40	2.00	2.00
10	70	5.00	10.00
			Total time 10.00

Column pneumatics: (pressure program)

Rate (psi/min)	Pressure (psi)	Time(min)	Total time (min)
Initial	15	10.00	10.00
			Total time 10.00

Detector (TCD) programing:

Heater (ON) at 95 °C

Electronics (ON)

Filament temperature at 235 °C

Filament temperature limit at 390 °C

TCD event table

Time (min)	**Range**	**Auto zero**	**Polarity**
Initial	0.05	YES	Negative

Gas sampling valve (GSV) programing:

Time (min)	**Gas sampling valve**
Initial	Fill
0.02	Inject

A3.3 Detail Purity Percentage of all Calibration Gases

Table A3.1 Detail purity percentage of all calibration gases

Name	Purity compositions
4 % CO_2 + 4 % N_2, balance Argon	CO_2 (99.999 %), N_2 (99.999 %), Ar (99.999 %), H_2O (< 2 ppm) and CO (< 0.5 ppm)
8 % CO_2 + 8 % N_2, balance Argon	CO_2 (99.999 %), N_2 (99.999 %), Ar (99.999 %), H_2O (< 2 ppm) and CO (< 0.5 ppm)
12 % CO_2 + 12 % N_2, balance Argon	CO_2 (99.999 %), N_2 (99.999 %), Ar (99.999 %), H_2O (< 2 ppm) and CO (< 0.5 ppm)
20 % CO_2, balance N_2	CO_2 (99.999 %), N_2 (99.999 %), H_2O (< 2 ppm) and CO (< 0.5 ppm)
40 % CO_2, balance N_2	CO_2 (99.999 %), N_2 (99.999 %), H_2O (< 2 ppm) and CO (< 0.5 ppm)
Pure CO_2	CO_2 (99.999 %)
Pure N_2	N_2 (99.999 %)
Pure H_2	H_2 (99.999%)

A3.4 Gas chromatography data of crosslinked PVA/PEG, PVA/PEG/Sil, PVA/PEG/APTMS-Sil (Permeation experiment)

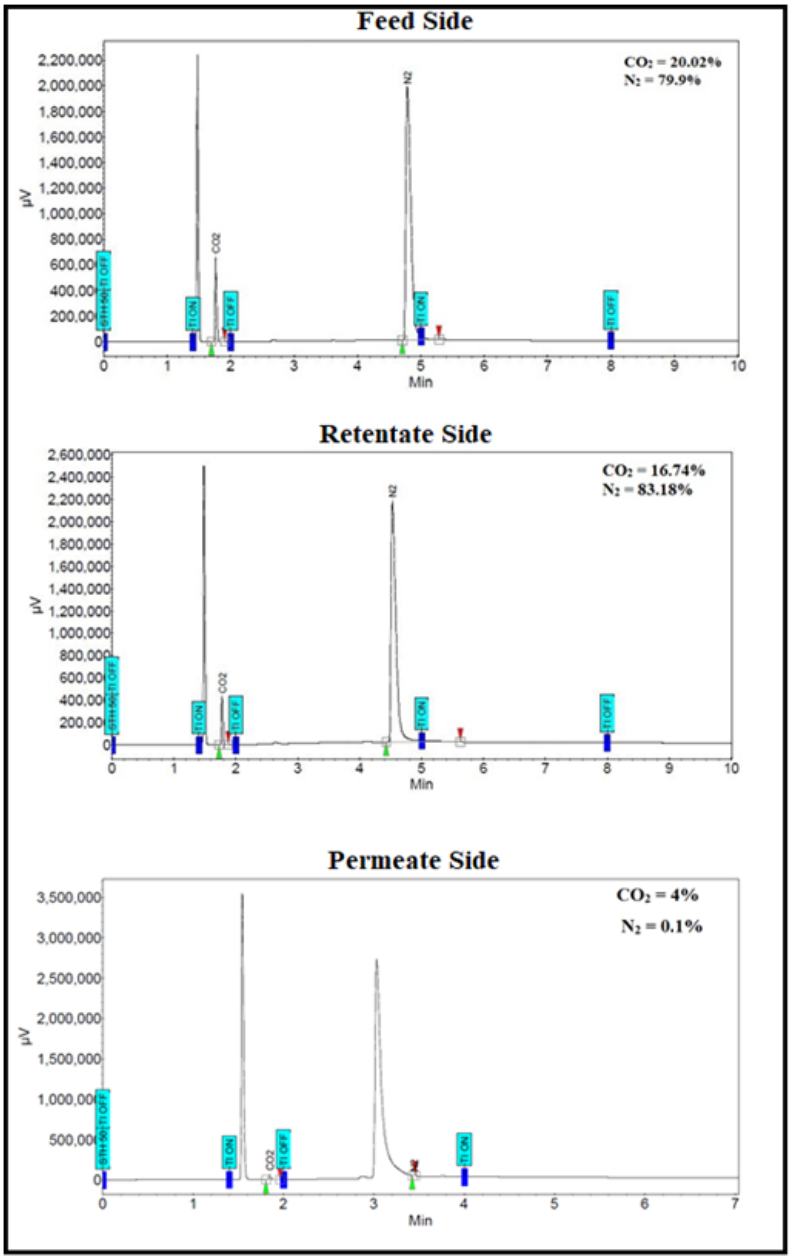

Figure A3.1 GC peaks of PVA/PEG membrane at 100 °C and absolute pressure = 2.5/1.2 atm (feed/sweep) having water flow rate of 0.03/0.04 ml/min (feed/sweep)

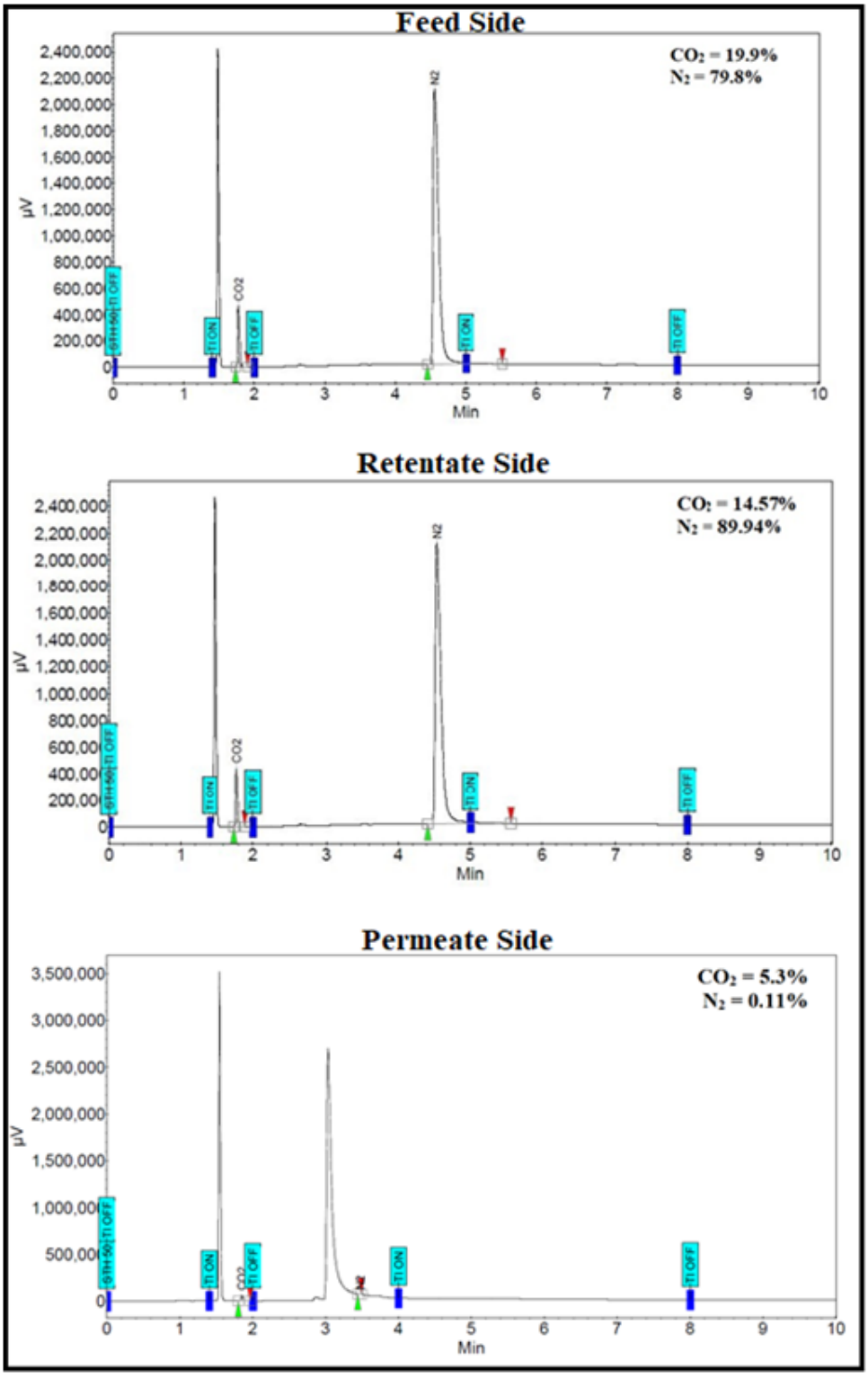

Figure A3.2 GC peaks of PVA/PEG/Sil membrane at 100 °C and absolute pressure = 2.5/1.2 atm (feed/sweep) having water flow rate of 0.03/0.04 ml/min (feed/sweep)

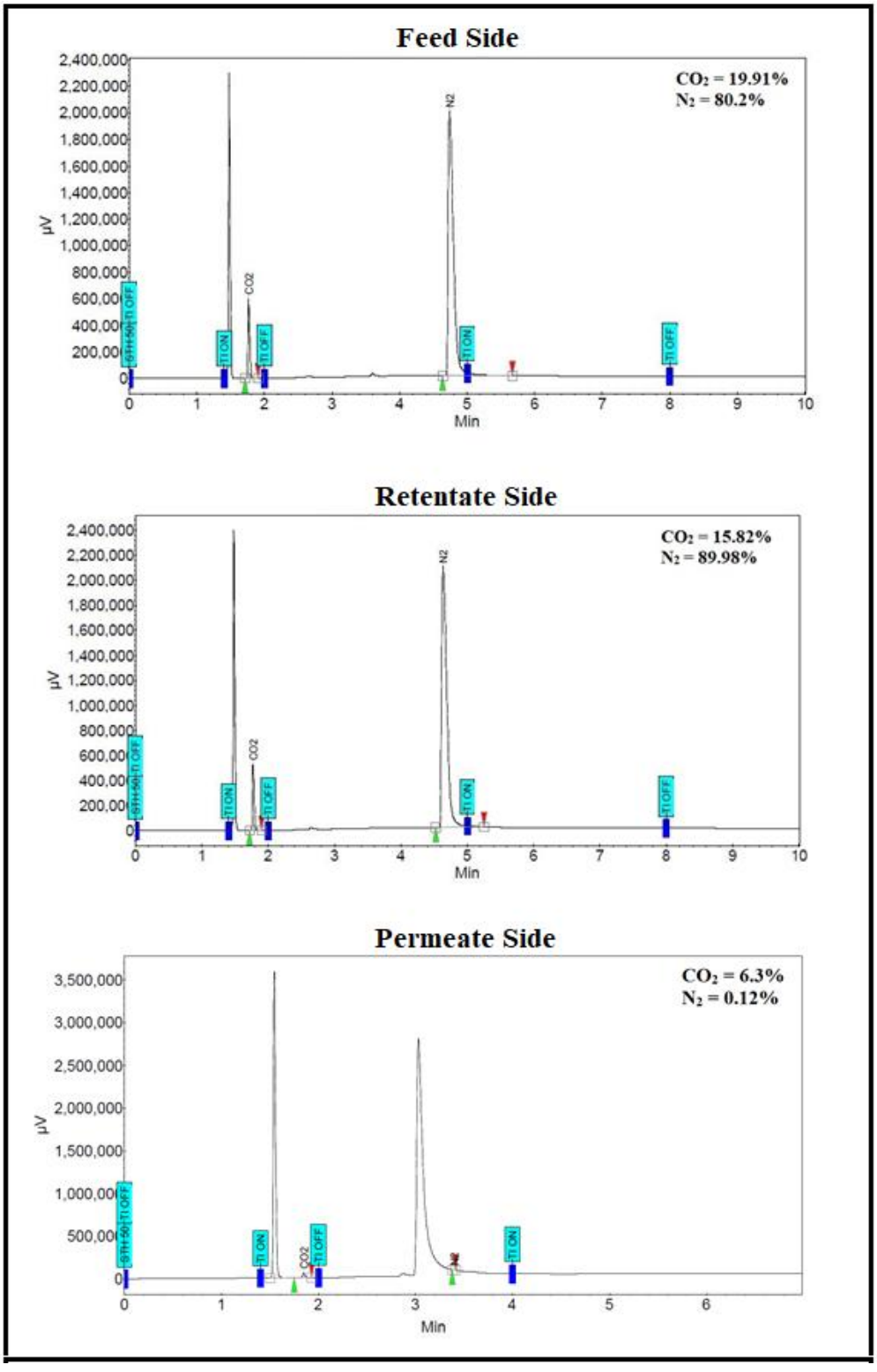

Figure A3.3 GC peaks of PVA/PEG/APTMS-Sil membrane at 100 °C and absolute pressure = 2.5/1.2 atm (feed/sweep) having water flow rate of 0.03/0.04 ml/min (feed/sweep)

A3.5 Gas chromatography data of crosslinked PVA/PG, PVA/PG/ZIF-8, PVA/PG/ZIF-8@PEI (Permeation experiment)

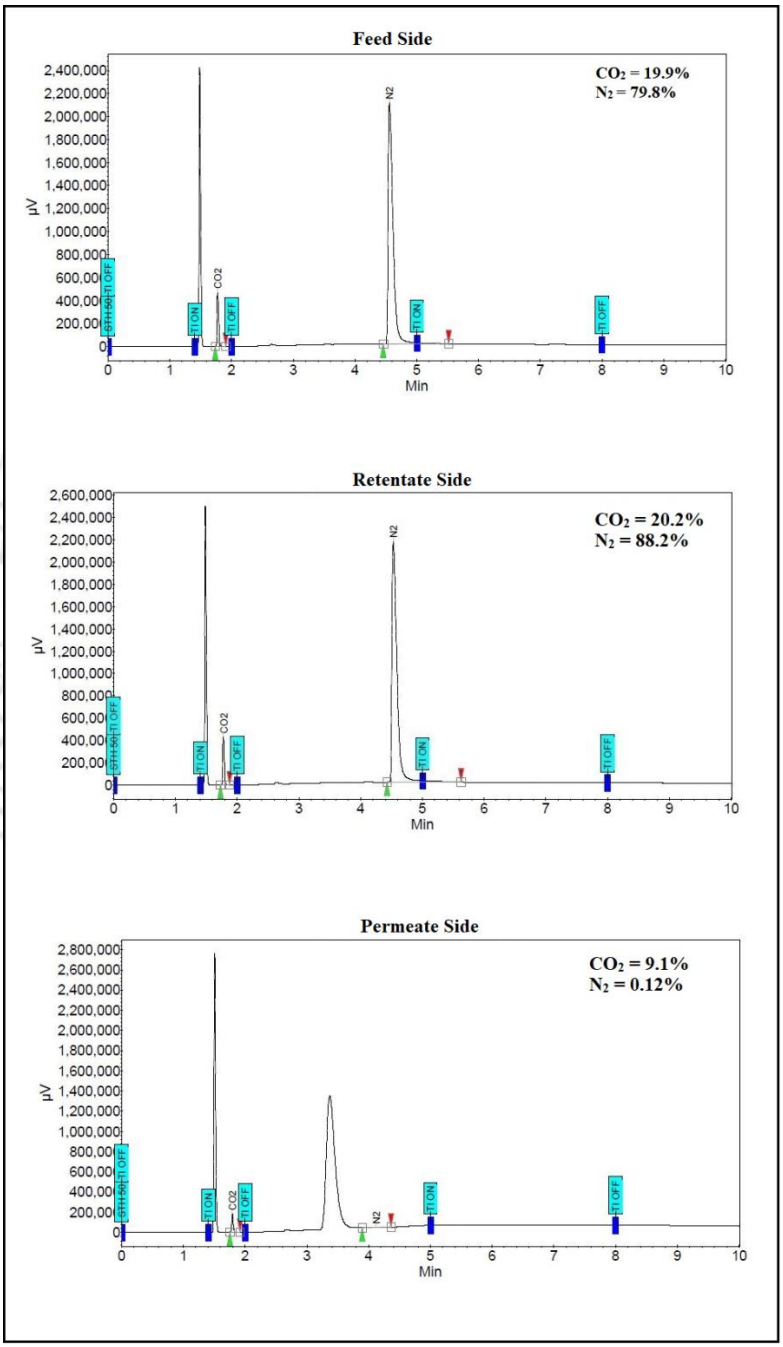

Figure A3.4 GC peaks of PVA/PG membrane at 100 °C and absolute pressure = 2.5/1.2 atm (feed/sweep) having water flow rate of 0.03/0.05 ml/min (feed/sweep)

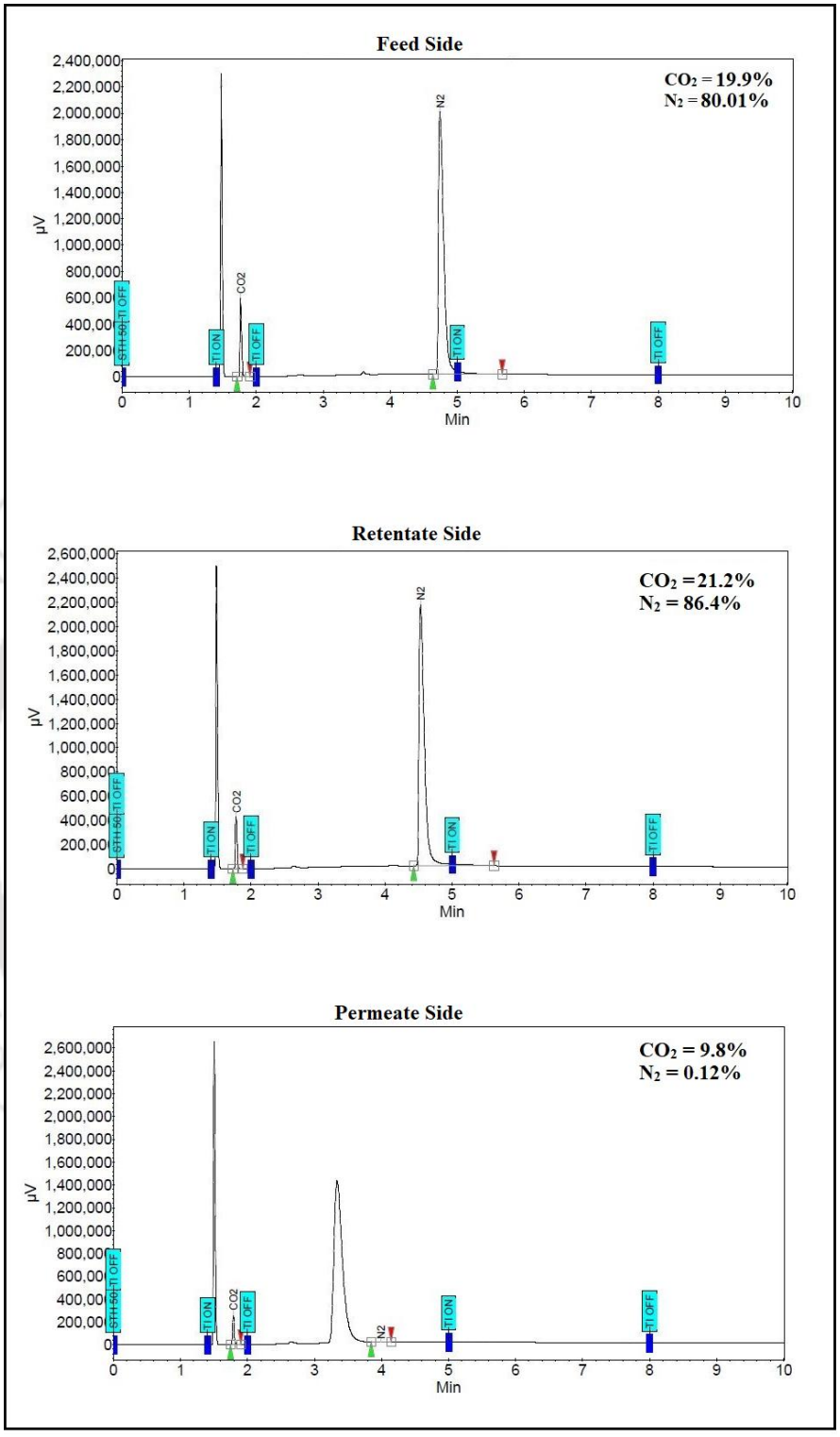

Figure A3.5 GC peaks of PVA/PG/ZIF-8 membrane at 100 °C and absolute pressure = 2.5/1.2 atm (feed/sweep) having water flow rate of 0.03/0.05 ml/min (feed/sweep)

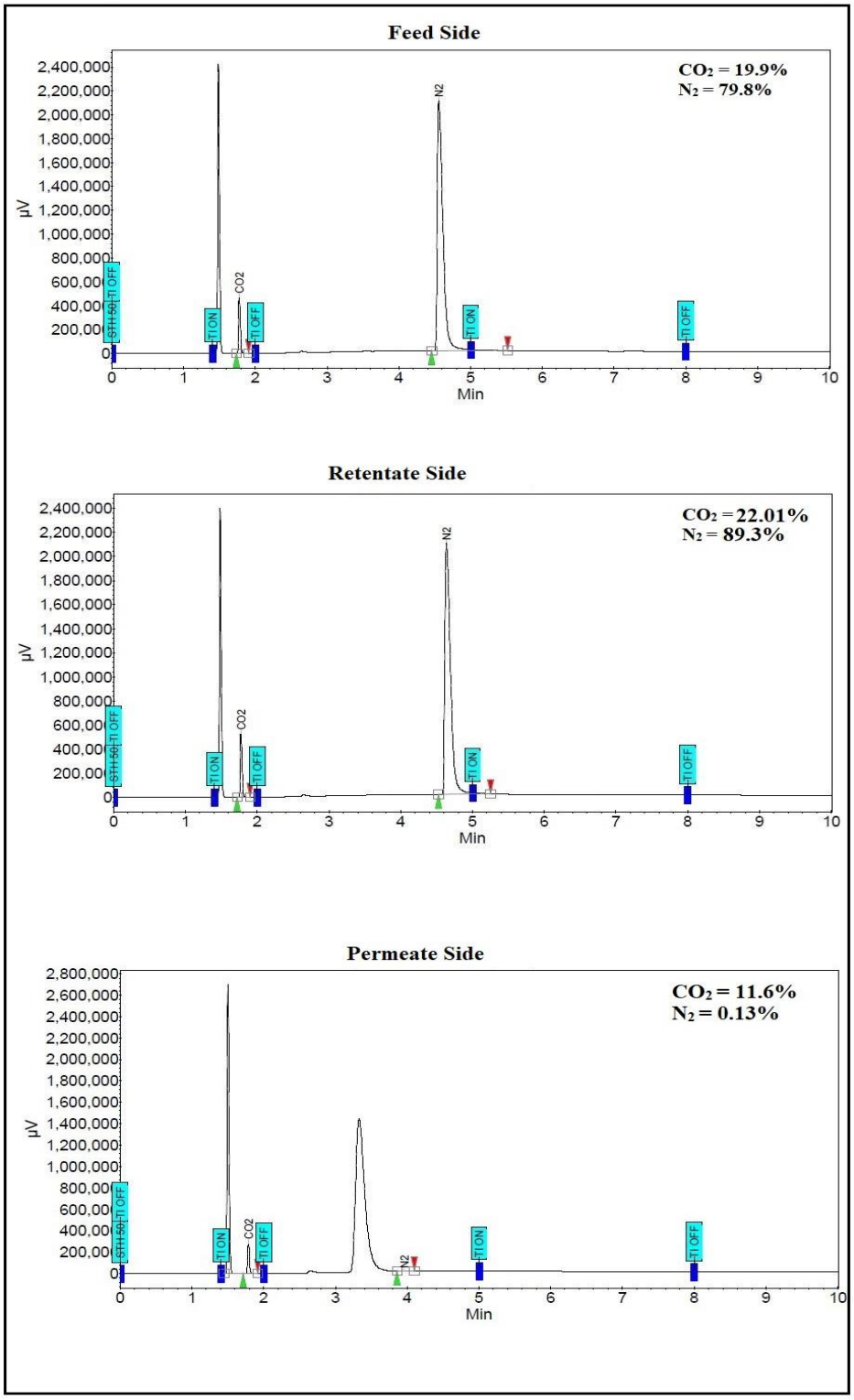

Figure A3.6 GC peaks of PVA/PG/ZIF-8@PEI membrane at 100 °C and absolute pressure = 2.5/1.2 atm (feed/sweep) having water flow rate of 0.03/0.05 ml/min (feed/sweep)

Research Output

Journal publications

Within Thesis work

1. **M. Barooah,** B. Mandal. "Enhanced CO_2 separation performance by PVA/PEG/silica mixed matrix membrane**",** *Journal of Applied Polymer Science,* 46481 (2018) 1-12. **(Wiley, Impact Factor 2.19).**

2. **M. Barooah,** B. Mandal. "Synthesis, characterization and CO_2 separation performance of novel PVA/PG/ZIF-8 mixed matrix membrane", *Journal of Membrane Science,* 572 (2019) 198-209. **(Elsevier, Impact Factor 7.015).**

3. **M. Barooah,** B. Mandal, B. Su, "Tailoring the properties of silica by amine functionalization a filler in mixed matrix membranes for enhanced CO_2 separation." **(to be communicated).**

4. **M. Barooah,** B. Mandal, "Effect of amino-functionalized ZIF-8 incorporated mixed matrix membrane for enhanced CO_2 separation." **(to be communicated).**

5. **M. Barooah,** B. Mandal, "Current status and development of mixed matrix membrane for gas separation: A review." **(to be communicated).**

Outside Thesis work

6. A. Mondal, **M. Barooah,** B. Mandal. "Effect of single and blended amine carriers on CO_2 separation from CO_2/N_2 mixtures using cross-linked thin-film poly (vinyl alcohol) composite membrane," *International Journal of Greenhouse Gas Control,* 39 (2015) 27–38. **(Elsevier, Impact Factor 3.28)**.

Research Output

National and International Conferences

1. **M. Barooah,** B. Mandal, (2019). "Synthesis and characterization of PVA/PG/Zeolite membrane for CO_2 separation". *1st Euro-Asia Conference on CO_2 Capture and Utilization (EACCO2CU 2019),* Aug. 6-7, Sunway University, Kuala Lumpur, Malaysia.

2. **M. Barooah,** B. Mandal, (2019). "Synthesis, characterization and gas permeation study of PVA mixed matrix membrane incorporated with silica and MOF fillers". *Student Academic Board (RESEARCH CONCLAVE 2019),* March 8-11, IIT Guwahati, INDIA.

3. **M. Barooah,** B. Mandal, (2018). "A review on membrane technology for CO_2 gas separation studies. *Student Academic Board (RESEARCH CONCLAVE 2018),* March 8-11, IIT Guwahati, INDIA.

4. **M. Barooah,** B. Mandal, (2018). "Synthesis and characterization of cross-linked poly (vinyl alcohol)/piperazine glycinate/polyethersulfone composite membrane for CO_2/N_2 gas separation". *Fourth International Symposium on Advances in Sustainable Polymers (ASP 17),* January 8-11, IIT Guwahati, INDIA.

5. **M. Barooah,** B. Mandal, (2017). "Application of sophisticated instruments for characterization studies of thin film composite polymer membranes". *International Conference on Sophisticated Instruments in Modern Research (ICSIMR 2017),* Centre for Instruments Facility (CIF), July 1, IIT Guwahati, INDIA.

6. **M. Barooah,** B. Mandal, (2017). "Synthesis and application of CO_2 selective thin film polymeric membrane for CO_2/N_2 gas separation". *Student Academic Board (RESEARCH CONCLAVE 2017),* March 16-19, IIT Guwahati, INDIA.

7. **M. Barooah,** R. Borgohain, B. Prasad, B. Mandal, (2016). "Novel CO_2 selective facilitated transport membrane for CO_2/N_2 separation"**.** *Gifu-U/IITG & Gifu-U/UKM Joint Symposium,* August 1, GIFU-JAPAN.

8. **M. Barooah,** R. Borgohain, B. Prasad, B. Mandal, (2016). "Novel CO_2 selective facilitated transport membrane for CO_2/N_2 separation". *International Symposium on Advances in Sustainable Polymers (ASP-16),* August 4-6, Kyoto Institute of Technology, Kyoto, JAPAN.

9. **M. Barooah,** R. Borgohain, B. Prasad, B. Mandal, (2016). "Synthesis and

characterization of cross-linked PVA membrane containing diethanolamine carrier for CO_2/N_2 separation". *The Indian Chemical Engineering Congress (CHEMCON 2016),* Dec 27-30, A.C. Tech, Anna University, Chennai, INDIA.

10. **M. Barooah,** B. Mandal, (2015). "Synthesis and characterization of mixed matrix composite membranes for CO_2/N_2 separation". *The Indian Chemical Engineering Congress (CHEMCON 2015),* Dec 27-30, IIT Guwahati, INDIA.

11. **M. Barooah,** B. Prasad, A. Mondal, B. Mandal, (2014). "CO_2 separation by facilitated transport polymer membrane containing monoethanolamine carrier". *The Indian Chemical Engineering Congress (CHEMCON 2014),* Dec 7–30, Chandigarh, INDIA.

12. **M. Barooah,** A. Mondal, A. Mandal, B. Mandal, (2014). "CO_2 selective poly (vinyl alcohol) membrane containing blends of poly(allylamine) and 2-amino-2-hydroxymethyl-1,3-propanediol**.** *International Symposium on Advances in Sustainable Polymers (ASP 14),* January 10-11, IIT Guwahati, INDIA.

Awards and Achievements

1. **Best poster awards (3rd position**), *The Indian Chemical Engineering Congress (CHEMCON 2016)*, Dec. 27-30, 2016, Chennai, India.

Front Page of the Papers Published in Various Reputed International Journals

Journal of Membrane Science 572 (2019) 198–209

Contents lists available at ScienceDirect

Journal of Membrane Science

journal homepage: www.elsevier.com/locate/memsci

Synthesis, characterization and CO_2 separation performance of novel PVA/PG/ZIF-8 mixed matrix membrane

Mridusmita Barooah, Bishnupada Mandal*

Department of Chemical Engineering, Indian Institute of Technology Guwahati, Guwahati 781039, Assam, India

ARTICLE INFO

Keywords:
Mixed matrix membranes (MMMs)
Poly (vinyl alcohol)
ZIF-8
Separation techniques
CO_2/N_2 gas separation

ABSTRACT

This work reports the synthesis of zeolitic imidazolate framework-8 (ZIF-8) having regular pore size (~0.35 nm) embedded to the poly (vinyl alcohol) (PVA)/piperazine glycinate (PG) solution. High performance mixed matrix membranes (MMMs) prepared by solution coating of PVA/PG/ZIF-8 solution onto a polyethersulfone (PES) support were utilized for CO_2/N_2 gas separation studies. Detailed thermal, structural and microscopic analysis of the synthesized ZIF-8 particles was conducted. The characterization studies and the performance evaluation tests were performed for the prepared MMMs. The excellent compatibility of ZIF-8 filler in the PVA/PG matrix resulted in enhancement of CO_2 permeance and CO_2/N_2 selectivity. The results depicted that PVA/PG membrane loaded with 5 wt% ZIF-8 (PVA/PG/ZIF-8(5)) showed a high CO_2 permeance of 82 GPU and CO_2/N_2 selectivity of 370 which was 82.2% and 76.2% higher when compared to pure PVA/PG membrane. Thus ZIF-8 doped PVA mixed matrix membrane serves as a potential candidate for industrial gas separation studies.

1. Introduction

CO_2 separation from flue gas is of considerable importance due to its regressive implication on the environmental ecology. The application of traditional CO_2 separation technique is restricted by its aggravated solvent regeneration cost and high energy intensity [1]. The two main constraints of CO_2 capture are restriction of huge amount of flue gas emitted from industrial plants and the separation of CO_2 present in a very low concentration (around 12–13%) in the flue gas [2]. Membrane-based technology has been formulated as a potential alternative to conventional techniques owing to its advantages of low cost, compact module, process flexibility and operational simplicity [3]. Polymer membranes have advantages of easy processing, low cost and high membrane flexibility [4–6]. However, its long-term usage is restricted by the permeability and selectivity restraint of the Robeson curve along with restricted long term stability [7,8]. Multistage process is required to obtain high purity leading to high CO_2/N_2 selectivity which increases both the capital and operating cost [9]. Cross-linking, blending and carrier meditated transport are introduced to tackle this low gas transport performance. Also, it has been observed that the large-scale application of thermally stable inorganic membranes having high chemical stability and prolonged stability is restricted by its brittle nature and the high cost [10].

To tackle these constraints, mixed matrix membranes (MMMs) comprising of inorganic particles embedded into the polymer matrix has been largely considered in the recent times [11,12]. Common inorganic fillers such as zeolite [13,14], silica nanoparticle [15,16], carbon nanotube [17–19], carbon molecular sieve [20,21], graphene oxide [22], and metal-organic framework [9,23] used for the MMMs fabrication has been extensively studied. The high-performance of MMM is achieved by the combination of excellent transport performance of the fillers along with the processability of the polymers. However, the major challenge is in the improvement of polymer-filler interface compatibility which otherwise leads to the occurrence of non-selective voids at the interface of the two phases. This leads to the high diffusion of gas molecules thereby leading to a steep decline in the overall selectivity of the membrane. Also, the good affinity between filler and polymer material during the fabrication process plays a major role in the formation of desired defect-free MMMs [24].

Recently, metal-organic frameworks (MOFs), a class of hybrid organic-inorganic crystalline nanoporous framework serve as potential filler material due to its high porosity, adjustable pore size, specific surface area and convenient synthesis process. When compared to zeolites, silica, or other porous materials, MOFs offer advantages of large surface area making it an attractive candidate for gas separation application. In addition to this, the highly tunable physical and chemical characteristic makes it a desirable filler material in MMMs [25–28]. Zeolitic imidazolate framework (ZIFs), a subclass of MOFs

* Corresponding author.
E-mail addresses: mridusmita@iitg.ac.in (M. Barooah), bpmandal@iitg.ac.in (B. Mandal).

https://doi.org/10.1016/j.memsci.2018.11.001
Received 1 August 2018; Received in revised form 31 October 2018; Accepted 3 November 2018
Available online 05 November 2018

TH-2301_136107039

Journal of Applied Polymer Science

Enhanced CO_2 separation performance by PVA/PEG/silica mixed matrix membrane

Mridusmita Barooah, Bishnupada Mandal
Department of Chemical Engineering, Indian Institute of Technology Guwahati, Guwahati, Assam 781039, India
Correspondence to: B. Mandal (E-mail: bpmandal@iitg.ernet.in)

ABSTRACT: This article focused on segregation of low concentration CO_2 from CO_2/N_2 mixture gas by implementing high-performance facilitated transport mixed matrix membranes (MMMs) in large-scale carbon capture techniques. These advanced, novel CO_2-selective membrane materials were developed by embedding silica nanoparticles at different loading into the poly(vinyl alcohol) (PVA)/poly(ethylene glycol) (PEG) matrix using solution casting. *In situ* sol–gel technique was applied for the synthesis of the hydrophilic SiO_2 nanoparticles. The compatibility of filler-polymer matrix plays a crucial role in the optimization of the membrane performance. The dispersion and interaction of the filler into the polymer matrix were confirmed by thermogravimetric analysis, differential scanning calorimetry, Fourier transform infrared spectroscopy, X-ray diffraction, field emission scanning electron microscopy, contact angle tests, and swelling ratio analysis. Field emission scanning electron microscopy analysis of the synthesized MMMs established the homogeneous dispersion of the fillers in the polymer matrix. Owing to its good compatibility with PVA/PEG matrix, the inclusion of fillers significantly increased the overall separation efficiency of CO_2 within the membrane. Compared to pristine PVA/PEG membrane, PVA/PEG/silica membrane with 3.34 wt % silica loading showed pronounced improvement in its gas separation properties with 78% augmentation in CO_2 permeability and 45% enhancement in CO_2/N_2 selectivity for fixed conditions pertaining to sweep side water flow rate of 0.04 mL/min and 100 °C temperature. © 2018 Wiley Periodicals, Inc. J. Appl. Polym. Sci. **2018**, *135*, 46481.

KEYWORDS: differential scanning calorimetry (DSC); films; membranes; separation techniques; swelling

Received 26 November 2017; accepted 20 February 2018
DOI: 10.1002/app.46481

INTRODUCTION

The capture and subsequent sequestration of carbon dioxide, a principal greenhouse gas, has been a major concern in recent times owing to its unparalleled contribution to global warming. The unprecedented increase in anthropogenic CO_2 emissions basically from industrial fossil fuel reserves has imposed a serious threat to the environmental ecology. As has been predicted, tackling the huge increase in the CO_2 concentration to about 800 ppm by 2100 would be a major challenge for researchers across the globe. To handle this, development of energy efficient, environmental friendly, and cost-effective membrane-based gas separation technology has been a major breakthrough study in the recent years.[1]

The capture of CO_2 from flue gas, produced by combustion of fossil fuel, by postcombustion techniques has been a study of great importance. The low CO_2 concentration of about 3–5 mol % in gas plants and 13–15 mol % in coal plants is the major challenge.[2] Sluijs *et al.*[3] studied the feasibility of post-combustion CO_2 separation using polymer gas separation membranes and reported that gas separation membrane with selectivity of at least 200 makes it a potential competitor with the conventional separation techniques. Thus, the separation of CO_2/N_2 mixture becomes a technique of commendable importance.

To tackle the restriction of low CO_2 permeability by glassy polymers, rubbery polymers containing CO_2-philic group are preferred for CO_2 separation.[4] Different modifications utilized for improved CO_2 transport performance include incorporation of suitable amine carriers into the polymer backbone, crosslinking, blending of polymer matrix, and mixed matrix membrane (MMM) composition and so forth.[5,6] The challenge imposed by the long-term usability of polymer membrane for industrial application is restricted by the instinctive trade-off limitation between permeability and selectivity as depicted by Robeson's curve.[7–9] On the other hand, the high separation properties of inorganic membranes even at high temperature is restricted by its high cost and lack of processability.[10] To address these issues, MMMs which combine the advantages of inorganic filler and polymer matrix have been extensively studied. In the synthesis

Additional Supporting Information may be found in the online version of this article.

International Journal of Greenhouse Gas Control 39 (2015) 27–38

Contents lists available at ScienceDirect

International Journal of Greenhouse Gas Control

journal homepage: www.elsevier.com/locate/ijggc

Effect of single and blended amine carriers on CO_2 separation from CO_2/N_2 mixtures using crosslinked thin-film poly(vinyl alcohol) composite membrane

Arijit Mondal, Mridusmita Barooah, Bishnupada Mandal*

Department of Chemical Engineering, Indian Institute of Technology Guwahati, Guwahati 781039, Assam, India

ARTICLE INFO

Article history:
Received 13 December 2014
Received in revised form 2 April 2015
Accepted 2 May 2015
Available online 15 May 2015

Keywords:
CO_2/N_2 separation
Formaldehyde cross-linking
PVA membrane
Blended amine

ABSTRACT

This article reports effect of different single and blended amine carriers on binary gas (20% CO_2 balance N_2) separation using novel CO_2-selective crosslinked thin-film poly(vinyl alcohol) composite membranes. The characterization of the thin-film active layer had been carried out by Thermogravimetric analysis (TGA), Differential scanning calorimetry (DSC), Fourier transform infrared spectroscopy (FTIR) and X-ray diffraction (XRD). The transport properties of CO_2 (CO_2 and N_2 fluxes, CO_2 and N_2 permeability, and CO_2/N_2 selectivity) across the membrane were examined using counter flow flat sheet membrane module. The effects of active layer thickness (41 to 84 micron), feed absolute pressure (1.7 to 6.2 atm), temperature (90 to 125 °C), and sweep side water flow rate (0.02 to 0.075 cm^3/min) on transport properties of CO_2 across the membrane were analyzed. The dense layer containing amine carrier displays both high selectivity and permeability. It has been seen that the composite membrane of 25 wt% poly(allylamine) and 15 wt% 2-amino-2-hydroxymethyl-1,3-propanediol with 44 micron active layer thickness is having maximum CO_2/N_2 selectivity of 434 and CO_2 permeability of 1826 Barrer at 2.8 atm feed side absolute pressure and 100 °C temperature.

1. Introduction

CO_2 emission has been a major environmental concern owing to the drastic climatic change in the recent times (Merkel et al., 2010). Its capture has wide applications like mitigating greenhouse gas effects, production of fuel with enhanced energy content, gas purification with the prevention of corrosion problems etc. (Zou and Ho, 2006). Conventional matured technologies such as amine absorption has large scale implementations. However, limitations of such technologies include high cost and are energy intensive. New advanced technologies like polymeric membrane based CO_2 separation is one of the most potential methods due to its low energy consumption, compact membrane module leading to enhanced weight and space efficiency. It is also an efficient environment-friendly alternative compared to other processes (Xing and Ho, 2009; Peters et al., 2011). Polymer membranes such as cellulose acetate, cellulose triacetate or polyimide are used industrially for CO_2 removal. These membranes are normally affected by low CO_2 permeability as well as low CO_2/N_2 selectivity. Wind et al. (2004) reported the CO_2 permeability of 4 Barrers and CO_2/N_2 selectivity of 26 for cellulose acetate membranes with the thickness of 50–75 micron at 35 °C temperature and 25 atm pressures. The permeability and selectivity of this membrane is quite low. Most of the industrially useful polymer membranes are made of common polymer materials and separation is governed by solution–diffusion mechanism. The selectivity of conventional polymeric membrane is limited by relative solubility and diffusivity of the components in the gas mixture. Blending of suitable amine carriers into the polymer matrix can enhance the CO_2 transport property by reacting reversibly with the targeted compound. Improvement of thermal stability of polymeric membrane is also important for high temperature application. Crosslinking as well as blending of thermally stable polymer matrix may improve thermal stability of polymer hydrogel. There are several investigations reported in the literature for improvement of thermal stability of polymers (Elashmawi and Abdel Baieth, 2012; Abdelrazek et al., 2010; Cassu and Felisberti, 1997, 1999; Qiao et al., 2010) as well as use of amine carrier to enhance CO_2 transport through the membrane (Cai et al., 2008; Deng et al., 2009a,b; Francisco et al., 2007; Kim et al., 2004a; Matsuyama et al., 1999a; Shen et al., 2006, 2008; Ward et al., 1976; Wu et al., 2006; Yegani et al., 2007; Mandal and Ho, 2007). In our

* Corresponding author. Tel.: +91 361 2582256; fax: +91 361 2690762.
E-mail addresses: a.mondal@iitg.ernet.in (A. Mondal), mridusmita@iitg.ernet.in (M. Barooah), bpmandal@iitg.ernet.in (B. Mandal).

http://dx.doi.org/10.1016/j.ijggc.2015.05.002
1750-5836/